

DIFFERENTIAL ANALYSIS OF FLUID FLOW

In this chapter we derive the differential equations of fluid motion, namely, conservation of mass (the *continuity equation*) and Newton's second law (the *Navier–Stokes equation*). These equations apply to every point in the flow field and thus enable us to solve for all details of the flow everywhere in the *flow domain*. Unfortunately, most differential equations encountered in fluid mechanics are very difficult to solve and often require the aid of a computer. Also, these equations must be combined when necessary with additional equations, such as an equation of state and an equation for energy and/or species transport. We provide a step-by-step procedure for solving this set of differential equations of fluid motion and obtain analytical solutions for several simple examples. We also introduce the concept of the *stream function*; curves of constant stream function turn out to be *streamlines* in two-dimensional flow fields.



OBJECTIVES

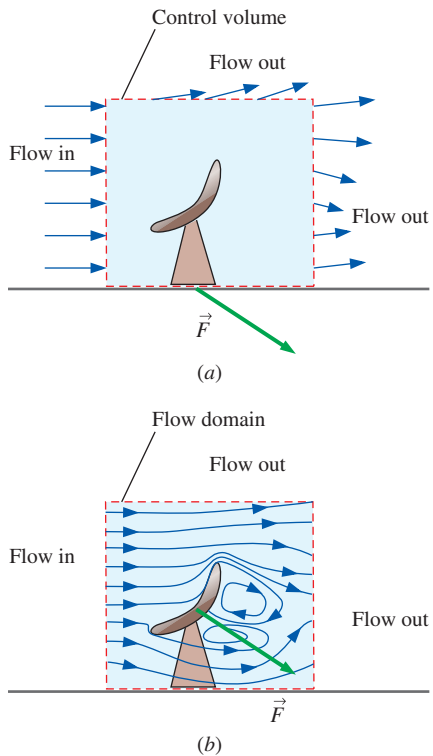
When you finish reading this chapter, you should be able to

- Understand how the differential equation of conservation of mass and the differential linear momentum equation are derived and applied
- Calculate the stream function and pressure field, and plot streamlines for a known velocity field
- Obtain analytical solutions of the equations of motion for simple flow fields

The fundamental differential equations of fluid motion are derived in this chapter, and we show how to solve them analytically for some simple flows. More complicated flows, such as the air flow induced by a tornado shown here, cannot be solved exactly although they can often be solved *approximately* with reasonable accuracy.

© Corbis RF



**FIGURE 9-1**

(a) In control volume analysis, the interior of the control volume is treated like a black box, but (b) in differential analysis, *all* the details of the flow are solved at *every* point within the flow domain.

9-1 • INTRODUCTION

In Chap. 5, we derived control volume versions of the laws of conservation of mass and energy, and in Chap. 6 we did the same for momentum. The control volume technique is useful when we are interested in the overall features of a flow, such as mass flow rate into and out of the control volume or net forces applied to bodies. An example is sketched in Fig. 9-1a for the case of wind flowing around a satellite dish. A rectangular control volume is taken around the vicinity of the satellite dish, as sketched. If we know the air velocity along the entire control surface, we can calculate the net reaction force on the stand without ever knowing any details about the geometry of the satellite dish. The interior of the control volume is in fact treated like a “black box” in control volume analysis—we *cannot* obtain detailed knowledge about flow properties such as velocity or pressure at points *inside* the control volume.

Differential analysis, on the other hand, involves application of differential equations of fluid motion to *any* and *every* point in the flow field over a region called the **flow domain**. You can think of the differential technique as the analysis of millions of tiny control volumes stacked end to end and on top of each other all throughout the flow field. In the limit as the number of tiny control volumes goes to infinity, and the size of each control volume shrinks to a point, the conservation equations simplify to a set of partial differential equations that are valid at any point in the flow. When solved, these differential equations yield details about the velocity, density, pressure, etc., at *every* point throughout the *entire* flow domain. In Fig. 9-1b, for example, differential analysis of airflow around the satellite dish yields streamline shapes, a detailed pressure distribution around the dish, etc. From these details, we can integrate to find gross features of the flow such as the net force on the satellite dish.

In a fluid flow problem such as the one illustrated in Fig. 9-1 in which air density and temperature changes are insignificant, it is sufficient to solve two differential equations of motion—conservation of mass and Newton’s second law (the linear momentum equation). For three-dimensional incompressible flow, there are *four unknowns* (velocity components u , v , w , and pressure P) and *four equations* (one from conservation of mass, which is a scalar equation, and three from Newton’s second law, which is a vector equation). As we shall see, the equations are **coupled**, meaning that some of the variables appear in all four equations; the set of differential equations must therefore be solved simultaneously for all four unknowns. In addition, **boundary conditions** for the variables must be specified at *all boundaries of the flow domain*, including inlets, outlets, and walls. Finally, if the flow is unsteady, we must march our solution along in time as the flow field changes. You can see how differential analysis of fluid flow can become quite complicated and difficult. Computers are a tremendous help here, as discussed in Chap. 15. Nevertheless, there is much we can do analytically, and we start by deriving the differential equation for conservation of mass.

9-2 • CONSERVATION OF MASS—THE CONTINUITY EQUATION

Through application of the Reynolds transport theorem (Chap. 4), we have the following general expression for conservation of mass as applied to a control volume:

Conservation of mass for a CV:

$$0 = \int_{CV} \frac{\partial \rho}{\partial t} dV + \int_{CS} \rho \vec{V} \cdot \vec{n} dA \quad (9-1)$$

Recall that Eq. 9–1 is valid for both fixed and moving control volumes, provided that the velocity vector is the *absolute* velocity (as seen by a fixed observer). When there are well-defined inlets and outlets, Eq. 9–1 is rewritten as

$$\int_{CV} \frac{\partial \rho}{\partial t} dV = \sum_{in} \dot{m} - \sum_{out} \dot{m} \quad (9-2)$$

In words, the net rate of change of mass within the control volume is equal to the rate at which mass flows into the control volume minus the rate at which mass flows out of the control volume. Equation 9–2 applies to *any* control volume, regardless of its size. To generate a differential equation for conservation of mass, we imagine the control volume shrinking to infinitesimal size, with dimensions dx , dy , and dz (Fig. 9–2). In the limit, the entire control volume shrinks to a *point* in the flow.

Derivation Using the Divergence Theorem

The quickest and most straightforward way to derive the differential form of conservation of mass is to apply the **divergence theorem** to Eq. 9–1. The divergence theorem is also called **Gauss's theorem**, named after the German mathematician Johann Carl Friedrich Gauss (1777–1855). The divergence theorem allows us to transform a volume integral of the divergence of a vector into an area integral over the surface that defines the volume. For any vector \vec{G} , the **divergence** of \vec{G} is defined as $\vec{\nabla} \cdot \vec{G}$, and the divergence theorem is written as

Divergence theorem: $\int_V \vec{\nabla} \cdot \vec{G} dV = \oint_A \vec{G} \cdot \vec{n} dA \quad (9-3)$

The circle on the area integral is used to emphasize that the integral must be evaluated around the *entire closed area A* that surrounds volume V . Note that the control surface of Eq. 9–1 is a closed area, even though we do not always add the circle to the integral symbol. Equation 9–3 applies to *any* volume, so we choose the control volume of Eq. 9–1. We also let $\vec{G} = \rho \vec{V}$ since \vec{G} can be any vector. Substitution of Eq. 9–3 into Eq. 9–1 converts the area integral into a volume integral,

$$0 = \int_{CV} \frac{\partial \rho}{\partial t} dV + \int_{CV} \vec{\nabla} \cdot (\rho \vec{V}) dV$$

We now combine the two volume integrals into one,

$$\int_{CV} \left[\frac{\partial \rho}{\partial t} + \vec{\nabla} \cdot (\rho \vec{V}) \right] dV = 0 \quad (9-4)$$

Finally, we argue that Eq. 9–4 must hold for *any* control volume regardless of its size or shape. This is possible only if the integrand (the terms within

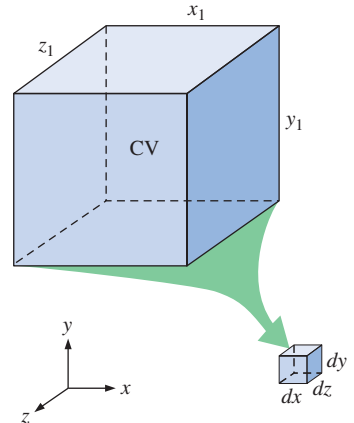


FIGURE 9-2

To derive a differential conservation equation, we imagine shrinking a control volume to infinitesimal size.

square brackets) is identically zero. Hence, we have a general differential equation for conservation of mass, better known as the **continuity equation**:

$$\text{Continuity equation: } \frac{\partial \rho}{\partial t} + \vec{\nabla} \cdot (\rho \vec{V}) = 0 \quad (9-5)$$

Equation 9–5 is the compressible form of the continuity equation since we have not assumed incompressible flow. It is valid at any point in the flow domain.

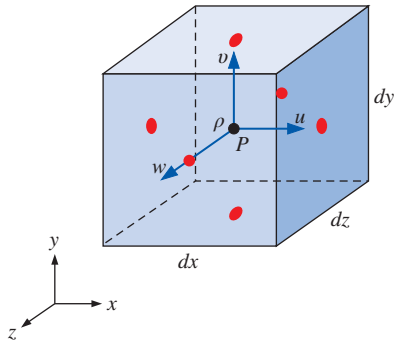


FIGURE 9–3

A small box-shaped control volume centered at point P is used for derivation of the differential equation for conservation of mass in Cartesian coordinates; the red dots indicate the center of each face.

Derivation Using an Infinitesimal Control Volume

We derive the continuity equation in a different way, by starting with a control volume on which we apply conservation of mass. Consider an infinitesimal box-shaped control volume aligned with the axes in Cartesian coordinates (Fig. 9–3). The dimensions of the box are dx , dy , and dz , and the center of the box is shown at some arbitrary point P from the origin (the box can be located anywhere in the flow field). At the center of the box we define the density as ρ and the velocity components as u , v , and w , as shown. At locations away from the center of the box, we use a **Taylor series expansion** about the center of the box (point P). [The series expansion is named in honor of its creator, the English mathematician Brook Taylor (1685–1731).] For example, the center of the right-most face of the box is located a distance $dx/2$ from the middle of the box in the x -direction; the value of ρu at that point is

$$(\rho u)_{\text{center of right face}} = \rho u + \frac{\partial(\rho u)}{\partial x} \frac{dx}{2} + \frac{1}{2!} \frac{\partial^2(\rho u)}{\partial x^2} \left(\frac{dx}{2} \right)^2 + \dots \quad (9-6)$$

As the box representing the control volume shrinks to a point, however, second-order and higher terms become negligible. For example, suppose $dx/L = 10^{-3}$, where L is some characteristic length scale of the flow domain. Then $(dx/L)^2 = 10^{-6}$, a factor of a thousand less than dx/L . In fact, the smaller dx , the better the assumption that second-order terms are negligible. Applying this truncated Taylor series expansion to the density times the normal velocity component at the center point of each of the six faces of the box, we have

$$\text{Center of right face: } (\rho u)_{\text{center of right face}} \cong \rho u + \frac{\partial(\rho u)}{\partial x} \frac{dx}{2}$$

$$\text{Center of left face: } (\rho u)_{\text{center of left face}} \cong \rho u - \frac{\partial(\rho u)}{\partial x} \frac{dx}{2}$$

$$\text{Center of front face: } (\rho w)_{\text{center of front face}} \cong \rho w + \frac{\partial(\rho w)}{\partial z} \frac{dz}{2}$$

$$\text{Center of rear face: } (\rho w)_{\text{center of rear face}} \cong \rho w - \frac{\partial(\rho w)}{\partial z} \frac{dz}{2}$$

$$\text{Center of top face: } (\rho v)_{\text{center of top face}} \cong \rho v + \frac{\partial(\rho v)}{\partial y} \frac{dy}{2}$$

$$\text{Center of bottom face: } (\rho v)_{\text{center of bottom face}} \cong \rho v - \frac{\partial(\rho v)}{\partial y} \frac{dy}{2}$$

The mass flow rate into or out of one of the faces is equal to the density times the normal velocity component at the center point of the face times the surface area of the face. In other words, $\dot{m} = \rho V_n A$ at each face, where V_n is the magnitude of the normal velocity through the face and A is the surface area of the face (Fig. 9–4). The mass flow rate through each face of our infinitesimal control volume is illustrated in Fig. 9–5. We could construct truncated Taylor series expansions at the center of each face for the remaining (nonnormal) velocity components as well, but this is unnecessary since these components are *tangential* to the face under consideration. For example, the value of ρv at the center of the right face can be estimated by a similar expansion, but since v is tangential to the right face of the box, it contributes nothing to the mass flow rate into or out of that face.

As the control volume shrinks to a point, the value of the volume integral on the left-hand side of Eq. 9–2 becomes

Rate of change of mass within CV:

$$\int_{CV} \frac{\partial \rho}{\partial t} dV \cong \frac{\partial \rho}{\partial t} dx dy dz \quad (9-7)$$

since the volume of the box is $dx dy dz$. We now apply the approximations of Fig. 9–5 to the right-hand side of Eq. 9–2. We add up all the mass flow rates into and out of the control volume through the faces. The left, bottom, and back faces contribute to mass *inflow*, and the first term on the right-hand side of Eq. 9–2 becomes

Net mass flow rate into CV:

$$\sum_{in} \dot{m} \cong \underbrace{\left(\rho u - \frac{\partial(\rho u)}{\partial x} \frac{dx}{2} \right) dy dz}_{\text{left face}} + \underbrace{\left(\rho v - \frac{\partial(\rho v)}{\partial y} \frac{dy}{2} \right) dx dz}_{\text{bottom face}} + \underbrace{\left(\rho w - \frac{\partial(\rho w)}{\partial z} \frac{dz}{2} \right) dx dy}_{\text{rear face}}$$

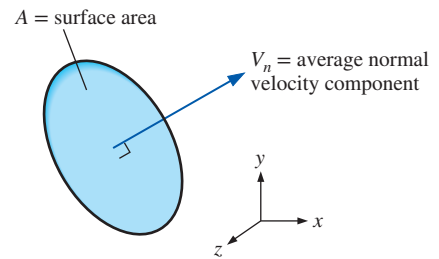


FIGURE 9-4

The mass flow rate through a surface is equal to $\rho V_n A$.

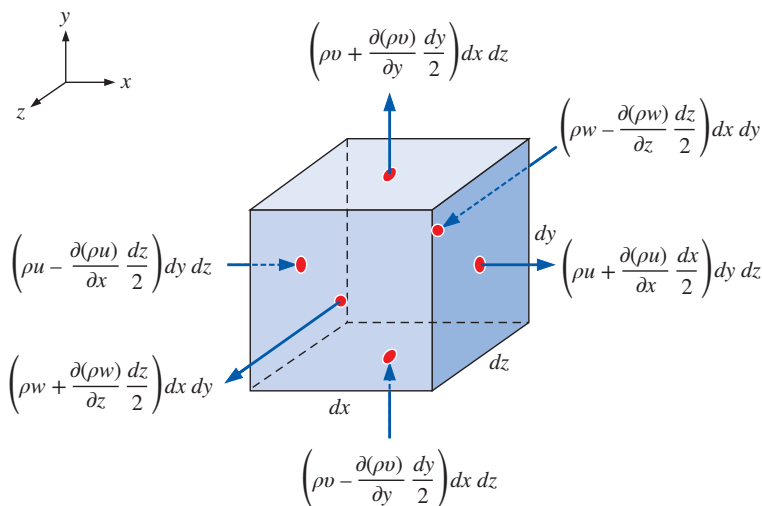
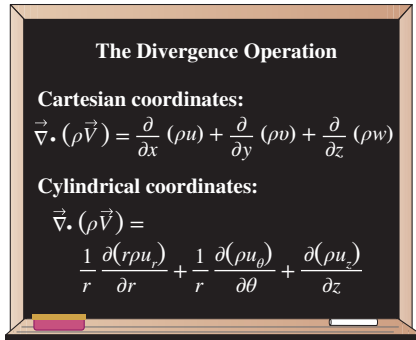


FIGURE 9-5

The inflow or outflow of mass through each face of the differential control volume; the red dots indicate the center of each face.

**FIGURE 9-6**

The divergence operation in Cartesian and cylindrical coordinates.

Similarly, the right, top, and front faces contribute to mass *outflow*, and the second term on the right-hand side of Eq. 9-2 becomes

Net mass flow rate out of CV:

$$\sum_{\text{out}} \dot{m} \cong \underbrace{\left(\rho u + \frac{\partial(\rho u)}{\partial x} \frac{dx}{2} \right) dy dz}_{\text{right face}} + \underbrace{\left(\rho v + \frac{\partial(\rho v)}{\partial y} \frac{dy}{2} \right) dx dz}_{\text{top face}} + \underbrace{\left(\rho w + \frac{\partial(\rho w)}{\partial z} \frac{dz}{2} \right) dx dy}_{\text{front face}}$$

We substitute Eq. 9-7 and these two equations for mass flow rate into Eq. 9-2. Many of the terms cancel each other out; after combining and simplifying the remaining terms, we are left with

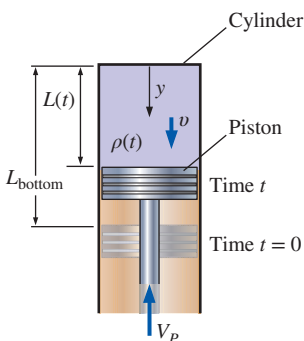
$$\frac{\partial \rho}{\partial t} dx dy dz = - \frac{\partial(\rho u)}{\partial x} dx dy dz - \frac{\partial(\rho v)}{\partial y} dx dy dz - \frac{\partial(\rho w)}{\partial z} dx dy dz$$

The volume of the box, $dx dy dz$, appears in each term and can be eliminated. After rearrangement we end up with the following differential equation for conservation of mass in Cartesian coordinates:

Continuity equation in Cartesian coordinates:

$$\frac{\partial \rho}{\partial t} + \frac{\partial(\rho u)}{\partial x} + \frac{\partial(\rho v)}{\partial y} + \frac{\partial(\rho w)}{\partial z} = 0 \quad (9-8)$$

Equation 9-8 is the compressible form of the continuity equation in Cartesian coordinates. It is written in more compact form by recognizing the divergence operation (Fig. 9-6), yielding the same equation as Eq. 9-5.

**FIGURE 9-7**

Fuel and air being compressed by a piston in a cylinder of an internal combustion engine.

EXAMPLE 9-1 Compression of an Air–Fuel Mixture

An air–fuel mixture is compressed by a piston in a cylinder of an internal combustion engine (Fig. 9-7). The origin of coordinate y is at the top of the cylinder, and y points straight down as shown. The piston is assumed to move up at constant speed V_p . The distance L between the top of the cylinder and the piston decreases with time according to the linear approximation $L = L_{\text{bottom}} - V_p t$, where L_{bottom} is the location of the piston when it is at the bottom of its cycle at time $t = 0$, as sketched in Fig. 9-7. At $t = 0$, the density of the air–fuel mixture in the cylinder is everywhere equal to $\rho(0)$. Estimate the density of the air–fuel mixture as a function of time and the given parameters during the piston's up stroke.

SOLUTION The density of the air–fuel mixture is to be estimated as a function of time and the given parameters in the problem statement.

Assumptions 1 Density varies with time, but not space; in other words, the density is uniform throughout the cylinder at any given time, but changes with time: $\rho = \rho(t)$. 2 Velocity component v varies with y and t , but not with x or z ; in other words $v = v(y, t)$ only. 3 $u = w = 0$. 4 No mass escapes from the cylinder during the compression.

Analysis First we need to establish an expression for velocity component v as a function of y and t . Clearly $v = 0$ at $y = 0$ (the top of the cylinder), and $v = -V_p$ at $y = L$. For simplicity, we approximate that v varies linearly between these two boundary conditions,

$$\text{Vertical velocity component: } v = -V_p \frac{y}{L} \quad (1)$$

where L is a function of time, as given. The compressible continuity equation in Cartesian coordinates (Eq. 9–8) is appropriate for solution of this problem.

$$\frac{\partial \rho}{\partial t} + \underbrace{\frac{\partial(\rho u)}{\partial x}}_{0 \text{ since } u=0} + \frac{\partial(\rho v)}{\partial y} + \underbrace{\frac{\partial(\rho w)}{\partial z}}_{0 \text{ since } w=0} = 0 \quad \rightarrow \quad \frac{\partial \rho}{\partial t} + \frac{\partial(\rho v)}{\partial y} = 0$$

By assumption 1, however, density is not a function of y and can therefore come out of the y -derivative. Substituting Eq. 1 for v and the given expression for L , differentiating, and simplifying, we obtain

$$\frac{\partial \rho}{\partial t} = -\rho \frac{\partial v}{\partial y} = -\rho \frac{\partial}{\partial y} \left(-V_P \frac{y}{L} \right) = \rho \frac{V_P}{L} = \rho \frac{V_P}{L_{\text{bottom}} - V_P t} \quad (2)$$

By assumption 1 again, we replace $\partial \rho / \partial t$ by $d\rho / dt$ in Eq. 2. After separating variables we obtain an expression that can be integrated analytically,

$$\int_{\rho=\rho(0)}^{\rho} \frac{d\rho}{\rho} = \int_{t=0}^t \frac{V_P}{L_{\text{bottom}} - V_P t} dt \quad \rightarrow \quad \ln \frac{\rho}{\rho(0)} = \ln \frac{L_{\text{bottom}}}{L_{\text{bottom}} - V_P t} \quad (3)$$

Finally then, we have the desired expression for ρ as a function of time,

$$\rho = \rho(0) \frac{L_{\text{bottom}}}{L_{\text{bottom}} - V_P t} \quad (4)$$

In keeping with the convention of nondimensionalizing results, Eq. 4 is rewritten as

$$\frac{\rho}{\rho(0)} = \frac{1}{1 - V_P t / L_{\text{bottom}}} \quad \rightarrow \quad \rho^* = \frac{1}{1 - t^*} \quad (5)$$

where $\rho^* = \rho / \rho(0)$ and $t^* = V_P t / L_{\text{bottom}}$. Equation 5 is plotted in Fig. 9–8.

Discussion At $t^* = 1$, the piston hits the top of the cylinder and ρ goes to infinity. In an actual internal combustion engine, the piston stops before reaching the top of the cylinder, forming what is called the *clearance volume*, which typically constitutes 4 to 12 percent of the maximum cylinder volume. The assumption of uniform density within the cylinder is the weakest link in this simplified analysis. In reality, ρ may be a function of both space and time.

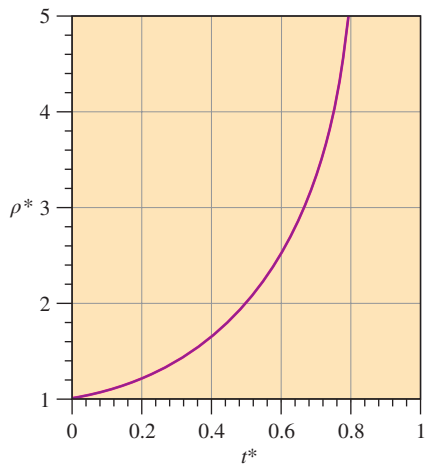


FIGURE 9–8

Nondimensional density as a function of nondimensional time for Example 9–1.

Alternative Form of the Continuity Equation

We expand Eq. 9–5 by using the product rule on the divergence term,

$$\frac{\partial \rho}{\partial t} + \vec{\nabla} \cdot (\rho \vec{V}) = \underbrace{\frac{\partial \rho}{\partial t}}_{\text{Material derivative of } \rho} + \vec{V} \cdot \vec{\nabla} \rho + \rho \vec{\nabla} \cdot \vec{V} = 0 \quad (9-9)$$

Recognizing the *material derivative* in Eq. 9–9 (see Chap. 4), and dividing by ρ , we write the compressible continuity equation in an alternative form,

Alternative form of the continuity equation:

$$\frac{1}{\rho} \frac{D\rho}{Dt} + \vec{\nabla} \cdot \vec{V} = 0 \quad (9-10)$$

Equation 9–10 shows that as we follow a fluid element through the flow field (we call this a **material element**), its density changes as $\vec{\nabla} \cdot \vec{V}$ changes (Fig. 9–9).

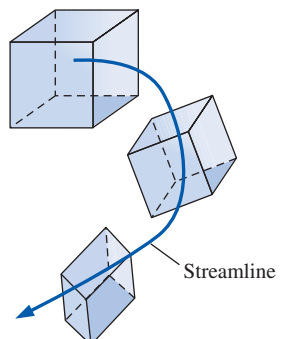


FIGURE 9–9

As a material element moves through a flow field, its density changes according to Eq. 9–10.

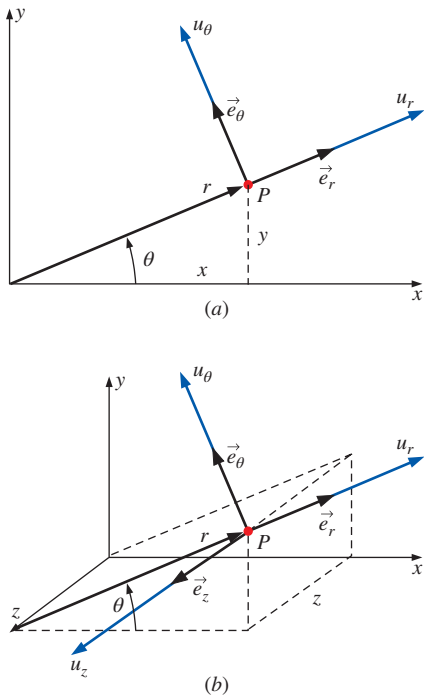


FIGURE 9-10

Velocity components and unit vectors in cylindrical coordinates: (a) two-dimensional flow in the xy - or $r\theta$ -plane, (b) three-dimensional flow.

On the other hand, if changes in the density of the material element are negligibly small compared to the magnitude of the density itself as the element moves around, then both terms in Eq. 9-10 are negligibly small; $\vec{\nabla} \cdot \vec{V} \cong 0$ and $\rho^{-1} D\rho/Dt \cong 0$, and the flow is approximated as **incompressible**.

Continuity Equation in Cylindrical Coordinates

Many problems in fluid mechanics are more conveniently solved in **cylindrical coordinates** (r, θ, z) (often called **cylindrical polar coordinates**), rather than in Cartesian coordinates. For simplicity, we introduce cylindrical coordinates in two dimensions first (Fig. 9-10a). By convention, r is the radial distance from the origin to some point (P), and θ is the angle measured from the x -axis (θ is always defined as mathematically positive in the counterclockwise direction). Velocity components, u_r and u_θ , and unit vectors, \vec{e}_r and \vec{e}_θ , are also shown in Fig. 9-10a. In three dimensions, imagine sliding everything in Fig. 9-10a out of the page along the z -axis (normal to the xy -plane) by some distance z . We have attempted to draw this in Fig. 9-10b. In three dimensions, we have a third velocity component, u_z , and a third unit vector, \vec{e}_z , also sketched in Fig. 9-10b.

The following coordinate transformations are obtained from Fig. 9-10:

Coordinate transformations:

$$r = \sqrt{x^2 + y^2} \quad x = r \cos \theta \quad y = r \sin \theta \quad \theta = \tan^{-1} \frac{y}{x} \quad (9-11)$$

Coordinate z is the same in cylindrical and Cartesian coordinates.

To obtain an expression for the continuity equation in cylindrical coordinates, we have two choices. First, we can use Eq. 9-5 directly, since it was derived without regard to our choice of coordinate system. We simply look up the expression for the divergence operator in cylindrical coordinates in a vector calculus book (e.g., Spiegel, 1968; see also Fig. 9-6). Second, we can draw a three-dimensional infinitesimal fluid element in cylindrical coordinates and analyze mass flow rates into and out of the element, similar to what we did before in Cartesian coordinates. Either way, we end up with

Continuity equation in cylindrical coordinates:

$$\frac{\partial \rho}{\partial t} + \frac{1}{r} \frac{\partial(r\rho u_r)}{\partial r} + \frac{1}{r} \frac{\partial(\rho u_\theta)}{\partial \theta} + \frac{\partial(\rho u_z)}{\partial z} = 0 \quad (9-12)$$

Details of the second method can be found in Fox and McDonald (1998).

Special Cases of the Continuity Equation

We now look at two special cases, or simplifications, of the continuity equation. In particular, we first consider steady compressible flow, and then incompressible flow.

Special Case 1: Steady Compressible Flow

If the flow is compressible but steady, $\partial/\partial t$ of any variable is equal to zero. Thus, Eq. 9-5 reduces to

Steady continuity equation:

$$\vec{\nabla} \cdot (\rho \vec{V}) = 0 \quad (9-13)$$

In Cartesian coordinates, Eq. 9–13 reduces to

$$\frac{\partial(\rho u)}{\partial x} + \frac{\partial(\rho v)}{\partial y} + \frac{\partial(\rho w)}{\partial z} = 0 \quad (9-14)$$

In cylindrical coordinates, Eq. 9–13 reduces to

$$\frac{1}{r} \frac{\partial(r \rho u_r)}{\partial r} + \frac{1}{r} \frac{\partial(\rho u_\theta)}{\partial \theta} + \frac{\partial(\rho u_z)}{\partial z} = 0 \quad (9-15)$$

Special Case 2: Incompressible Flow

If the flow is approximated as incompressible, density is not a function of time or space. Thus the unsteady term in Eq. 9–5 disappears and ρ can be taken outside of the divergence operator. Equation 9–5 therefore reduces to

Incompressible continuity equation:

$$\vec{\nabla} \cdot \vec{V} = 0 \quad (9-16)$$

The same result is obtained if we start with Eq. 9–10 and recognize that for an incompressible flow, density does not change appreciably following a fluid particle, as pointed out previously. Thus the material derivative of ρ is approximately zero, and Eq. 9–10 reduces immediately to Eq. 9–16.

You may have noticed that *no time derivatives remain in Eq. 9–16*. We conclude from this that *even if the flow is unsteady, Eq. 9–16 applies at any instant in time*. Physically, this means that as the velocity field changes in one part of an incompressible flow field, the entire rest of the flow field immediately adjusts to the change such that Eq. 9–16 is satisfied at all times. For compressible flow this is not the case. In fact, a disturbance in one part of the flow is not even felt by fluid particles some distance away until the sound wave from the disturbance reaches that distance. Very loud noises, such as that from a gun or explosion, generate a **shock wave** that actually travels *faster* than the speed of sound. (The shock wave produced by an explosion is illustrated in Fig. 9–11.) Shock waves and other manifestations of compressible flow are discussed in Chap. 12.

In Cartesian coordinates, Eq. 9–16 is

Incompressible continuity equation in Cartesian coordinates:

$$\frac{\partial u}{\partial x} + \frac{\partial v}{\partial y} + \frac{\partial w}{\partial z} = 0 \quad (9-17)$$

Equation 9–17 is the form of the continuity equation you will probably encounter most often. It applies to steady or unsteady, incompressible, three-dimensional flow, and you would do well to memorize it.

In cylindrical coordinates, Eq. 9–16 is

Incompressible continuity equation in cylindrical coordinates:

$$\frac{1}{r} \frac{\partial(r u_r)}{\partial r} + \frac{1}{r} \frac{\partial(u_\theta)}{\partial \theta} + \frac{\partial(u_z)}{\partial z} = 0 \quad (9-18)$$

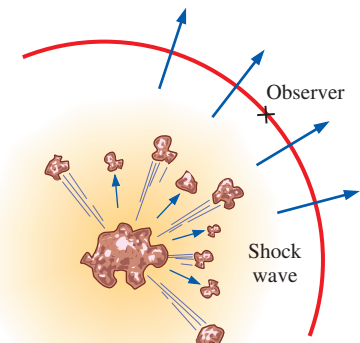


FIGURE 9–11

The disturbance from an explosion is not felt until the shock wave reaches the observer.

EXAMPLE 9–2 Design of a Compressible Converging Duct

- A two-dimensional converging duct is being designed for a high-speed wind tunnel. The bottom wall of the duct is to be flat and horizontal, and the top wall is to be curved in such a way that the axial wind speed u increases approximately linearly from $u_1 = 100$ m/s at section (1) to $u_2 = 300$ m/s at section

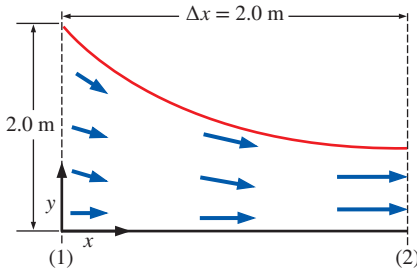


FIGURE 9-12

Converging duct, designed for a high-speed wind tunnel (not to scale).

(2) (Fig. 9-12). Meanwhile, the air density ρ is to decrease approximately linearly from $\rho_1 = 1.2 \text{ kg/m}^3$ at section (1) to $\rho_2 = 0.85 \text{ kg/m}^3$ at section (2). The converging duct is 2.0 m long and is 2.0 m high at section (1). (a) Predict the y -component of velocity, $v(x, y)$, in the duct. (b) Plot the approximate shape of the duct, ignoring friction on the walls. (c) How high should the duct be at section (2), the exit of the duct?

SOLUTION For given velocity component u and density ρ , we are to predict velocity component v , plot an approximate shape of the duct, and predict its height at the duct exit.

Assumptions 1 The flow is steady and two-dimensional in the xy -plane. 2 Friction on the walls is ignored. 3 Axial velocity u increases linearly with x , and density ρ decreases linearly with x .

Properties The fluid is air at room temperature (25°C). The speed of sound is about 346 m/s, so the flow is subsonic, but compressible.

Analysis (a) We write expressions for u and ρ , forcing them to be linear in x ,

$$u = u_1 + C_u x \quad \text{where} \quad C_u = \frac{u_2 - u_1}{\Delta x} = \frac{(300 - 100) \text{ m/s}}{2.0 \text{ m}} = 100 \text{ s}^{-1} \quad (1)$$

and

$$\rho = \rho_1 + C_\rho x \quad \text{where} \quad C_\rho = \frac{\rho_2 - \rho_1}{\Delta x} = \frac{(0.85 - 1.2) \text{ kg/m}^3}{2.0 \text{ m}} \\ = -0.175 \text{ kg/m}^4 \quad (2)$$

The steady continuity equation (Eq. 9-14) for this two-dimensional compressible flow simplifies to

$$\frac{\partial(\rho u)}{\partial x} + \frac{\partial(\rho v)}{\partial y} + \underbrace{\frac{\partial(\rho w)}{\partial z}}_{0 \text{ (2-D)}} = 0 \quad \rightarrow \quad \frac{\partial(\rho v)}{\partial y} = -\frac{\partial(\rho u)}{\partial x} \quad (3)$$

Substituting Eqs. 1 and 2 into Eq. 3 and noting that C_u and C_ρ are constants,

$$\frac{\partial(\rho v)}{\partial y} = -\frac{\partial[(\rho_1 + C_\rho x)(u_1 + C_u x)]}{\partial x} = -(\rho_1 C_u + u_1 C_\rho) - 2C_u C_\rho x$$

Integration with respect to y gives

$$\rho v = -(\rho_1 C_u + u_1 C_\rho)y - 2C_u C_\rho xy + f(x) \quad (4)$$

Note that since the integration is a *partial* integration, we have added an arbitrary function of x instead of simply a constant of integration. Next, we apply boundary conditions. We argue that since the bottom wall is flat and horizontal, v must equal zero at $y = 0$ for any x . This is possible only if $f(x) = 0$. Solving Eq. 4 for v gives

$$v = \frac{-(\rho_1 C_u + u_1 C_\rho)y - 2C_u C_\rho xy}{\rho} \quad \rightarrow \quad v = \frac{-(\rho_1 C_u + u_1 C_\rho)y - 2C_u C_\rho xy}{\rho_1 + C_\rho x} \quad (5)$$

(b) Using Eqs. 1 and 5 and the technique described in Chap. 4, we plot several streamlines between $x = 0$ and $x = 2.0 \text{ m}$ in Fig. 9-13. The streamline starting at $x = 0, y = 2.0 \text{ m}$ approximates the top wall of the duct.

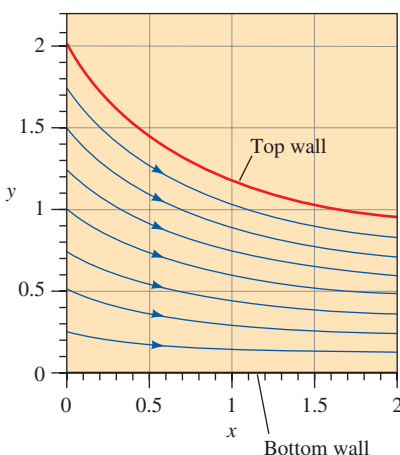


FIGURE 9-13

Streamlines for the converging duct of Example 9-2.

(c) At section (2), the top streamline crosses $y = 0.941$ m at $x = 2.0$ m. Thus, the predicted height of the duct at section (2) is **0.941 m**.

Discussion You can verify that the combination of Eqs. 1, 2, and 5 satisfies the continuity equation. However, this alone does not guarantee that the density and velocity components will actually *follow* these equations if the duct were to be built as designed here. The actual flow depends on the *pressure drop* between sections (1) and (2); only one unique pressure drop can yield the desired flow acceleration. Temperature may also change considerably in this kind of compressible flow in which the air accelerates toward sonic speeds.

EXAMPLE 9–3 Incompressibility of an Unsteady Two-Dimensional Flow

- Consider the velocity field of Example 4–5—an unsteady, two-dimensional velocity field given by $\vec{V} = (u, v) = (0.5 + 0.8x)\vec{i} + [1.5 + 2.5 \sin(\omega t) - 0.8y]\vec{j}$, where angular frequency ω is equal to 2π rad/s (a physical frequency of 1 Hz). Verify that this flow field can be approximated as incompressible.

SOLUTION We are to verify that a given velocity field is incompressible.

Assumptions 1 The flow is two-dimensional, implying no z -component of velocity and no variation of u or v with z .

Analysis The components of velocity in the x - and y -directions, respectively, are

$$u = 0.5 + 0.8x \quad \text{and} \quad v = 1.5 + 2.5 \sin(\omega t) - 0.8y$$

If the flow is incompressible, Eq. 9–16 must apply. More specifically, in Cartesian coordinates Eq. 9–17 must apply. Let's check:

$$\underbrace{\frac{\partial u}{\partial x}}_{0.8} + \underbrace{\frac{\partial v}{\partial y}}_{-0.8} + \underbrace{\frac{\partial v}{\partial z}}_{0 \text{ since 2-D}} = 0 \quad \rightarrow \quad 0.8 - 0.8 = 0$$

So we see that the incompressible continuity equation is indeed satisfied at any instant in time, and **this flow field may be approximated as incompressible**.

Discussion Although there is an unsteady term in v , it has no y -derivative and drops out of the continuity equation.

EXAMPLE 9–4 Finding a Missing Velocity Component

- The u velocity component of a steady, two-dimensional, incompressible flow field is $u = ax + by$, where a and b are constants. Velocity component v is missing (Fig. 9–14). Generate an expression for v as a function of x and y .

SOLUTION We are to find the y component of velocity v , using a given expression for u .

Assumptions 1 The flow is steady. 2 The flow is incompressible. 3 The flow is two-dimensional in the xy -plane, implying that $w = 0$ and neither u nor v depends on z .

Analysis We plug the velocity components into the steady incompressible continuity equation,

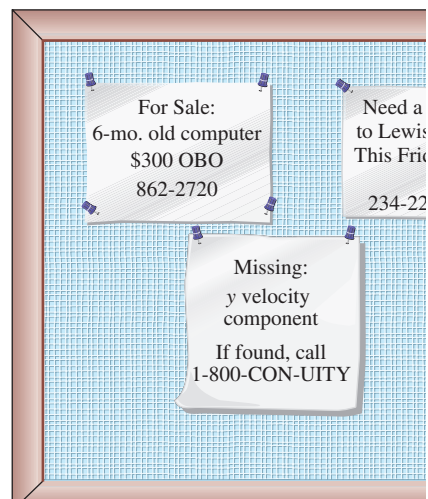


FIGURE 9–14
The continuity equation can be used to find a missing velocity component.

Condition for incompressibility:

$$\frac{\partial v}{\partial y} = -\underbrace{\frac{\partial u}{\partial x}}_a - \underbrace{\frac{\partial w}{\partial z}}_0 \rightarrow \frac{\partial v}{\partial y} = -a$$

Next we integrate with respect to y . Note that since the integration is a *partial* integration, we must add some arbitrary function of x instead of simply a constant of integration.

Solution:

$$v = -ay + f(x)$$

If the flow were three-dimensional, we would add a function of x and z instead.

Discussion To satisfy the incompressible continuity equation, any function of x will work since there are no derivatives of v with respect to x in the continuity equation. Not all functions of x are necessarily physically possible, however, since the flow may not be able to satisfy the steady conservation of momentum equation.

EXAMPLE 9–5 Two-Dimensional, Incompressible, Vortical Flow

Consider a two-dimensional, incompressible flow in cylindrical coordinates; the tangential velocity component is $u_\theta = K/r$, where K is a constant. This represents a class of vortical flows. Generate an expression for the other velocity component, u_r .

SOLUTION For a given tangential velocity component, we are to generate an expression for the radial velocity component.

Assumptions 1 The flow is two-dimensional in the xy - ($r\theta$ -) plane (velocity is not a function of z , and $u_z = 0$ everywhere). 2 The flow is incompressible.

Analysis The incompressible continuity equation (Eq. 9–18) for this two-dimensional case simplifies to

$$\frac{1}{r} \frac{\partial(ru_r)}{\partial r} + \frac{1}{r} \frac{\partial u_\theta}{\partial \theta} + \underbrace{\frac{\partial u_z}{\partial z}}_{0 \text{ (2-D)}} = 0 \rightarrow \frac{\partial(ru_r)}{\partial r} = -\frac{\partial u_\theta}{\partial \theta} \quad (1)$$

The given expression for u_θ is not a function of θ , and therefore Eq. 1 reduces to

$$\frac{\partial(ru_r)}{\partial r} = 0 \rightarrow ru_r = f(\theta, t) \quad (2)$$

where we have introduced an arbitrary function of θ and t instead of a constant of integration, since we performed a *partial* integration with respect to r .

Solving for u_r ,

$$u_r = \frac{f(\theta, t)}{r} \quad (3)$$

Thus, any radial velocity component of the form given by Eq. 3 yields a two-dimensional, incompressible velocity field that satisfies the continuity equation.

We discuss some specific cases. The simplest case is when $f(\theta, t) = 0$ ($u_r = 0$, $u_\theta = K/r$). This yields the **line vortex** discussed in Chap. 4, as sketched in Fig. 9–15a. Another simple case is when $f(\theta, t) = C$, where C is a constant. This yields a radial velocity whose magnitude decays as $1/r$. For negative C , imagine a spiraling line vortex/sink flow, in which fluid elements not only revolve around the origin, but get sucked into a sink at the origin (actually a line sink along the z -axis). This is illustrated in Fig. 9–15b.

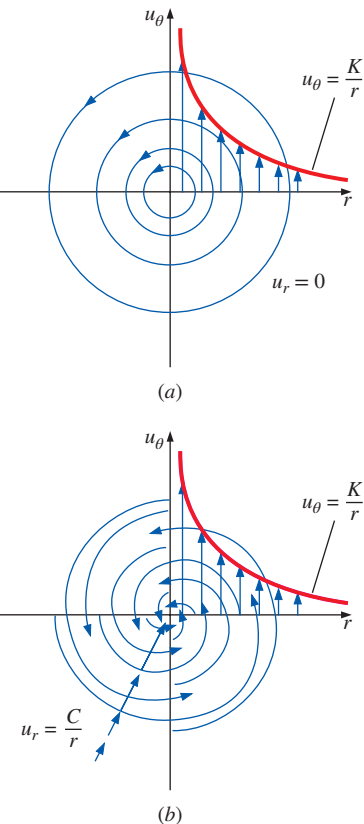


FIGURE 9–15

Streamlines and velocity profiles for (a) a line vortex flow and (b) a spiraling line vortex/sink flow.

Discussion Other more complicated flows can be obtained by setting $f(\theta, t)$ to some other function. For any function $f(\theta, t)$, the flow satisfies the two-dimensional, incompressible continuity equation at a given instant in time.

EXAMPLE 9–6 Comparison of Continuity and Volumetric Strain Rate

Recall the *volumetric strain rate*, defined in Chap. 4. In Cartesian coordinates,

$$\frac{1}{V} \frac{DV}{Dt} = \epsilon_{xx} + \epsilon_{yy} + \epsilon_{zz} = \frac{\partial u}{\partial x} + \frac{\partial v}{\partial y} + \frac{\partial w}{\partial z} \quad (1)$$

Show that volumetric strain rate is zero for incompressible flow. Discuss the physical interpretation of volumetric strain rate for incompressible and compressible flows.

SOLUTION We are to show that volumetric strain rate is zero in an incompressible flow, and discuss its physical significance in incompressible and compressible flow.

Analysis If the flow is incompressible, Eq. 9–16 applies. More specifically, Eq. 9–17, in Cartesian coordinates, applies. Comparing Eq. 9–17 to Eq. 1,

$$\frac{1}{V} \frac{DV}{Dt} = 0 \quad \text{for incompressible flow}$$

Thus, *volumetric strain rate is zero in an incompressible flow field*. In fact, you can *define* incompressibility by $DV/Dt = 0$. Physically, as we follow a fluid element, parts of it may stretch while other parts shrink, and the element may translate, distort, and rotate, but its volume remains constant along its entire path through the flow field (Fig. 9–16a). This is true whether the flow is steady or unsteady, as long as it is incompressible. If the flow were compressible, the volumetric strain rate would not be zero, implying that fluid elements may expand in volume (dilate) or shrink in volume as they move around in the flow field (Fig. 9–16b). Specifically, consider Eq. 9–10, an alternative form of the continuity equation for compressible flow. By definition, $\rho = m/V$, where m is the mass of a fluid element. For a material element (following the fluid element as it moves through the flow field), m must be constant. Applying some algebra to Eq. 9–10 yields

$$\frac{1}{\rho} \frac{D\rho}{Dt} = \frac{V}{m} \frac{D(m/V)}{Dt} = -\frac{V}{m} \frac{m}{V^2} \frac{DV}{Dt} = -\frac{1}{V} \frac{DV}{Dt} = -\vec{\nabla} \cdot \vec{V} \rightarrow \frac{1}{V} \frac{DV}{Dt} = \vec{\nabla} \cdot \vec{V}$$

Discussion The final result is general—not limited to Cartesian coordinates. It applies to unsteady as well as steady flows.

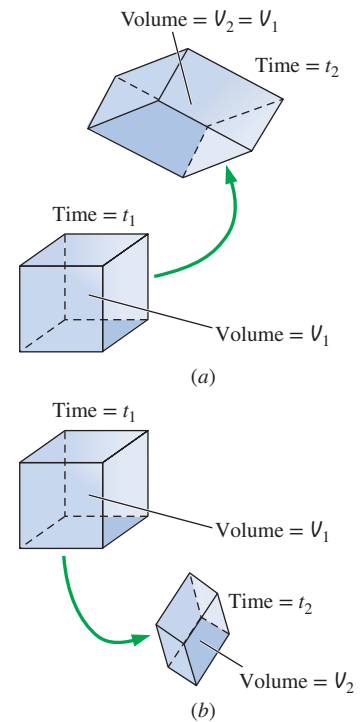


FIGURE 9–16

(a) In an incompressible flow field, fluid elements may translate, distort, and rotate, but they do not grow or shrink in volume; (b) in a compressible flow field, fluid elements may grow or shrink in volume as they translate, distort, and rotate.

EXAMPLE 9–7 Conditions for Incompressible Flow

Consider a steady velocity field given by $\vec{V} = (u, v, w) = a(x^2y + y^2)\vec{i} + bxy^2\vec{j} + cx\vec{k}$, where a , b , and c are constants. Under what conditions is this flow field incompressible?

SOLUTION We are to determine a relationship between constants a , b , and c that ensures incompressibility.

Assumptions 1 The flow is steady. 2 The flow is incompressible (under certain constraints to be determined).

Analysis We apply Eq. 9–17 to the given velocity field,

$$\underbrace{\frac{\partial u}{\partial x}}_{2axy} + \underbrace{\frac{\partial v}{\partial y}}_{2bxy} + \underbrace{\frac{\partial w}{\partial z}}_0 = 0 \quad \rightarrow \quad 2axy + 2bxy = 0$$

Thus to guarantee incompressibility, constants a and b must be equal in magnitude but opposite in sign.

Condition for incompressibility:

$$a = -b$$

Discussion If a were not equal to $-b$, this might still be a valid flow field, but density would have to vary with location in the flow field. In other words, the flow would be *compressible*, and Eq. 9–14 would need to be satisfied in place of Eq. 9–17.

9–3 ■ THE STREAM FUNCTION

The Stream Function in Cartesian Coordinates

Consider the simple case of incompressible, two-dimensional flow in the xy -plane. The continuity equation (Eq. 9–17) in Cartesian coordinates reduces to

$$\frac{\partial u}{\partial x} + \frac{\partial v}{\partial y} = 0 \quad (9-19)$$

A clever variable transformation enables us to rewrite Eq. 9–19 in terms of *one* dependent variable (ψ) instead of *two* dependent variables (u and v). We define the **stream function** ψ as (Fig. 9–17)

Incompressible, two-dimensional stream function in Cartesian coordinates:

$$u = \frac{\partial \psi}{\partial y} \quad \text{and} \quad v = -\frac{\partial \psi}{\partial x} \quad (9-20)$$

The stream function and the corresponding velocity potential function (Chap. 10) were first introduced by the Italian mathematician Joseph Louis Lagrange (1736–1813). Substitution of Eq. 9–20 into Eq. 9–19 yields

$$\frac{\partial}{\partial x} \left(\frac{\partial \psi}{\partial y} \right) + \frac{\partial}{\partial y} \left(-\frac{\partial \psi}{\partial x} \right) = \frac{\partial^2 \psi}{\partial x \partial y} - \frac{\partial^2 \psi}{\partial y \partial x} = 0$$

which is identically satisfied for any smooth function $\psi(x, y)$, because the order of differentiation (y then x versus x then y) is irrelevant.

You may ask why we chose to put the negative sign on v rather than on u . (We could have defined the stream function with the signs reversed, and continuity would still have been identically satisfied.) The answer is that although the sign is arbitrary, the definition of Eq. 9–20 leads to flow from left to right as ψ increases in the y -direction, which is usually preferred. Most fluid mechanics books define ψ in this way, although sometimes ψ is

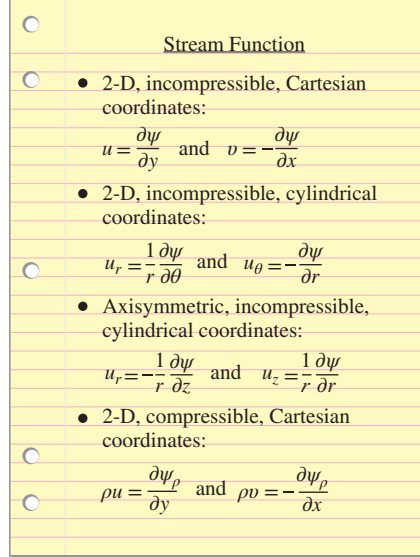


FIGURE 9–17

There are several definitions of the stream function, depending on the type of flow under consideration as well as the coordinate system being used.

defined with the opposite signs (e.g., in some British textbooks and in the indoor air quality field, Heinsohn and Cimbala, 2003).

What have we gained by this transformation? First, as already mentioned, a single variable (ψ) replaces two variables (u and v)—once ψ is known, we can generate both u and v via Eq. 9–20, and we are guaranteed that the solution satisfies continuity, Eq. 9–19. Second, it turns out that the stream function has useful physical significance (Fig. 9–18). Namely,

Curves of constant ψ are streamlines of the flow.

This is easily proven by considering a streamline in the xy -plane, as sketched in Fig. 9–19. Recall from Chap. 4 that along such a streamline,

$$\text{Along a streamline: } \frac{dy}{dx} = \frac{v}{u} \rightarrow -v \frac{dx}{dy} + u \frac{dy}{dx} = 0$$

where we have applied Eq. 9–20, the definition of ψ . Thus,

$$\text{Along a streamline: } \frac{\partial \psi}{\partial x} dx + \frac{\partial \psi}{\partial y} dy = 0 \quad (9-21)$$

But for any smooth function ψ of two variables x and y , we know by the chain rule of mathematics that the total change of ψ from point (x, y) to another point $(x + dx, y + dy)$ some infinitesimal distance away is

$$\text{Total change of } \psi: \quad d\psi = \frac{\partial \psi}{\partial x} dx + \frac{\partial \psi}{\partial y} dy \quad (9-22)$$

By comparing Eq. 9–21 to Eq. 9–22 we see that $d\psi = 0$ along a streamline; thus we have proven the statement that ψ is constant along streamlines.

EXAMPLE 9–8 Calculation of the Velocity Field from the Stream Function

- A steady, two-dimensional, incompressible flow field in the xy -plane has a stream function given by $\psi = ax^3 + by + cx$, where a , b , and c are constants: $a = 0.50 \text{ (m}\cdot\text{s)}^{-1}$, $b = -2.0 \text{ m/s}$, and $c = -1.5 \text{ m/s}$. (a) Obtain expressions for velocity components u and v . (b) Verify that the flow field satisfies the incompressible continuity equation. (c) Plot several streamlines of the flow in the upper-right quadrant.

SOLUTION For a given stream function, we are to calculate the velocity components, verify incompressibility, and plot flow streamlines.

Assumptions 1 The flow is steady. 2 The flow is incompressible (this assumption is to be verified). 3 The flow is two-dimensional in the xy -plane, implying that $w = 0$ and neither u nor v depend on z .

Analysis (a) We use Eq. 9–20 to obtain expressions for u and v by differentiating the stream function,

$$u = \frac{\partial \psi}{\partial y} = b \quad \text{and} \quad v = -\frac{\partial \psi}{\partial x} = -3ax^2 - c$$

(b) Since u is not a function of x , and v is not a function of y , we see immediately that the two-dimensional, incompressible continuity equation (Eq. 9–19) is satisfied. In fact, since ψ is smooth in x and y , the two-dimensional, incompressible

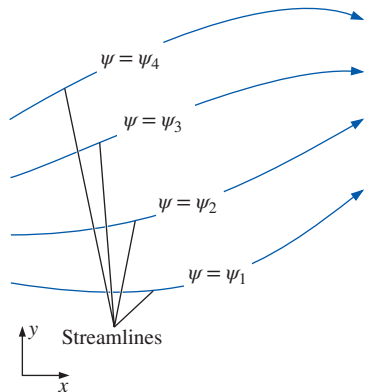


FIGURE 9–18

Curves of constant stream function represent streamlines of the flow.

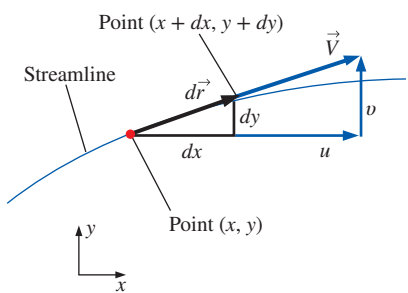


FIGURE 9–19

Arc length $d\vec{r} = (dx, dy)$ and local velocity vector $\vec{V} = (u, v)$ along a two-dimensional streamline in the xy -plane.

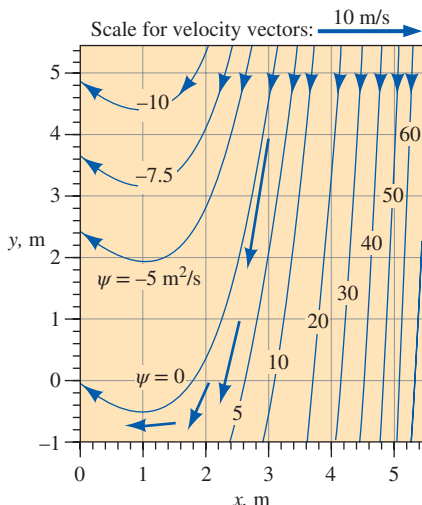


FIGURE 9-20

Streamlines for the velocity field of Example 9-8; the value of constant ψ is indicated for each streamline, and velocity vectors are shown at four locations.

continuity equation in the xy -plane is automatically satisfied by the very definition of ψ . We conclude that **the flow is indeed incompressible**.

(c) To plot streamlines, we solve the given equation for either y as a function of x and ψ , or x as a function of y and ψ . In this case, the former is easier, and we have

Equation for a streamline:

$$y = \frac{\psi - ax^3 - cx}{b}$$

This equation is plotted in Fig. 9-20 for several values of ψ , and for the provided values of a , b , and c . The flow is nearly straight down at large values of x , but veers upward for $x < 1$ m.

Discussion You can verify that $v = 0$ at $x = 1$ m. In fact, v is negative for $x > 1$ m and positive for $x < 1$ m. The direction of the flow can also be determined by picking an arbitrary point in the flow, say ($x = 3$ m, $y = 4$ m), and calculating the velocity there. We get $u = -2.0$ m/s and $v = -12.0$ m/s at this point, either of which shows that fluid flows to the lower left in this region of the flow field. For clarity, the velocity vector at this point is also plotted in Fig. 9-20; it is clearly parallel to the streamline near that point. Velocity vectors at three other locations are also plotted.

EXAMPLE 9-9 Calculation of Stream Function for a Known Velocity Field

Consider a steady, two-dimensional, incompressible velocity field with $u = ax + b$ and $v = -ay + cx$, where a , b , and c are constants: $a = 0.50 \text{ s}^{-1}$, $b = 1.5 \text{ m/s}$, and $c = 0.35 \text{ s}^{-1}$. Generate an expression for the stream function and plot some streamlines of the flow in the upper-right quadrant.

SOLUTION For a given velocity field we are to generate an expression for ψ and plot several streamlines for given values of constants a , b , and c .

Assumptions 1 The flow is steady. 2 The flow is incompressible. 3 The flow is two-dimensional in the xy -plane, implying that $w = 0$ and neither u nor v depend on z .

Analysis We start by picking one of the two parts of Eq. 9-20 that define the stream function (it doesn't matter which part we choose—the solution will be identical).

$$\frac{\partial \psi}{\partial y} = u = ax + b$$

Next we integrate with respect to y , noting that this is a *partial* integration, so we add an arbitrary function of the other variable, x , rather than a constant of integration,

$$\psi = axy + by + g(x) \quad (1)$$

Now we choose the other part of Eq. 9-20, differentiate Eq. 1, and rearrange as follows:

$$v = -\frac{\partial \psi}{\partial x} = -ay - g'(x) \quad (2)$$

where $g'(x)$ denotes dg/dx since g is a function of only one variable, x . We now have two expressions for velocity component v , the equation given in the

problem statement and Eq. 2. We equate these and integrate with respect to x to find $g(x)$,

$$v = -ay + cx = -ay - g'(x) \rightarrow g'(x) = -cx \rightarrow g(x) = -c \frac{x^2}{2} + C \quad (3)$$

Note that here we have added an arbitrary constant of integration C since g is a function of x only. Finally, substituting Eq. 3 into Eq. 1 yields the final expression for ψ ,

Solution: $\psi = axy + by - c \frac{x^2}{2} + C \quad (4)$

To plot the streamlines, we note that Eq. 4 represents a *family* of curves, one unique curve for each value of the constant ($\psi - C$). Since C is arbitrary, it is common to set it equal to zero, although it can be set to any desired value. For simplicity we set $C = 0$ and solve Eq. 4 for y as a function of x , yielding

Equation for streamlines: $y = \frac{\psi + cx^2/2}{ax + b} \quad (5)$

For the given values of constants a , b , and c , we plot Eq. 5 for several values of ψ in Fig. 9–21; these curves of constant ψ are streamlines of the flow. From Fig. 9–21 we see that this is a smoothly converging flow in the upper-right quadrant.

Discussion It is always good to check your algebra. In this example, you should substitute Eq. 4 into Eq. 9–20 to verify that the correct velocity components are obtained.

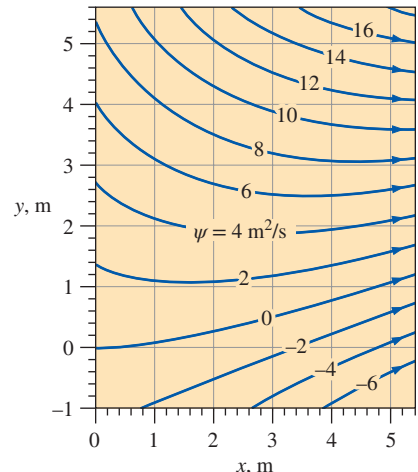


FIGURE 9–21

Streamlines for the velocity field of Example 9–9; the value of constant ψ is indicated for each streamline.

There is another physically significant fact about the stream function:

The difference in the value of ψ from one streamline to another is equal to the volume flow rate per unit width between the two streamlines.

This statement is illustrated in Fig. 9–22. Consider two streamlines, ψ_1 and ψ_2 , and imagine two-dimensional flow in the xy -plane, of unit width into the page (1 m in the $-z$ -direction). By definition, *no flow can cross a streamline*. Thus, the fluid that happens to occupy the space between these two streamlines remains confined between the same two streamlines. It follows that the mass flow rate through any cross-sectional slice between the streamlines is the same at any instant in time. The cross-sectional slice can be any shape, provided that it starts at streamline 1 and ends at streamline 2. In Fig. 9–22, for example, slice A is a smooth arc from one streamline to the other while slice B is wavy. For steady, incompressible, two-dimensional flow in the xy -plane, the volume flow rate \dot{V} between the two streamlines (per unit width) must therefore be a constant. If the two streamlines spread apart, as they do from cross-sectional slice A to cross-sectional slice B, the average velocity between the two streamlines decreases accordingly, such that the volume flow rate remains the same ($\dot{V}_A = \dot{V}_B$). In Fig. 9–20 of Example 9–8, velocity vectors at four locations in the flow field between streamlines $\psi = 0 \text{ m}^2/\text{s}$ and $\psi = 5 \text{ m}^2/\text{s}$ are plotted. You can clearly see that as the streamlines diverge from each other, the velocity vector decays in magnitude. Likewise, when streamlines *converge*, the average velocity between them must increase.

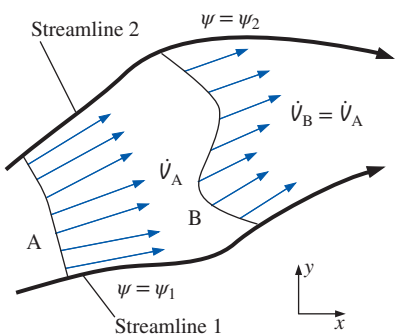
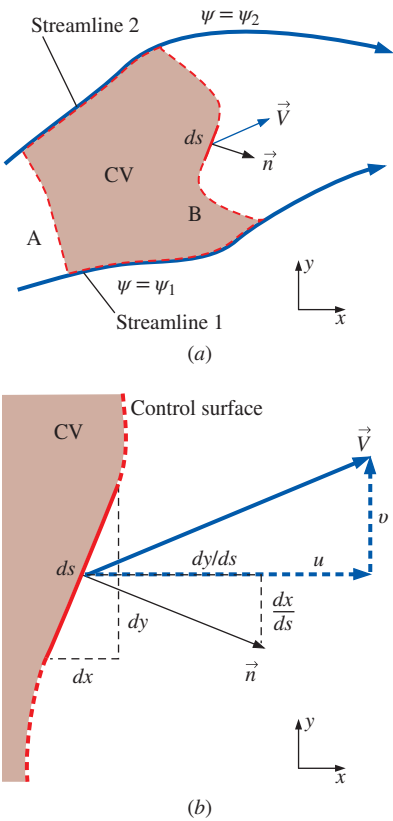


FIGURE 9–22

For two-dimensional streamlines in the xy -plane, the volume flow rate \dot{V} per unit width between two streamlines is the same through any cross-sectional slice.

**FIGURE 9-23**

(a) Control volume bounded by streamlines ψ_1 and ψ_2 and slices A and B in the xy -plane; (b) magnified view of the region around infinitesimal length ds .

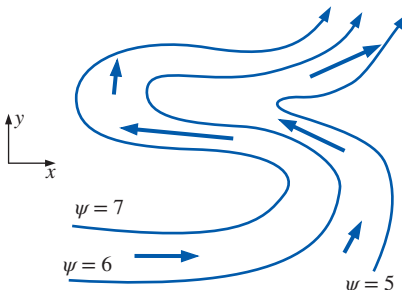
**FIGURE 9-24**

Illustration of the “left-side convention.” In the xy -plane, the value of the stream function always increases to the left of the flow direction.

We prove the given statement mathematically by considering a control volume bounded by the two streamlines of Fig. 9-22 and by cross-sectional slice A and cross-sectional slice B (Fig. 9-23). An infinitesimal length ds along slice B is illustrated in Fig. 9-23a, along with its unit normal vector \vec{n} . A magnified view of this region is sketched in Fig. 9-23b for clarity. As shown, the two components of ds are dx and dy ; thus the unit normal vector is

$$\vec{n} = \frac{dy}{ds} \vec{i} - \frac{dx}{ds} \vec{j}$$

The volume flow rate per unit width through segment ds of the control surface is

$$d\dot{V} = \underbrace{\vec{V} \cdot \vec{n}}_{ds} dA = (u\vec{i} + v\vec{j}) \cdot \left(\frac{dy}{ds} \vec{i} - \frac{dx}{ds} \vec{j} \right) ds \quad (9-23)$$

where $dA = ds$ times 1 = ds , where the 1 indicates a unit width into the page, regardless of the unit system. When we expand the dot product of Eq. 9-23 and apply Eq. 9-20, we get

$$d\dot{V} = u dy - v dx = \frac{\partial \psi}{\partial y} dy + \frac{\partial \psi}{\partial x} dx = d\psi \quad (9-24)$$

We find the total volume flow rate through cross-sectional slice B by integrating Eq. 9-24 from streamline 1 to streamline 2,

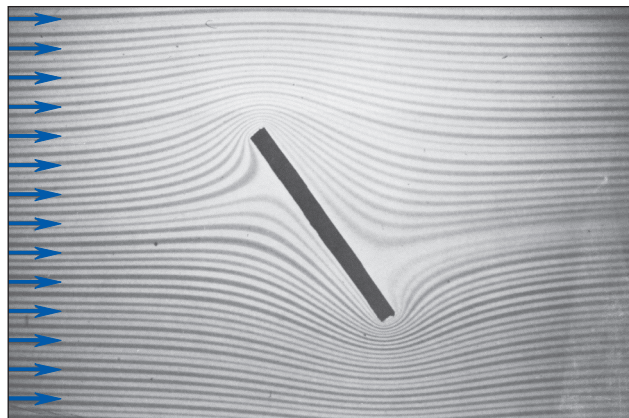
$$\dot{V}_B = \int_B \vec{V} \cdot \vec{n} dA = \int_B d\dot{V} = \int_{\psi=\psi_1}^{\psi=\psi_2} d\psi = \psi_2 - \psi_1 \quad (9-25)$$

Thus, the volume flow rate per unit width through slice B is equal to the difference between the values of the two stream functions that bound slice B. Now consider the entire control volume of Fig. 9-23a. Since we know that no flow crosses the streamlines, conservation of mass demands that the volume flow rate into the control volume through slice A be identical to the volume flow rate out of the control volume through slice B. Finally, since we may choose a cross-sectional slice of any shape or location between the two streamlines, the statement is proven.

When dealing with stream functions, the direction of flow is obtained by what we might call the “**left-side convention**.” Namely, if you are looking down the z -axis at the xy -plane (Fig. 9-24) and are moving in the direction of the flow, the stream function increases to your left.

The value of ψ increases to the left of the direction of flow in the xy -plane.

In Fig. 9-24, for example, the stream function increases to the left of the flow direction, regardless of how much the flow twists and turns. Notice also that when the streamlines are far apart (lower right of Fig. 9-24), the magnitude of velocity (the fluid speed) in that vicinity is small relative to the speed in locations where the streamlines are close together (middle region of Fig. 9-24). This is easily explained by conservation of mass. As the streamlines converge, the cross-sectional area between them decreases, and the velocity must increase to maintain the flow rate between the streamlines.

**FIGURE 9-25**

Streaklines produced by Hele–Shaw flow over an inclined plate. The streaklines model streamlines of potential flow (Chap. 10) over a two-dimensional inclined plate of the same cross-sectional shape.

Original © D.H. Peregrine, School of Mathematics, University of Bristol. Courtesy of Onno Bokhove and Valerie Zwart.

EXAMPLE 9-10 Relative Velocity Deduced from Streamlines

Hele–Shaw flow is produced by forcing a liquid through a thin gap between parallel plates. An example of Hele–Shaw flow is provided in Fig. 9–25 for flow over an inclined plate. Streaklines are generated by introducing dye at evenly spaced points upstream of the field of view. Since the flow is steady, the streaklines are coincident with streamlines. The fluid is water and the glass plates are 1.0 mm apart. Discuss how you can tell from the streamline pattern whether the flow speed in a particular region of the flow field is (relatively) large or small.

SOLUTION For the given set of streamlines, we are to discuss how we can tell the relative speed of the fluid.

Assumptions 1 The flow is steady. 2 The flow is incompressible. 3 The flow models two-dimensional potential flow in the xy -plane.

Analysis When equally spaced streamlines of a stream function spread away from each other, it indicates that the flow speed has decreased in that region. Likewise, if the streamlines come closer together, the flow speed has increased in that region. In Fig. 9–25 we infer that the flow far upstream of the plate is straight and uniform, since the streamlines are equally spaced. The fluid decelerates as it approaches the underside of the plate, especially near the stagnation point, as indicated by the wide gap between streamlines. The flow accelerates rapidly to very high speeds around the sharp corners of the plate, as indicated by the tightly spaced streamlines.

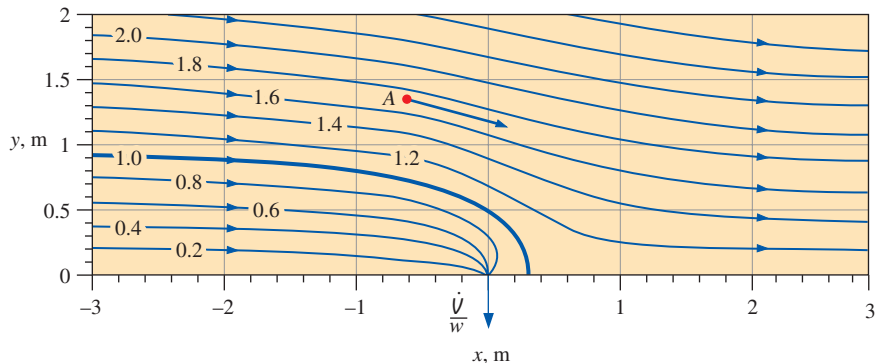
Discussion The streaklines of Hele–Shaw flow turn out to be similar to those of potential flow, which is discussed in Chap. 10.

EXAMPLE 9-11 Volume Flow Rate Deduced from Streamlines

Water is sucked through a narrow slot on the bottom wall of a water channel. The water in the channel flows from left to right at uniform velocity $V = 1.0 \text{ m/s}$. The slot is perpendicular to the xy -plane, and runs along the z -axis across the entire channel, which is $w = 2.0 \text{ m}$ wide. The flow is thus approximately two-dimensional in the xy -plane. Several streamlines of the flow are plotted and labeled in Fig. 9–26.

FIGURE 9–26

Streamlines for free-stream flow along a wall with a narrow suction slot; streamline values are shown in units of m^2/s ; the thick streamline is the dividing streamline. The direction of the velocity vector at point A is determined by the left-side convention.



The thick streamline in Fig. 9–26 is called the **dividing streamline** because it divides the flow into two parts. Namely, all the water below this dividing streamline gets sucked into the slot, while all the water above the dividing streamline continues on its way downstream. What is the volume flow rate of water being sucked through the slot? Estimate the magnitude of the velocity at point A.

SOLUTION For the given set of streamlines, we are to determine the volume flow rate through the slot and estimate the fluid speed at a point.

Assumptions 1 The flow is steady. 2 The flow is incompressible. 3 The flow is two-dimensional in the xy -plane. 4 Friction along the bottom wall is neglected.

Analysis By Eq. 9–25, the volume flow rate per unit width between the bottom wall ($\psi_{\text{wall}} = 0$) and the dividing streamline ($\psi_{\text{dividing}} = 1.0 \text{ m}^2/\text{s}$) is

$$\frac{\dot{V}}{w} = \psi_{\text{dividing}} - \psi_{\text{wall}} = (1.0 - 0) \text{ m}^2/\text{s} = 1.0 \text{ m}^2/\text{s}$$

All of this flow must go through the slot. Since the channel is 2.0 m wide, the total volume flow rate through the slot is

$$\dot{V} = \frac{\dot{V}}{w} w = (1.0 \text{ m}^2/\text{s})(2.0 \text{ m}) = \mathbf{2.0 \text{ m}^3/\text{s}}$$

To estimate the speed at point A, we measure the distance δ between the two streamlines that enclose point A. We find that streamline 1.8 is about 0.21 m away from streamline 1.6 in the vicinity of point A. The volume flow rate per unit width (into the page) between these two streamlines is equal to the difference in value of the stream function. We thus estimate the speed at point A,

$$V_A \cong \frac{\dot{V}}{w\delta} = \frac{1}{\delta} \frac{\dot{V}}{w} = \frac{1}{\delta} (\psi_{1.8} - \psi_{1.6}) = \frac{1}{0.21 \text{ m}} (1.8 - 1.6) \text{ m}^2/\text{s} = \mathbf{0.95 \text{ m/s}}$$

Our estimate is close to the known free-stream speed (1.0 m/s), indicating that the fluid in the vicinity of point A flows at nearly the same speed as the free-stream flow, but points slightly downward.

Discussion The streamlines of Fig. 9–26 were generated by superposition of a uniform stream and a line sink, assuming irrotational (potential) flow. We discuss such superposition in Chap. 10.

The Stream Function in Cylindrical Coordinates

For two-dimensional flow in the xy -plane, we can also define the stream function in cylindrical coordinates, which is more convenient for many problems. Note that by *two-dimensional* we mean that there are only two relevant independent spatial coordinates—with no dependence on the third component. There are two possibilities. The first is **planar flow**, just like that of Eqs. 9–19 and 9–20, but in terms of (r, θ) and (u_r, u_θ) instead of (x, y) and (u, v) (see Fig. 9–10a). In this case, there is no dependence on coordinate z . We simplify the incompressible continuity equation, Eq. 9–18, for two-dimensional planar flow in the $r\theta$ -plane,

$$\frac{\partial(ru_r)}{\partial r} + \frac{\partial(u_\theta)}{\partial\theta} = 0 \quad (9-26)$$

We define the stream function as follows:

Incompressible, planar stream function in cylindrical coordinates:

$$u_r = \frac{1}{r} \frac{\partial\psi}{\partial\theta} \quad \text{and} \quad u_\theta = -\frac{\partial\psi}{\partial r} \quad (9-27)$$

We note again that the signs are reversed in some textbooks. You can substitute Eq. 9–27 into Eq. 9–26 to convince yourself that Eq. 9–26 is identically satisfied for any smooth function $\psi(r, \theta)$, since the order of differentiation (r then θ versus θ then r) is irrelevant for a smooth function.

The second type of two-dimensional flow in cylindrical coordinates is **axisymmetric flow**, in which r and z are the relevant spatial variables, u_r and u_z are the nonzero velocity components, and there is no dependence on θ (Fig. 9–27). Examples of axisymmetric flow include flow around spheres, bullets, and the fronts of many objects like torpedoes and missiles, which would be axisymmetric everywhere if not for their fins. For incompressible axisymmetric flow, the continuity equation is

$$\frac{1}{r} \frac{\partial(ru_r)}{\partial r} + \frac{\partial(u_z)}{\partial z} = 0 \quad (9-28)$$

The stream function ψ is defined such that it satisfies Eq. 9–28 exactly, provided of course that ψ is a smooth function of r and z ,

Incompressible, axisymmetric stream function in cylindrical coordinates:

$$u_r = -\frac{1}{r} \frac{\partial\psi}{\partial z} \quad \text{and} \quad u_z = \frac{1}{r} \frac{\partial\psi}{\partial r} \quad (9-29)$$

We also note that there is another way to describe axisymmetric flows, namely, by using Cartesian coordinates (x, y) and (u, v) , but forcing coordinate x to be the axis of symmetry. This can lead to confusion because the equations of motion must be modified accordingly to account for the axisymmetry. Nevertheless, this is often the approach used in CFD codes. The advantage is that after one sets up a grid in the xy -plane, the *same* grid can be used for both planar flow (flow in the xy -plane with no z -dependence) and axisymmetric flow (flow in the xy -plane with rotational symmetry about the x -axis). We do not discuss the equations for this alternative description of axisymmetric flows.

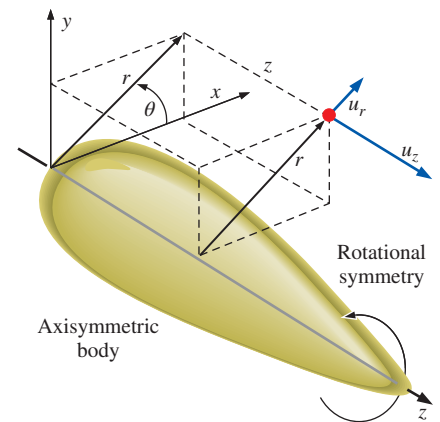


FIGURE 9–27

Flow over an axisymmetric body in cylindrical coordinates with rotational symmetry about the z -axis; neither the geometry nor the velocity field depend on θ , and $u_\theta = 0$.

EXAMPLE 9–12 Stream Function in Cylindrical Coordinates

Consider a line vortex, defined as steady, planar, incompressible flow in which the velocity components are $u_r = 0$ and $u_\theta = K/r$, where K is a constant. This flow is represented in Fig. 9–15a. Derive an expression for the stream function $\psi(r, \theta)$, and prove that the streamlines are circles.

SOLUTION For a given velocity field in cylindrical coordinates, we are to derive an expression for the stream function and show that the streamlines are circular.

Assumptions 1 The flow is steady. 2 The flow is incompressible. 3 The flow is planar in the $r\theta$ -plane.

Analysis We use the definition of stream function given by Eq. 9–27. We can choose either component to start with; we choose the tangential component,

$$\frac{\partial \psi}{\partial r} = -u_\theta = -\frac{K}{r} \quad \rightarrow \quad \psi = -K \ln r + f(\theta) \quad (1)$$

Now we use the other component of Eq. 9–27,

$$u_r = \frac{1}{r} \frac{\partial \psi}{\partial \theta} = \frac{1}{r} f'(\theta) \quad (2)$$

where the prime denotes a derivative with respect to θ . By equating u_r from the given information to Eq. 2, we see that

$$f'(\theta) = 0 \quad \rightarrow \quad f(\theta) = C$$

where C is an arbitrary constant of integration. Equation 1 is thus

$$\text{Solution:} \quad \psi = -K \ln r + C \quad (3)$$

Finally, we see from Eq. 3 that curves of constant ψ are produced by setting r to a constant value. Since curves of constant r are circles by definition, **streamlines (curves of constant ψ) must therefore be circles about the origin, as in Fig. 9–15a.**

For given values of C and ψ , we solve Eq. 3 for r to plot the streamlines,

$$\text{Equation for streamlines:} \quad r = e^{-(\psi - C)/K} \quad (4)$$

For $K = 10 \text{ m}^2/\text{s}$ and $C = 0$, streamlines from $\psi = 0$ to 22 are plotted in Fig. 9–28.

Discussion Notice that for a uniform increment in the value of ψ , the streamlines get closer and closer together near the origin as the tangential velocity increases. This is a direct result of the statement that the difference in the value of ψ from one streamline to another is equal to the volume flow rate per unit width between the two streamlines.

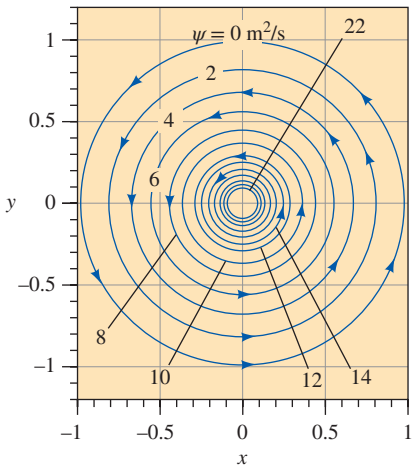


FIGURE 9–28

Streamlines for the velocity field of Example 9–12, with $K = 10 \text{ m}^2/\text{s}$ and $C = 0$; the value of constant ψ is indicated for several streamlines.

The Compressible Stream Function*

We extend the stream function concept to steady, *compressible*, two-dimensional flow in the xy -plane. The compressible continuity equation (Eq. 9–14) in Cartesian coordinates reduces to the following for steady two-dimensional flow:

$$\frac{\partial(\rho u)}{\partial x} + \frac{\partial(\rho v)}{\partial y} = 0 \quad (9-30)$$

* This section can be skipped without loss of continuity (no pun intended).

We introduce a **compressible stream function**, which we denote as ψ_ρ ,

Steady, compressible, two-dimensional stream function in Cartesian coordinates:

$$\rho u = \frac{\partial \psi_\rho}{\partial y} \quad \text{and} \quad \rho v = -\frac{\partial \psi_\rho}{\partial x} \quad (9-31)$$

By definition, ψ_ρ of Eq. 9-31 satisfies Eq. 9-30 exactly, provided that ψ_ρ is a smooth function of x and y . Many of the features of the compressible stream function are the same as those of the incompressible ψ as discussed previously. For example, curves of constant ψ_ρ are still streamlines. However, the difference in ψ_ρ from one streamline to another is *mass* flow rate per unit width rather than volume flow rate per unit width. Although not as popular as its incompressible counterpart, the compressible stream function finds use in some commercial CFD codes.

9-4 • THE DIFFERENTIAL LINEAR MOMENTUM EQUATION—CAUCHY'S EQUATION

Through application of the Reynolds transport theorem (Chap. 4), we have the general expression for the linear momentum equation as applied to a control volume,

$$\sum \vec{F} = \int_{CV} \rho \vec{g} dV + \int_{CS} \sigma_{ij} \cdot \vec{n} dA = \int_{CV} \frac{\partial}{\partial t} (\rho \vec{V}) dV + \int_{CS} (\rho \vec{V}) \vec{V} \cdot \vec{n} dA \quad (9-32)$$

where σ_{ij} is the **stress tensor** introduced in Chap. 6. Components of σ_{ij} on the positive faces of an infinitesimal rectangular control volume are shown in Fig. 9-29. Equation 9-32 applies to both fixed and moving control volumes, provided that \vec{V} is the absolute velocity (as seen from a fixed observer). For the special case of flow with well defined inlets and outlets, Eq. 9-32 is simplified as follows:

$$\sum \vec{F} = \sum \vec{F}_{\text{body}} + \sum \vec{F}_{\text{surface}} = \int_{CV} \frac{\partial}{\partial t} (\rho \vec{V}) dV + \sum_{\text{out}} \beta \dot{m} \vec{V} - \sum_{\text{in}} \beta \dot{m} \vec{V} \quad (9-33)$$

where \vec{V} in the last two terms is taken as the average velocity at an inlet or outlet, and β is the momentum flux correction factor (Chap. 6). In words, the total force acting on the control volume is equal to the rate at which momentum changes within the control volume plus the rate at which momentum flows out of the control volume minus the rate at which momentum flows into the control volume. Equation 9-33 applies to *any* control volume, regardless of its size. To generate a differential linear momentum equation, we imagine the control volume shrinking to infinitesimal size. In the limit, the entire control volume shrinks to a *point* in the flow (Fig. 9-2). We take the same approach here as we did for conservation of mass; namely, we show more than one way to derive the differential form of the linear momentum equation.

Derivation Using the Divergence Theorem

The most straightforward (and most elegant) way to derive the differential form of the momentum equation is to apply the divergence theorem of Eq. 9-3. A more general form of the divergence theorem applies not only to vectors, but to other quantities as well, such as tensors, as illustrated in

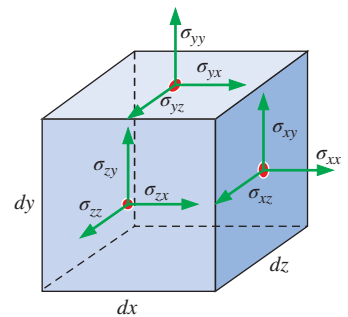
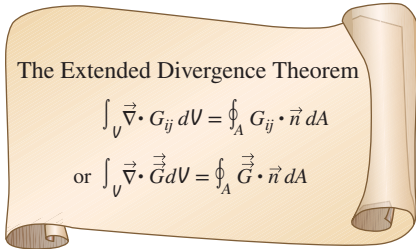
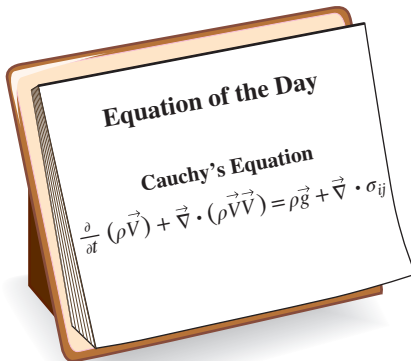


FIGURE 9-29

Positive components of the stress tensor in Cartesian coordinates on the positive (right, top, and front) faces of an infinitesimal rectangular control volume. The red dots indicate the center of each face. Positive components on the negative (left, bottom, and back) faces are in the opposite direction of those shown here.

**FIGURE 9–30**

An extended form of the divergence theorem is useful not only for vectors, but also for tensors. In the equation, G_{ij} (or \vec{G}) is a second-order tensor, V is a volume, and A is the surface area that encloses and defines the volume.

**FIGURE 9–31**

Cauchy's equation is a differential form of the linear momentum equation. It applies to any type of fluid.

Fig. 9–30. Specifically, if we replace G_{ij} in the extended divergence theorem of Fig. 9–30 with the quantity $(\rho\vec{V})\vec{V}$, a second-order tensor, the last term in Eq. 9–32 becomes

$$\int_{CS} (\rho\vec{V})\vec{V} \cdot \vec{n} dA = \int_{CV} \vec{\nabla} \cdot (\rho\vec{V}\vec{V}) dV \quad (9-34)$$

where $\vec{V}\vec{V}$ is a vector product called the *outer product* of the velocity vector with itself. (The outer product of two vectors is *not* the same as the inner or dot product, nor is it the same as the cross product of the two vectors.) Similarly, if we replace G_{ij} in Fig. 9–30 by the stress tensor σ_{ij} , the second term on the left-hand side of Eq. 9–32 becomes

$$\int_{CS} \sigma_{ij} \cdot \vec{n} dA = \int_{CV} \vec{\nabla} \cdot \sigma_{ij} dV \quad (9-35)$$

Thus, the two surface integrals of Eq. 9–32 become volume integrals by applying Eqs. 9–34 and 9–35. We combine and rearrange the terms, and rewrite Eq. 9–32 as

$$\int_{CV} \left[\frac{\partial}{\partial t} (\rho\vec{V}) + \vec{\nabla} \cdot (\rho\vec{V}\vec{V}) - \rho\vec{g} - \vec{\nabla} \cdot \sigma_{ij} \right] dV = 0 \quad (9-36)$$

Finally, we argue that Eq. 9–36 must hold for *any* control volume regardless of its size or shape. This is possible only if the integrand (enclosed by square brackets) is identically zero. Hence, we have a general differential equation for linear momentum, known as **Cauchy's equation**,

$$\text{Cauchy's equation: } \frac{\partial}{\partial t} (\rho\vec{V}) + \vec{\nabla} \cdot (\rho\vec{V}\vec{V}) = \rho\vec{g} + \vec{\nabla} \cdot \sigma_{ij} \quad (9-37)$$

Equation 9–37 is named in honor of the French engineer and mathematician Augustin Louis de Cauchy (1789–1857). It is valid for compressible as well as incompressible flow since we have not made any assumptions about incompressibility. It is valid at any point in the flow domain (Fig. 9–31). Note that Eq. 9–37 is a *vector* equation, and thus represents three scalar equations, one for each coordinate axis in three-dimensional problems.

Derivation Using an Infinitesimal Control Volume

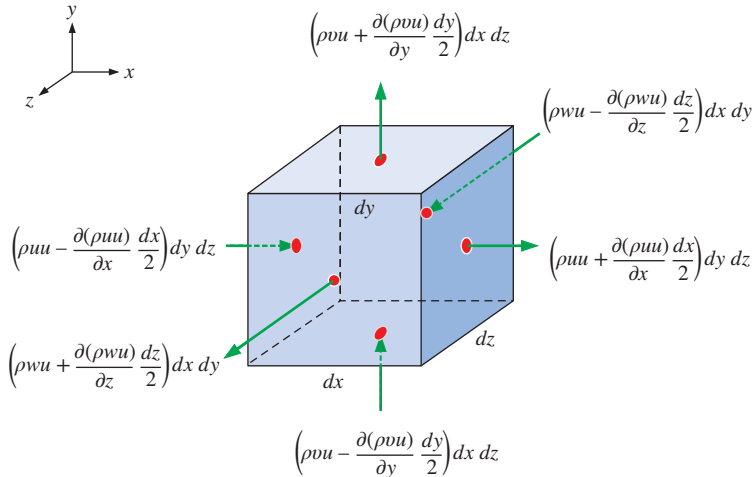
We derive Cauchy's equation a second way, using an infinitesimal control volume on which we apply the linear momentum equation (Eq. 9–33). We consider the same box-shaped control volume we used to derive the continuity equation (Fig. 9–3). At the center of the box, as previously, we define the density as ρ and the velocity components as u , v , and w . We also define the stress tensor as σ_{ij} at the center of the box. For simplicity, we consider the x -component of Eq. 9–33, obtained by setting $\Sigma\vec{F}$ equal to its x -component, ΣF_x , and \vec{V} equal to its x -component, u . This not only simplifies the diagrams, but enables us to work with a scalar equation, namely,

$$\Sigma F_x = \Sigma F_{x, \text{body}} + \Sigma F_{x, \text{surface}} = \int_{CV} \frac{\partial}{\partial t} (\rho u) dV + \sum_{\text{out}} \beta \dot{m} u - \sum_{\text{in}} \beta \dot{m} u \quad (9-38)$$

As the control volume shrinks to a point, the first term on the right-hand side of Eq. 9–38 becomes

Rate of change of x -momentum within the control volume:

$$\int_{CV} \frac{\partial}{\partial t} (\rho u) dV = \frac{\partial}{\partial t} (\rho u) dx dy dz \quad (9-39)$$

**FIGURE 9-32**

Inflow and outflow of the x -component of linear momentum through each face of an infinitesimal control volume; the red dots indicate the center of each face.

since the volume of the differential element is $dx dy dz$. We apply first-order truncated Taylor series expansions at locations away from the center of the control volume to approximate the inflow and outflow of momentum in the x -direction. Figure 9-32 shows these momentum fluxes at the center point of each of the six faces of the infinitesimal control volume. Only the *normal* velocity component at each face needs to be considered, since the tangential velocity components contribute no mass flow out of (or into) the face, and hence no momentum flow through the face either.

By summing all the outflows and subtracting all the inflows shown in Fig. 9-32, we obtain an approximation for the last two terms of Eq. 9-38,

Net outflow of x -momentum through the control surface:

$$\sum_{\text{out}} \beta \dot{m} u - \sum_{\text{in}} \beta \dot{m} u \approx \left(\frac{\partial}{\partial x} (\rho u u) + \frac{\partial}{\partial y} (\rho v u) + \frac{\partial}{\partial z} (\rho w u) \right) dx dy dz \quad (9-40)$$

where β is set equal to one at all faces, consistent with our first-order approximation.

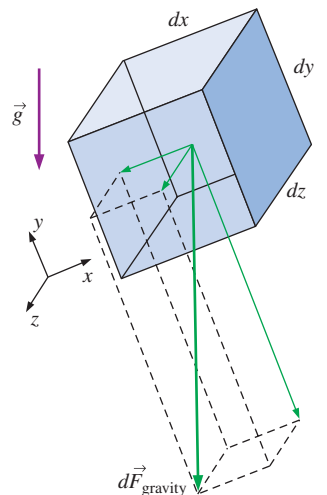
Next, we sum all the forces acting on our infinitesimal control volume in the x -direction. As was done in Chap. 6, we need to consider both body forces and surface forces. Gravity force (weight) is the only body force we take into account. For the general case in which the coordinate system may not be aligned with the z -axis (or with any coordinate axis for that matter), as sketched in Fig. 9-33, the gravity vector is written as

$$\vec{g} = g_x \vec{i} + g_y \vec{j} + g_z \vec{k}$$

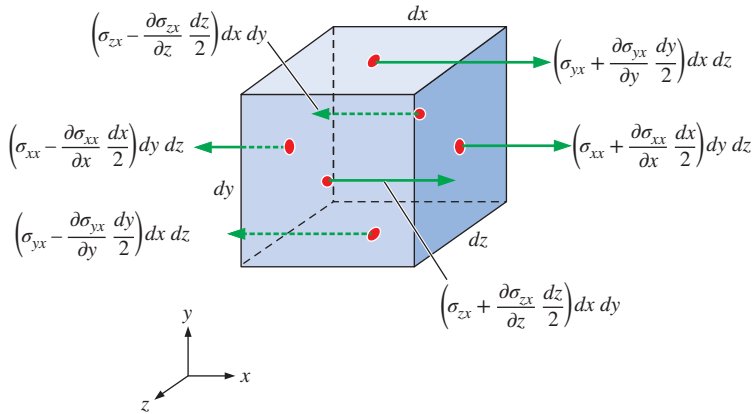
Thus, in the x -direction, the body force on the control volume is

$$\sum dF_{x, \text{body}} = \sum dF_{x, \text{gravity}} = \rho g x dx dy dz \quad (9-41)$$

Next we consider the net surface force in the x -direction. Recall that stress tensor σ_{ij} has dimensions of force per unit area. Thus, to obtain a force, we must multiply each stress component by the surface area of the face on

**FIGURE 9-33**

The gravity vector is not necessarily aligned with any particular axis, in general, and there are three components of the body force acting on an infinitesimal fluid element.

**FIGURE 9-34**

Sketch illustrating the surface forces acting in the x -direction due to the appropriate stress tensor component on each face of the differential control volume; the red dots indicate the center of each face.

which it acts. We need to consider only those components that point in the x - (or $-x$ -) direction. (The other components of the stress tensor, although they may be nonzero, do not contribute to a net force in the x -direction.) Using truncated Taylor series expansions, we sketch all the surface forces that contribute to a net x -component of surface force acting on our differential fluid element (Fig. 9-34).

Summing all the surface forces illustrated in Fig. 9-34, we obtain an approximation for the net surface force acting on the differential fluid element in the x -direction,

$$\sum dF_{x, \text{surface}} = \left(\frac{\partial}{\partial x} \sigma_{xx} + \frac{\partial}{\partial y} \sigma_{yx} + \frac{\partial}{\partial z} \sigma_{zx} \right) dx dy dz \quad (9-42)$$

We now substitute Eqs. 9-39 through 9-42 into Eq. 9-38, noting that the volume of the differential element of fluid, $dx dy dz$, appears in all terms and can be eliminated. After some rearrangement we obtain the differential form of the x -momentum equation,

$$\frac{\partial(\rho u)}{\partial t} + \frac{\partial(\rho uu)}{\partial x} + \frac{\partial(\rho vu)}{\partial y} + \frac{\partial(\rho wu)}{\partial z} = \rho g_x + \frac{\partial}{\partial x} \sigma_{xx} + \frac{\partial}{\partial y} \sigma_{yx} + \frac{\partial}{\partial z} \sigma_{zx} \quad (9-43)$$

In similar fashion, we generate differential forms of the y - and z -momentum equations,

$$\frac{\partial(\rho v)}{\partial t} + \frac{\partial(\rho uv)}{\partial x} + \frac{\partial(\rho vv)}{\partial y} + \frac{\partial(\rho wv)}{\partial z} = \rho g_y + \frac{\partial}{\partial x} \sigma_{xy} + \frac{\partial}{\partial y} \sigma_{yy} + \frac{\partial}{\partial z} \sigma_{zy} \quad (9-44)$$

and

$$\frac{\partial(\rho w)}{\partial t} + \frac{\partial(\rho uw)}{\partial x} + \frac{\partial(\rho vw)}{\partial y} + \frac{\partial(\rho ww)}{\partial z} = \rho g_z + \frac{\partial}{\partial x} \sigma_{xz} + \frac{\partial}{\partial y} \sigma_{yz} + \frac{\partial}{\partial z} \sigma_{zz} \quad (9-45)$$

respectively. Finally, we combine Eqs. 9-43 through 9-45 into one vector equation,

$$\text{Cauchy's equation: } \frac{\partial}{\partial t} (\rho \vec{V}) + \vec{\nabla} \cdot (\rho \vec{V} \vec{V}) = \rho \vec{g} + \vec{\nabla} \cdot \vec{\sigma}_{ij}$$

This equation is identical to Cauchy's equation (Eq. 9-37); thus we confirm that our derivation using the differential fluid element yields the same result

as our derivation using the divergence theorem. Note that the product $\vec{V}\vec{V}$ is a second-order tensor (Fig. 9–35).

Alternative Form of Cauchy's Equation

Applying the product rule to the first term on the left side of Eq. 9–37, we get

$$\frac{\partial}{\partial t}(\rho\vec{V}) = \rho \frac{\partial\vec{V}}{\partial t} + \vec{V} \frac{\partial\rho}{\partial t} \quad (9-46)$$

The second term of Eq. 9–37 is written as

$$\vec{V} \cdot (\rho\vec{V}\vec{V}) = \vec{V} \vec{V} \cdot (\rho\vec{V}) + \rho(\vec{V} \cdot \vec{V})\vec{V} \quad (9-47)$$

Thus we have eliminated the second-order tensor represented by $\vec{V}\vec{V}$. After some rearrangement, substitution of Eqs. 9–46 and 9–47 into Eq. 9–37 yields

$$\rho \frac{\partial\vec{V}}{\partial t} + \vec{V} \left[\frac{\partial\rho}{\partial t} + \vec{V} \cdot (\rho\vec{V}) \right] + \rho(\vec{V} \cdot \vec{V})\vec{V} = \rho\vec{g} + \vec{V} \cdot \sigma_{ij}$$

But the expression in square brackets in this equation is identically zero by the continuity equation, Eq. 9–5. By combining the remaining two terms on the left side, we write

Alternative form of Cauchy's equation:

$$\rho \left[\frac{\partial\vec{V}}{\partial t} + (\vec{V} \cdot \vec{V})\vec{V} \right] = \rho \frac{D\vec{V}}{Dt} = \rho\vec{g} + \vec{V} \cdot \sigma_{ij} \quad (9-48)$$

where we have recognized the expression in square brackets as the material acceleration—the acceleration following a fluid particle (see Chap. 4).

Derivation Using Newton's Second Law

We derive Cauchy's equation by yet a third method. Namely, we take the differential fluid element as a *material element* instead of a control volume. In other words, we think of the fluid within the differential element as a tiny system of fixed identity, moving with the flow (Fig. 9–36). The acceleration of this fluid element is $\vec{a} = D\vec{V}/Dt$ by definition of the material acceleration. By Newton's second law applied to a material element of fluid,

$$\sum d\vec{F} = dm\vec{a} = dm \frac{D\vec{V}}{Dt} = \rho dx dy dz \frac{D\vec{V}}{Dt} \quad (9-49)$$

At the instant in time represented in Fig. 9–36, the net force on the differential fluid element is found in the same way as that calculated earlier on the differential control volume. Thus the total force acting on the fluid element is the sum of Eqs. 9–41 and 9–42, extended to vector form. Substituting these into Eq. 9–49 and dividing by $dx dy dz$, we once again generate the alternative form of Cauchy's equation,

$$\rho \frac{D\vec{V}}{Dt} = \rho\vec{g} + \vec{V} \cdot \sigma_{ij} \quad (9-50)$$

Equation 9–50 is identical to Eq. 9–48. In hindsight, we could have started with Newton's second law from the beginning, avoiding some algebra. Nevertheless, derivation of Cauchy's equation by three methods certainly boosts our confidence in the validity of the equation!

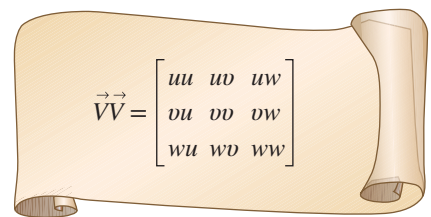


FIGURE 9-35

The outer product of vector $\vec{V} = (u, v, w)$ with itself is a second-order tensor. The product shown is in Cartesian coordinates and is illustrated as a nine-component matrix.

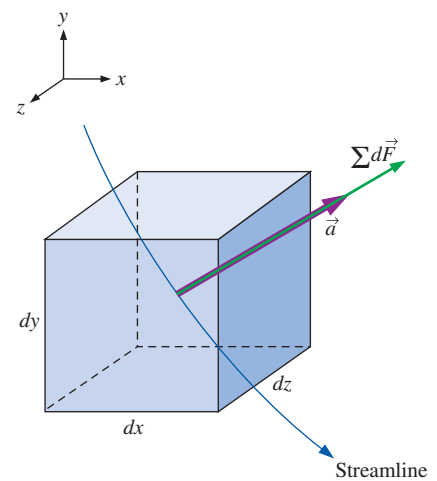


FIGURE 9-36

If the differential fluid element is a material element, it moves with the flow and Newton's second law applies directly.

We must be very careful when expanding the last term of Eq. 9–50, which is the divergence of a second-order tensor. In Cartesian coordinates, the three components of Cauchy's equation are

$$x\text{-component: } \rho \frac{Du}{Dt} = \rho g_x + \frac{\partial \sigma_{xx}}{\partial x} + \frac{\partial \sigma_{yx}}{\partial y} + \frac{\partial \sigma_{zx}}{\partial z} \quad (9-51a)$$

$$y\text{-component: } \rho \frac{Dv}{Dt} = \rho g_y + \frac{\partial \sigma_{xy}}{\partial x} + \frac{\partial \sigma_{yy}}{\partial y} + \frac{\partial \sigma_{zy}}{\partial z} \quad (9-51b)$$

$$z\text{-component: } \rho \frac{Dw}{Dt} = \rho g_z + \frac{\partial \sigma_{xz}}{\partial x} + \frac{\partial \sigma_{yz}}{\partial y} + \frac{\partial \sigma_{zz}}{\partial z} \quad (9-51c)$$

We conclude this section by noting that we cannot solve any fluid mechanics problems using Cauchy's equation by itself (even when combined with continuity). The problem is that the stress tensor σ_{ij} needs to be expressed in terms of the primary unknowns in the problem, namely, density, pressure, and velocity. This is done for the most common type of fluid in Section 9–5.

9–5 ■ THE NAVIER–STOKES EQUATION

Introduction

Cauchy's equation (Eq. 9–37 or its alternative form Eq. 9–48) is not very useful to us as is, because the stress tensor σ_{ij} contains nine components, six of which are independent (because of symmetry). Thus, in addition to density and the three velocity components, there are six additional unknowns, for a total of 10 unknowns. (In Cartesian coordinates the unknowns are ρ , u , v , w , σ_{xx} , σ_{xy} , σ_{xz} , σ_{yy} , σ_{yz} , and σ_{zz}) Meanwhile, we have discussed only four equations so far—continuity (one equation) and Cauchy's equation (three equations). Of course, to be mathematically solvable, the number of equations must equal the number of unknowns, and thus we need six more equations. These equations are called **constitutive equations**, and they enable us to write the components of the stress tensor in terms of the velocity field and pressure field.

The first thing we do is separate the pressure stresses and the viscous stresses. When a fluid is at rest, the only stress acting at *any* surface of *any* fluid element is pressure P , which always acts *inward* and *normal* to the surface (Fig. 9–37). Thus, regardless of the orientation of the coordinate axes, for a fluid at rest the stress tensor reduces to

$$\text{Fluid at rest: } \sigma_{ij} = \begin{pmatrix} \sigma_{xx} & \sigma_{xy} & \sigma_{xz} \\ \sigma_{yx} & \sigma_{yy} & \sigma_{yz} \\ \sigma_{zx} & \sigma_{zy} & \sigma_{zz} \end{pmatrix} = \begin{pmatrix} -P & 0 & 0 \\ 0 & -P & 0 \\ 0 & 0 & -P \end{pmatrix} \quad (9-52)$$

Pressure P in Eq. 9–52 is the same as the **thermodynamic pressure** with which we are familiar from our study of thermodynamics. P is related to temperature and density through some type of **equation of state** (e.g., the ideal gas law). As a side note, this further complicates a compressible fluid flow analysis because we introduce yet another unknown, namely, temperature T . This new unknown requires another equation—the differential form of the energy equation—which is not discussed in this text.

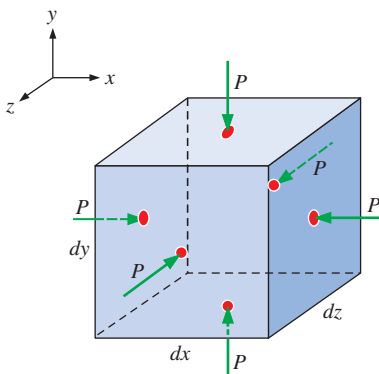


FIGURE 9–37

For fluids at rest, the only stress on a fluid element is the hydrostatic pressure, which always acts inward and normal to any surface. Note that we are ignoring gravity in this case; otherwise pressure would increase in the direction of the gravitational acceleration.

When a fluid is *moving*, pressure still acts inwardly normal, but viscous stresses may also exist. We generalize Eq. 9–52 for moving fluids as

Moving fluids:

$$\sigma_{ij} = \begin{pmatrix} \sigma_{xx} & \sigma_{xy} & \sigma_{xz} \\ \sigma_{yx} & \sigma_{yy} & \sigma_{yz} \\ \sigma_{zx} & \sigma_{zy} & \sigma_{zz} \end{pmatrix} = \begin{pmatrix} -P & 0 & 0 \\ 0 & -P & 0 \\ 0 & 0 & -P \end{pmatrix} + \begin{pmatrix} \tau_{xx} & \tau_{xy} & \tau_{xz} \\ \tau_{yx} & \tau_{yy} & \tau_{yz} \\ \tau_{zx} & \tau_{zy} & \tau_{zz} \end{pmatrix} \quad (9-53)$$

where we have introduced a new tensor, τ_{ij} , called the **viscous stress tensor** or the **deviatoric stress tensor**. Mathematically, we have not helped the situation because we have replaced the six unknown components of σ_{ij} with six unknown components of τ_{ij} , and have added *another* unknown, pressure P . Fortunately, however, there are constitutive equations that express τ_{ij} in terms of the velocity field and measurable fluid properties such as viscosity. The actual form of the constitutive relations depends on the type of fluid, as discussed shortly.

As a side note, there are some subtleties associated with the pressure in Eq. 9–53. If the fluid is *incompressible*, we have no equation of state (it is replaced by the equation $\rho = \text{constant}$), and we can no longer define P as the thermodynamic pressure. Instead, we define P in Eq. 9–53 as the **mechanical pressure**,

Mechanical pressure: $P_m = -\frac{1}{3}(\sigma_{xx} + \sigma_{yy} + \sigma_{zz}) \quad (9-54)$

We see from Eq. 9–54 that *mechanical pressure is the mean normal stress acting inwardly on a fluid element*. It is therefore also called **mean pressure** by some authors. Thus, when dealing with incompressible fluid flows, pressure variable P is always interpreted as the mechanical pressure P_m . For *compressible* flow fields however, pressure P in Eq. 9–53 is the thermodynamic pressure, but the mean normal stress felt on the surfaces of a fluid element is not necessarily the same as P (pressure variable P and mechanical pressure P_m are not necessarily equivalent). You are referred to Panton (1996) or Kundu et al. (2011) for a more detailed discussion of mechanical pressure.

Newtonian versus Non-Newtonian Fluids

The study of the deformation of flowing fluids is called **rheology**; the rheological behavior of various fluids is sketched in Fig. 9–38. In this text, we concentrate on **Newtonian fluids**, defined as *fluids for which the stress tensor is linearly proportional to the strain rate tensor*. Newtonian fluids (stress proportional to strain rate) are analogous to elastic solids (Hooke's law: stress proportional to strain). Many common fluids, such as air and other gases, water, kerosene, gasoline, and other oil-based liquids, are Newtonian fluids. Fluids for which the stress tensor is *not* linearly related to the strain rate tensor are called **non-Newtonian fluids**. Examples include slurries and colloidal suspensions, polymer solutions, blood, paste, and cake batter. Some non-Newtonian fluids exhibit a "memory"—the shear stress depends not only on the local strain rate, but also on its *history*. A fluid that returns (partially) to its original shape after the applied stress is released is called **viscoelastic**.

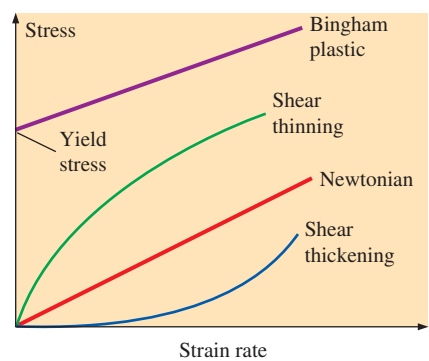
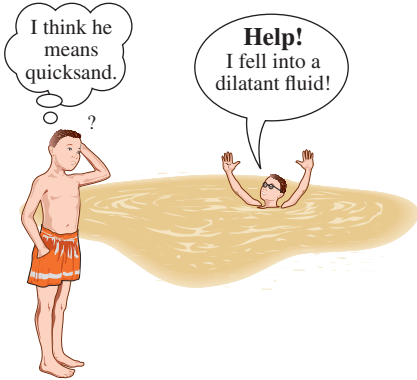


FIGURE 9–38
Rheological behavior of fluids—stress as a function of strain rate.

**FIGURE 9-39**

When an engineer falls into quicksand (a *dilatant fluid*), the faster he tries to move, the more viscous the fluid becomes.

Some non-Newtonian fluids are called **shear thinning fluids** or **pseudoplastic fluids**, because the more the fluid is sheared, the less viscous it becomes. A good example is paint. Paint is very viscous when poured from the can or when picked up by a paintbrush, since the shear rate is small. However, as we apply the paint to the wall, the thin layer of paint between the paintbrush and the wall is subjected to a large shear rate, and it becomes much less viscous. **Plastic fluids** are those in which the shear thinning effect is extreme. In some fluids a finite stress called the **yield stress** is required before the fluid begins to flow at all; such fluids are called **Bingham plastic fluids**. Certain pastes such as acne cream and toothpaste are examples of Bingham plastic fluids. If you hold the tube upside down, the paste does not flow, even though there is a nonzero stress due to gravity. However, if you squeeze the tube (greatly increasing the stress), the paste flows like a very viscous fluid. Other fluids show the opposite effect and are called **shear thickening fluids** or **dilatant fluids**; the more the fluid is sheared, the *more* viscous it becomes. The best example is quicksand, a thick mixture of sand and water. As we all know from Hollywood movies, it is easy to move *slowly* through quicksand, since the viscosity is low; but if you panic and try to move quickly, the viscous resistance increases considerably and you get “stuck” (Fig. 9-39). You can create your own quicksand by mixing two parts cornstarch with one part water—try it! Shear thickening fluids are used in some exercise equipment—the faster you pull, the more resistance you encounter.

Derivation of the Navier–Stokes Equation for Incompressible, Isothermal Flow

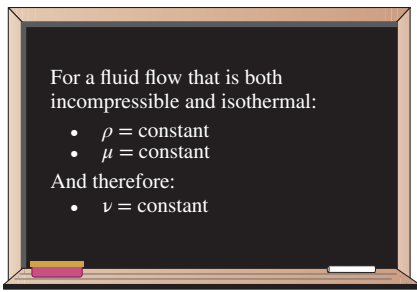
From this point on, we limit our discussion to Newtonian fluids, where by definition the stress tensor is linearly proportional to the strain rate tensor. The general result (for compressible flow) is rather involved and is not included here. Instead, we assume incompressible flow ($\rho = \text{constant}$). We also assume nearly isothermal flow—namely, that local changes in temperature are small or nonexistent; this eliminates the need for a differential energy equation. A further consequence of the latter assumption is that fluid properties, such as dynamic viscosity μ and kinematic viscosity ν , are constant as well (Fig. 9-40). With these assumptions, it can be shown (Kundu et al., 2011) that the viscous stress tensor reduces to

Viscous stress tensor for an incompressible Newtonian fluid with constant properties:

$$\tau_{ij} = 2\mu\epsilon_{ij} \quad (9-55)$$

where ϵ_{ij} is the strain rate tensor defined in Chap. 4. Equation 9-55 shows that stress is linearly proportional to strain. In Cartesian coordinates, the nine components of the viscous stress tensor are listed, only six of which are independent due to symmetry:

$$\tau_{ij} = \begin{pmatrix} \tau_{xx} & \tau_{xy} & \tau_{xz} \\ \tau_{yx} & \tau_{yy} & \tau_{yz} \\ \tau_{zx} & \tau_{zy} & \tau_{zz} \end{pmatrix} = \begin{pmatrix} 2\mu \frac{\partial u}{\partial x} & \mu \left(\frac{\partial u}{\partial y} + \frac{\partial v}{\partial x} \right) & \mu \left(\frac{\partial u}{\partial z} + \frac{\partial w}{\partial x} \right) \\ \mu \left(\frac{\partial v}{\partial x} + \frac{\partial u}{\partial y} \right) & 2\mu \frac{\partial v}{\partial y} & \mu \left(\frac{\partial v}{\partial z} + \frac{\partial w}{\partial y} \right) \\ \mu \left(\frac{\partial w}{\partial x} + \frac{\partial u}{\partial z} \right) & \mu \left(\frac{\partial w}{\partial y} + \frac{\partial v}{\partial z} \right) & 2\mu \frac{\partial w}{\partial z} \end{pmatrix} \quad (9-56)$$

**FIGURE 9-40**

The incompressible flow approximation implies constant density, and the isothermal approximation implies constant viscosity.

In Cartesian coordinates the stress tensor of Eq. 9–53 thus becomes

$$\sigma_{ij} = \begin{pmatrix} -P & 0 & 0 \\ 0 & -P & 0 \\ 0 & 0 & -P \end{pmatrix} + \begin{pmatrix} 2\mu \frac{\partial u}{\partial x} & \mu \left(\frac{\partial u}{\partial y} + \frac{\partial v}{\partial x} \right) & \mu \left(\frac{\partial u}{\partial z} + \frac{\partial w}{\partial x} \right) \\ \mu \left(\frac{\partial v}{\partial x} + \frac{\partial u}{\partial y} \right) & 2\mu \frac{\partial v}{\partial y} & \mu \left(\frac{\partial v}{\partial z} + \frac{\partial w}{\partial y} \right) \\ \mu \left(\frac{\partial w}{\partial x} + \frac{\partial u}{\partial z} \right) & \mu \left(\frac{\partial w}{\partial y} + \frac{\partial v}{\partial z} \right) & 2\mu \frac{\partial w}{\partial z} \end{pmatrix} \quad (9-57)$$

Now we substitute Eq. 9–57 into the three Cartesian components of Cauchy's equation. Let's consider the *x-component* first. Equation 9–51a becomes

$$\rho \frac{Du}{Dt} = -\frac{\partial P}{\partial x} + \rho g_x + 2\mu \frac{\partial^2 u}{\partial x^2} + \mu \frac{\partial}{\partial y} \left(\frac{\partial v}{\partial x} + \frac{\partial u}{\partial y} \right) + \mu \frac{\partial}{\partial z} \left(\frac{\partial w}{\partial x} + \frac{\partial u}{\partial z} \right) \quad (9-58)$$

Notice that since pressure consists of a normal stress only, it contributes only one term to Eq. 9–58. However, since the viscous stress tensor consists of both normal and shear stresses, it contributes *three* terms. (This is a direct result of taking the divergence of a second-order tensor, by the way.)

We note that as long as the velocity components are smooth functions of *x*, *y*, and *z*, the order of differentiation is irrelevant. For example, the first part of the last term in Eq. 9–58 can be rewritten as

$$\mu \frac{\partial}{\partial z} \left(\frac{\partial w}{\partial x} \right) = \mu \frac{\partial}{\partial x} \left(\frac{\partial w}{\partial z} \right)$$

After some clever rearrangement of the viscous terms in Eq. 9–58,

$$\begin{aligned} \rho \frac{Du}{Dt} &= -\frac{\partial P}{\partial x} + \rho g_x + \mu \left[\frac{\partial^2 u}{\partial x^2} + \frac{\partial}{\partial x} \frac{\partial u}{\partial x} + \frac{\partial}{\partial x} \frac{\partial v}{\partial y} + \frac{\partial^2 u}{\partial y^2} + \frac{\partial}{\partial x} \frac{\partial w}{\partial z} + \frac{\partial^2 u}{\partial z^2} \right] \\ &= -\frac{\partial P}{\partial x} + \rho g_x + \mu \left[\frac{\partial}{\partial x} \left(\frac{\partial u}{\partial x} + \frac{\partial v}{\partial y} + \frac{\partial w}{\partial z} \right) + \frac{\partial^2 u}{\partial x^2} + \frac{\partial^2 u}{\partial y^2} + \frac{\partial^2 u}{\partial z^2} \right] \end{aligned}$$

The term in parentheses is zero because of the continuity equation for incompressible flow (Eq. 9–17). We also recognize the last three terms as the **Laplacian** of velocity component *u* in Cartesian coordinates (Fig. 9–41). Thus, we write the *x*-component of the momentum equation as

$$\rho \frac{Du}{Dt} = -\frac{\partial P}{\partial x} + \rho g_x + \mu \nabla^2 u \quad (9-59a)$$

Similarly, the *y*- and *z*-components of the momentum equation reduce to

$$\rho \frac{Dv}{Dt} = -\frac{\partial P}{\partial y} + \rho g_y + \mu \nabla^2 v \quad (9-59b)$$

and

$$\rho \frac{Dw}{Dt} = -\frac{\partial P}{\partial z} + \rho g_z + \mu \nabla^2 w \quad (9-59c)$$

respectively. Finally, we combine the three components into one vector equation; the result is the **Navier–Stokes equation** for incompressible flow with constant viscosity.

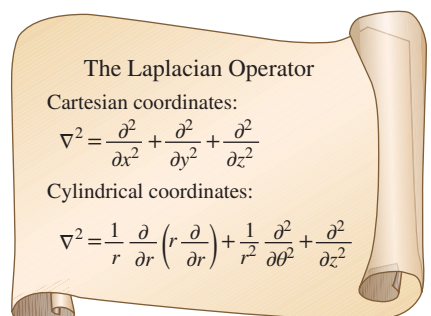
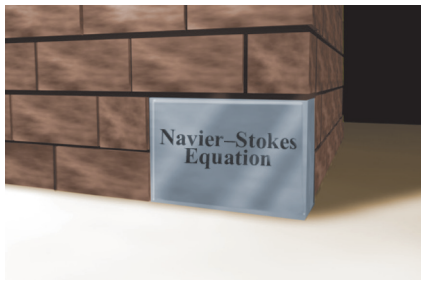


FIGURE 9–41

The Laplacian operator, shown here in both Cartesian and cylindrical coordinates, appears in the viscous term of the incompressible Navier–Stokes equation.

**FIGURE 9–42**

The Navier–Stokes equation is the cornerstone of fluid mechanics.

Incompressible Navier–Stokes equation:

$$\rho \frac{D\vec{V}}{Dt} = -\vec{\nabla}P + \rho\vec{g} + \mu\nabla^2\vec{V} \quad (9-60)$$

Although we derived the components of Eq. 9–60 in Cartesian coordinates, the vector form of Eq. 9–60 is valid in any orthogonal coordinate system. This famous equation is named in honor of the French engineer Louis Marie Henri Navier (1785–1836) and the English mathematician Sir George Gabriel Stokes (1819–1903), who both developed the viscous terms, although independently of each other.

The Navier–Stokes equation is the cornerstone of fluid mechanics (Fig. 9–42). It may look harmless enough, but it is an unsteady, nonlinear, second-order, partial differential equation. If we were able to solve this equation for flows of any geometry, this book would be about half as thick. Unfortunately, analytical solutions are unobtainable except for very simple flow fields. It is not too far from the truth to say that the rest of this book is devoted to solving Eq. 9–60! In fact, many researchers have spent their entire careers trying to solve the Navier–Stokes equation.

Equation 9–60 has four unknowns (three velocity components and pressure), yet it represents only three equations (three components since it is a vector equation). Obviously we need another equation to make the problem solvable. The fourth equation is the incompressible continuity equation (Eq. 9–16). Before we attempt to solve this set of differential equations, we need to choose a coordinate system and expand the equations in that coordinate system.

Continuity and Navier–Stokes Equations in Cartesian Coordinates

The continuity equation (Eq. 9–16) and the Navier–Stokes equation (Eq. 9–60) are expanded in Cartesian coordinates (x, y, z) and (u, v, w):

Incompressible continuity equation:

$$\frac{\partial u}{\partial x} + \frac{\partial v}{\partial y} + \frac{\partial w}{\partial z} = 0 \quad (9-61a)$$

x-component of the incompressible Navier–Stokes equation:

$$\rho \left(\frac{\partial u}{\partial t} + u \frac{\partial u}{\partial x} + v \frac{\partial u}{\partial y} + w \frac{\partial u}{\partial z} \right) = -\frac{\partial P}{\partial x} + \rho g_x + \mu \left(\frac{\partial^2 u}{\partial x^2} + \frac{\partial^2 u}{\partial y^2} + \frac{\partial^2 u}{\partial z^2} \right) \quad (9-61b)$$

y-component of the incompressible Navier–Stokes equation:

$$\rho \left(\frac{\partial v}{\partial t} + u \frac{\partial v}{\partial x} + v \frac{\partial v}{\partial y} + w \frac{\partial v}{\partial z} \right) = -\frac{\partial P}{\partial y} + \rho g_y + \mu \left(\frac{\partial^2 v}{\partial x^2} + \frac{\partial^2 v}{\partial y^2} + \frac{\partial^2 v}{\partial z^2} \right) \quad (9-61c)$$

z-component of the incompressible Navier–Stokes equation:

$$\rho \left(\frac{\partial w}{\partial t} + u \frac{\partial w}{\partial x} + v \frac{\partial w}{\partial y} + w \frac{\partial w}{\partial z} \right) = -\frac{\partial P}{\partial z} + \rho g_z + \mu \left(\frac{\partial^2 w}{\partial x^2} + \frac{\partial^2 w}{\partial y^2} + \frac{\partial^2 w}{\partial z^2} \right) \quad (9-61d)$$

Continuity and Navier–Stokes Equations in Cylindrical Coordinates

The continuity equation (Eq. 9–16) and the Navier–Stokes equation (Eq. 9–60) are expanded in cylindrical coordinates (r, θ, z) and (u_r, u_θ, u_z):

$$\text{Incompressible continuity equation: } \frac{1}{r} \frac{\partial(ru_r)}{\partial r} + \frac{1}{r} \frac{\partial(u_\theta)}{\partial \theta} + \frac{\partial(u_z)}{\partial z} = 0 \quad (9-62a)$$

r-component of the incompressible Navier–Stokes equation:

$$\begin{aligned} \rho \left(\frac{\partial u_r}{\partial t} + u_r \frac{\partial u_r}{\partial r} + \frac{u_\theta}{r} \frac{\partial u_r}{\partial \theta} - \frac{u_\theta^2}{r} + u_z \frac{\partial u_r}{\partial z} \right) \\ = -\frac{\partial P}{\partial r} + \rho g_r + \mu \left[\frac{1}{r} \frac{\partial}{\partial r} \left(r \frac{\partial u_r}{\partial r} \right) - \frac{u_r}{r^2} + \frac{1}{r^2} \frac{\partial^2 u_r}{\partial \theta^2} - \frac{2}{r^2} \frac{\partial u_\theta}{\partial \theta} + \frac{\partial^2 u_r}{\partial z^2} \right] \end{aligned} \quad (9-62b)$$

θ-component of the incompressible Navier–Stokes equation:

$$\begin{aligned} \rho \left(\frac{\partial u_\theta}{\partial t} + u_r \frac{\partial u_\theta}{\partial r} + \frac{u_\theta}{r} \frac{\partial u_\theta}{\partial \theta} + \frac{u_r u_\theta}{r} + u_z \frac{\partial u_\theta}{\partial z} \right) \\ = -\frac{1}{r} \frac{\partial P}{\partial \theta} + \rho g_\theta + \mu \left[\frac{1}{r} \frac{\partial}{\partial r} \left(r \frac{\partial u_\theta}{\partial r} \right) - \frac{u_\theta}{r^2} + \frac{1}{r^2} \frac{\partial^2 u_\theta}{\partial \theta^2} + \frac{2}{r^2} \frac{\partial u_r}{\partial \theta} + \frac{\partial^2 u_\theta}{\partial z^2} \right] \end{aligned} \quad (9-62c)$$

z-component of the incompressible Navier–Stokes equation:

$$\begin{aligned} \rho \left(\frac{\partial u_z}{\partial t} + u_r \frac{\partial u_z}{\partial r} + \frac{u_\theta}{r} \frac{\partial u_z}{\partial \theta} + u_z \frac{\partial u_z}{\partial z} \right) \\ = -\frac{\partial P}{\partial z} + \rho g_z + \mu \left[\frac{1}{r} \frac{\partial}{\partial r} \left(r \frac{\partial u_z}{\partial r} \right) + \frac{1}{r^2} \frac{\partial^2 u_z}{\partial \theta^2} + \frac{\partial^2 u_z}{\partial z^2} \right] \end{aligned} \quad (9-62d)$$

The first two viscous terms in Eqs. 9–62b and 9–62c can be manipulated to a different form that is often more useful when solving these equations (Fig. 9–43). The derivation is left as an exercise. The “extra” terms on both sides of the *r*- and *θ*-components of the Navier–Stokes equation (Eqs. 9–62b and 9–62c) arise because of the special nature of cylindrical coordinates. Namely, as we move in the *θ*-direction, the unit vector \vec{e}_r also changes direction; thus the *r*- and *θ*-components are *coupled* (Fig. 9–44). (This coupling effect is not present in Cartesian coordinates, and thus there are no “extra” terms in Eqs. 9–61.)

For completeness, the six independent components of the viscous stress tensor are listed here in cylindrical coordinates,

$$\begin{aligned} \tau_{ij} &= \begin{pmatrix} \tau_{rr} & \tau_{r\theta} & \tau_{rz} \\ \tau_{\theta r} & \tau_{\theta\theta} & \tau_{\theta z} \\ \tau_{zr} & \tau_{z\theta} & \tau_{zz} \end{pmatrix} \\ &= \begin{pmatrix} 2\mu \frac{\partial u_r}{\partial r} & \mu \left[r \frac{\partial}{\partial r} \left(\frac{u_\theta}{r} \right) + \frac{1}{r} \frac{\partial u_r}{\partial \theta} \right] & \mu \left(\frac{\partial u_r}{\partial z} + \frac{\partial u_z}{\partial r} \right) \\ \mu \left[r \frac{\partial}{\partial r} \left(\frac{u_\theta}{r} \right) + \frac{1}{r} \frac{\partial u_r}{\partial \theta} \right] & 2\mu \left(\frac{1}{r} \frac{\partial u_\theta}{\partial \theta} + \frac{u_r}{r} \right) & \mu \left(\frac{\partial u_\theta}{\partial z} + \frac{1}{r} \frac{\partial u_z}{\partial \theta} \right) \\ \mu \left(\frac{\partial u_r}{\partial z} + \frac{\partial u_z}{\partial r} \right) & \mu \left(\frac{\partial u_\theta}{\partial z} + \frac{1}{r} \frac{\partial u_z}{\partial \theta} \right) & 2\mu \frac{\partial u_z}{\partial z} \end{pmatrix} \end{aligned} \quad (9-63)$$

- Alternative Form of the Viscous Terms
- It can be shown that

$$\begin{aligned} \frac{1}{r} \frac{\partial}{\partial r} \left(r \frac{\partial u_r}{\partial r} \right) - \frac{u_r}{r^2} \\ = \frac{\partial}{\partial r} \left(\frac{1}{r} \frac{\partial}{\partial r} (ru_r) \right) \end{aligned}$$
- and

$$\begin{aligned} \frac{1}{r} \frac{\partial}{\partial r} \left(r \frac{\partial u_\theta}{\partial r} \right) - \frac{u_\theta}{r^2} \\ = \frac{\partial}{\partial r} \left(\frac{1}{r} \frac{\partial}{\partial r} (ru_\theta) \right) \end{aligned}$$
-
-

FIGURE 9–43

An alternative form for the first two viscous terms in the *r*- and *θ*-components of the Navier–Stokes equation.

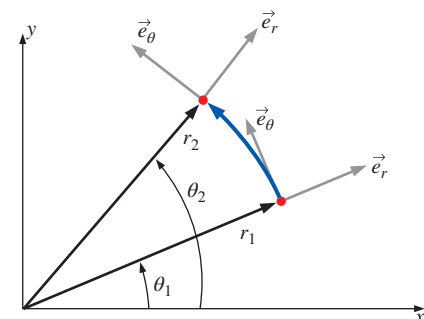


FIGURE 9–44

Unit vectors \vec{e}_r and \vec{e}_θ in cylindrical coordinates are *coupled*: movement in the *θ*-direction causes \vec{e}_r to change direction, and leads to extra terms in the *r*- and *θ*-components of the Navier–Stokes equation.

Three-Dimensional Incompressible Flow

Four variables or unknowns:

- Pressure P
- Three components of velocity \vec{V}

Four equations of motion:

- Continuity, $\vec{\nabla} \cdot \vec{V} = 0$
- Three components of Navier–Stokes, $\rho \frac{D\vec{V}}{Dt} = -\vec{\nabla} P + \rho \vec{g} + \mu \nabla^2 \vec{V}$

FIGURE 9–45

A general three-dimensional but incompressible flow field with constant properties requires four equations to solve for four unknowns.

9–6 ▪ DIFFERENTIAL ANALYSIS OF FLUID FLOW PROBLEMS

In this section we show how to apply the differential equations of motion in both Cartesian and cylindrical coordinates. There are two types of problems for which the differential equations (continuity and Navier–Stokes) are useful:

- Calculating the pressure field for a known velocity field
- Calculating both the velocity and pressure fields for a flow of known geometry and known boundary conditions

For simplicity, we consider only incompressible flow, eliminating calculation of ρ as a variable. In addition, the form of the Navier–Stokes equation derived in Section 9–5 is valid only for Newtonian fluids with constant properties (viscosity, thermal conductivity, etc.). Finally, we assume negligible temperature variations, so that T is not a variable. We are left with four variables or unknowns (pressure plus three components of velocity), and we have four differential equations (Fig. 9–45).

Calculation of the Pressure Field for a Known Velocity Field

The first set of examples involves calculation of the pressure field for a known velocity field. Since pressure does not appear in the continuity equation, we can theoretically generate a velocity field based solely on conservation of mass. However, since velocity appears in both the continuity equation and the Navier–Stokes equation, these two equations are *coupled*. In addition, pressure appears in all three components of the Navier–Stokes equation, and thus the velocity and pressure fields are also coupled. This intimate coupling between velocity and pressure enables us to calculate the pressure field for a known velocity field.

EXAMPLE 9–13 Calculating the Pressure Field in Cartesian Coordinates

Consider the steady, two-dimensional, incompressible velocity field of Example 9–9, namely, $\vec{V} = (u, v) = (ax + b)\vec{i} + (-ay + cx)\vec{j}$. Calculate the pressure as a function of x and y .

SOLUTION For a given velocity field, we are to calculate the pressure field.

Assumptions 1 The flow is steady and incompressible. 2 The fluid has constant properties. 3 The flow is two-dimensional in the xy -plane. 4 Gravity does not act in either the x - or y -direction.

Analysis First we check whether the given velocity field satisfies the two-dimensional, incompressible continuity equation:

$$\underbrace{\frac{\partial u}{\partial x}}_a + \underbrace{\frac{\partial v}{\partial y}}_{-a} + \underbrace{\frac{\partial w}{\partial z}}_{0(2-D)} = a - a = 0 \quad (1)$$

Thus, continuity is indeed satisfied by the given velocity field. If continuity were *not* satisfied, we would stop our analysis—the given velocity field would not be physically possible, and we could not calculate a pressure field.

Next, we consider the y -component of the Navier–Stokes equation:

$$\rho \left(\underbrace{\frac{\partial p}{\partial t}}_{0 \text{ (steady)}} + u \underbrace{\frac{\partial v}{\partial x}}_{(ax+b)c} + v \underbrace{\frac{\partial v}{\partial y}}_{(-ay+cx)(-a)} + w \underbrace{\frac{\partial p}{\partial z}}_{0 \text{ (2-D)}} \right) = - \frac{\partial P}{\partial y} + \underbrace{\rho g_y}_{0} + \mu \left(\underbrace{\frac{\partial^2 p}{\partial x^2}}_0 + \underbrace{\frac{\partial^2 p}{\partial y^2}}_0 + \underbrace{\frac{\partial^2 p}{\partial z^2}}_0 \right)$$

The y -momentum equation reduces to

$$\frac{\partial P}{\partial y} = \rho(-acx - bc - a^2y + acx) = \rho(-bc - a^2y) \quad (2)$$

The y -momentum equation is satisfied if we can generate a pressure field that satisfies Eq. 2. In similar fashion, the x -momentum equation reduces to

$$\frac{\partial P}{\partial x} = \rho(-a^2x - ab) \quad (3)$$

The x -momentum equation is satisfied if we can generate a pressure field that satisfies Eq. 3.

In order for a steady flow solution to exist, P cannot be a function of time. Furthermore, a physically realistic steady, incompressible flow field requires a pressure field $P(x, y)$ that is a smooth function of x and y (there can be no sudden discontinuities in either P or a derivative of P). Mathematically, this requires that the order of differentiation (x then y versus y then x) should not matter (Fig. 9–46). We check whether this is so by cross-differentiating Eqs. 2 and 3, respectively,

$$\frac{\partial^2 P}{\partial x \partial y} = \frac{\partial}{\partial x} \left(\frac{\partial P}{\partial y} \right) = 0 \quad \text{and} \quad \frac{\partial^2 P}{\partial y \partial x} = \frac{\partial}{\partial y} \left(\frac{\partial P}{\partial x} \right) = 0 \quad (4)$$

Equation 4 shows that P is indeed a smooth function of x and y . Thus, *the given velocity field satisfies the steady, two-dimensional, incompressible Navier–Stokes equation.*

If at this point in the analysis, the cross-differentiation of pressure were to yield two incompatible relationships (in other words if the equation in Fig. 9–46 were not satisfied) we would conclude that the given velocity field could not satisfy the steady, two-dimensional, incompressible Navier–Stokes equation, and we would abandon our attempt to calculate a steady pressure field.

To calculate $P(x, y)$, we partially integrate Eq. 2 (with respect to y)

Pressure field from y -momentum:

$$P(x, y) = \rho \left(-bcy - \frac{a^2y^2}{2} \right) + g(x) \quad (5)$$

Note that we add an arbitrary function of the other variable x rather than a constant of integration since this is a partial integration. We then take the partial derivative of Eq. 5 with respect to x to obtain

$$\frac{\partial P}{\partial x} = g'(x) = \rho(-a^2x - ab) \quad (6)$$

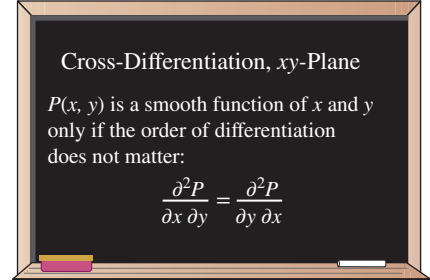


FIGURE 9–46

For a two-dimensional flow field in the xy -plane, cross-differentiation reveals whether pressure P is a smooth function.

where we have equated our result to Eq. 3 for consistency. We now integrate Eq. 6 to obtain the function $g(x)$:

$$g(x) = \rho \left(-\frac{a^2 x^2}{2} - abx \right) + C_1 \quad (7)$$

where C_1 is an arbitrary constant of integration. Finally, we substitute Eq. 7 into Eq. 5 to obtain our final expression for $P(x, y)$. The result is

$$P(x, y) = \rho \left(-\frac{a^2 x^2}{2} - \frac{a^2 y^2}{2} - abx - bcy \right) + C_1 \quad (8)$$

Discussion For practice, and as a check of our algebra, you should differentiate Eq. 8 with respect to both y and x , and compare to Eqs. 2 and 3. In addition, try to obtain Eq. 8 by starting with Eq. 3 rather than Eq. 2; you should get the same answer.

Notice that the final equation (Eq. 8) for pressure in Example 9–13 contains an arbitrary constant C_1 . This illustrates an important point about the pressure field in an incompressible flow; namely,

The velocity field in an incompressible flow is not affected by the absolute magnitude of pressure, but only by pressure differences.

This should not be surprising if we look at the Navier–Stokes equation, where P appears only as a *gradient*, never by itself. Another way to explain this statement is that it is not the absolute magnitude of pressure that matters, but only pressure *differences* (Fig. 9–47). A direct result of the statement is that we can calculate the pressure field to within an arbitrary constant, but in order to determine that constant (C_1 in Example 9–13), we must measure (or otherwise obtain) P somewhere in the flow field. In other words, we require a pressure boundary condition.

We illustrate this point with an example generated using **computational fluid dynamics (CFD)**, where the continuity and Navier–Stokes equations are solved numerically (Chap. 15). Consider downward flow of air through a channel in which there is a nonsymmetrical blockage (Fig. 9–48). (Note that the computational flow domain extends much further upstream and downstream than shown in Fig. 9–48.) We calculate two cases that are identical except for the pressure condition. In case 1 we set the gage pressure far downstream of the blockage to zero. In case 2 we set the pressure at the same location to 500 Pa gage pressure. The gage pressure at the top center of the field of view and at the bottom center of the field of view are shown in Fig. 9–48 for both cases, as generated by the two CFD solutions. You can see that the pressure field for case 2 is identical to that of case 1 except that the pressure is everywhere increased by 500 Pa. Also shown in Fig. 9–48 are a velocity vector plot and a streamline plot for each case. The results are identical, confirming our statement that the velocity field is not affected by the absolute magnitude of the pressure, but only by pressure *differences*. Subtracting the pressure at the bottom from that at the top, we see that $\Delta P = 12.784$ Pa for both cases.

The statement about pressure differences is *not* true for *compressible* flow fields, where P is the thermodynamic pressure rather than the mechanical

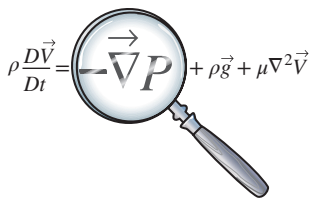


FIGURE 9–47

Since pressure appears only as a gradient in the incompressible Navier–Stokes equation, the absolute magnitude of pressure is not relevant—only pressure *differences* matter.

pressure. In such cases, P is coupled with density and temperature through an equation of state, and the absolute magnitude of pressure *is* important. A compressible flow solution requires not only mass and momentum equations, but also an energy equation and an equation of state.

We take this opportunity to comment further about the CFD results shown in Fig. 9–48. You can learn a lot about the physics of fluid flow by studying relatively simple flows like this. Notice that most of the pressure drop occurs across the throat of the channel where the flow is rapidly accelerated. There is also flow separation downstream of the blockage; rapidly moving air cannot turn around a sharp corner, and the flow separates off the walls as it exits the opening. The streamlines indicate large recirculating regions on both sides of the channel downstream of the blockage. Pressure is low in these recirculating regions. The velocity vectors indicate an inverse bell-shaped velocity profile exiting the opening—much like an exhaust jet. Because of the nonsymmetric nature of the geometry, the jet turns to the right, and the flow reattaches to the right wall much sooner than to the left wall. The pressure increases somewhat in the region where the jet impinges on the right wall, as you might expect. Finally, notice that as the air accelerates to squeeze through the orifice, the streamlines converge (as discussed in Section 9–3). As the jet of air fans out downstream, the streamlines diverge somewhat. Notice also that the streamlines in the recirculating zones are very far apart, indicating that the velocities are relatively small there; this is verified by the velocity vector plots.

Finally, we note that most CFD codes do *not* calculate pressure by integration of the Navier–Stokes equation as we have done in Example 9–13. Instead, some kind of **pressure correction algorithm** is used. Most of the commonly used algorithms work by combining the continuity and Navier–Stokes equations in such a way that pressure appears in the continuity equation. The most popular pressure correction algorithms result in a form of **Poisson's equation** for the change in pressure ΔP from one iteration (n) to the next ($n + 1$),

$$\text{Poisson's equation for } \Delta P: \quad \nabla^2(\Delta P) = \text{RHS}_{(n)} \quad (9-64)$$

Then, as the computer iterates toward a solution, the modified continuity equation is used to “correct” the pressure field at iteration ($n + 1$) from its values at iteration (n),

$$\text{Correction for } P: \quad P_{(n+1)} = P_{(n)} + \Delta P$$

Details associated with the development of pressure correction algorithms is beyond the scope of the present text. An example for two-dimensional flows is developed in Gerhart, Gross, and Hochstein (1992).

EXAMPLE 9–14 Calculating the Pressure Field in Cylindrical Coordinates

- Consider the steady, two-dimensional, incompressible velocity field of Example 9–5 with function $f(\theta, t)$ equal to 0. This represents a line vortex whose axis lies along the z -coordinate (Fig. 9–49). The velocity components are $u_r = 0$ and $u_\theta = K/r$, where K is a constant. Calculate the pressure as a function of r and θ .

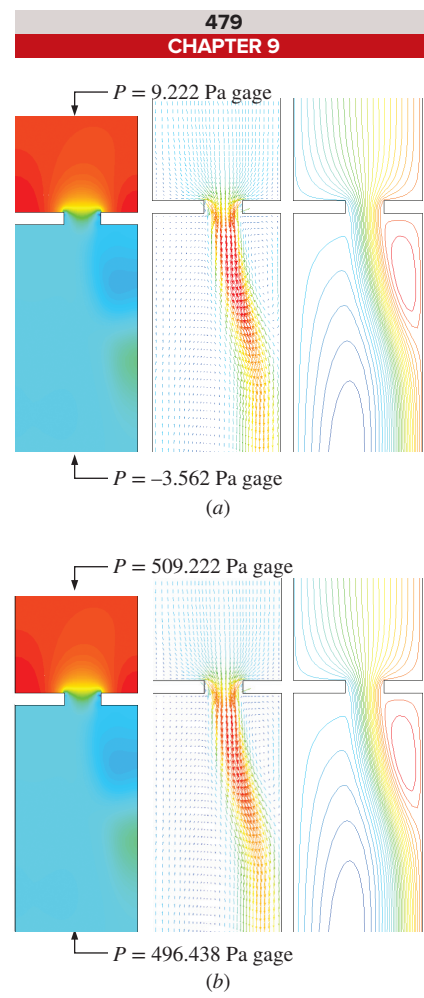
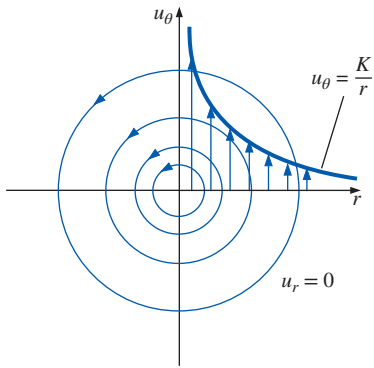


FIGURE 9–48
Filled pressure contour plot, velocity vector plot, and streamlines for downward flow of air through a channel with blockage: (a) case 1; (b) case 2—identical to case 1, except P is everywhere increased by 500 Pa.
On the contour plots, blue is low pressure and red is high pressure.

**FIGURE 9-49**

Streamlines and velocity profiles for a line vortex.

SOLUTION For a given velocity field, we are to calculate the pressure field.

Assumptions 1 The flow is steady. 2 The fluid is incompressible with constant properties. 3 The flow is two-dimensional in the $r\theta$ -plane. 4 Gravity does not act in either the r - or the θ -direction.

Analysis The flow field must satisfy both the continuity and the momentum equations, Eqs. 9-62. For steady, two-dimensional, incompressible flow,

$$\text{Incompressible continuity: } \frac{1}{r} \underbrace{\frac{\partial(ru_r)}{\partial r}}_0 + \frac{1}{r} \underbrace{\frac{\partial(u_\theta)}{\partial \theta}}_0 + \underbrace{\frac{\partial(u_z)}{\partial z}}_0 = 0$$

Thus, the incompressible continuity equation is satisfied. Now we look at the θ component of the Navier-Stokes equation (Eq. 9-62c):

$$\begin{aligned} & \rho \left(\underbrace{\frac{\partial u_\theta}{\partial t} + u_r \frac{\partial u_\theta}{\partial r} + \frac{u_\theta}{r} \frac{\partial u_\theta}{\partial \theta}}_{0 \text{ (steady)}} + \frac{u_r u_\theta}{r} + u_z \frac{\partial u_\theta}{\partial z} \right) \\ & \quad (0)(0)\left(-\frac{K}{r^2}\right) \quad \left(\frac{K}{r^2}\right)(0) \quad 0 \quad 0 \text{ (2-D)} \\ & = -\frac{1}{r} \underbrace{\frac{\partial P}{\partial \theta}}_0 + \rho g_\theta + \mu \left(\underbrace{\frac{1}{r} \frac{\partial}{\partial r} \left(r \frac{\partial u_\theta}{\partial r} \right)}_{\frac{K}{r^3}} - \frac{u_\theta}{r^2} + \underbrace{\frac{1}{r^2} \frac{\partial^2 u_\theta}{\partial \theta^2}}_0 + \underbrace{\frac{2}{r^2} \frac{\partial u_r}{\partial \theta}}_0 + \underbrace{\frac{\partial^2 u_\theta}{\partial z^2}}_0 \right) \end{aligned}$$

The θ -momentum equation therefore reduces to

$$\text{θ-momentum: } \frac{\partial P}{\partial \theta} = 0 \quad (1)$$

Thus, the θ -momentum equation is satisfied if we can generate an appropriate pressure field that satisfies Eq. 1. In similar fashion, the r -momentum equation (Eq. 9-62b) reduces to

$$\text{r-momentum: } \frac{\partial P}{\partial r} = \rho \frac{K^2}{r^3} \quad (2)$$

Thus, the r -momentum equation is satisfied if we can generate a pressure field that satisfies Eq. 2.

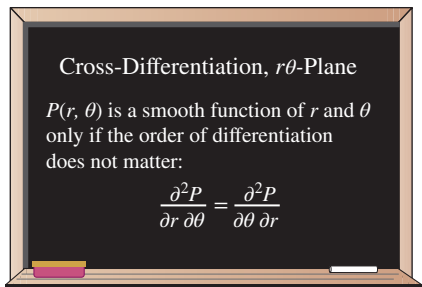
In order for a steady flow solution to exist, P cannot be a function of time. Furthermore, a physically realistic steady, incompressible flow field requires a pressure field $P(r, \theta)$ that is a smooth function of r and θ . Mathematically, this requires that the order of differentiation (r then θ versus θ then r) should not matter (Fig. 9-50). We check whether this is so by cross-differentiating the pressure:

$$\frac{\partial^2 P}{\partial r \partial \theta} = \frac{\partial}{\partial r} \left(\frac{\partial P}{\partial \theta} \right) = 0 \quad \text{and} \quad \frac{\partial^2 P}{\partial \theta \partial r} = \frac{\partial}{\partial \theta} \left(\frac{\partial P}{\partial r} \right) = 0 \quad (3)$$

Equation 3 shows that P is indeed a smooth function of r and θ . Thus, the given velocity field satisfies the steady, two-dimensional, incompressible Navier-Stokes equation.

We integrate Eq. 1 with respect to θ to obtain an expression for $P(r, \theta)$,

$$\text{Pressure field from θ-momentum: } P(r, \theta) = 0 + g(r) \quad (4)$$

**FIGURE 9-50**

For a two-dimensional flow field in the $r\theta$ -plane, cross-differentiation reveals whether pressure P is a smooth function.

Note that we added an arbitrary function of the other variable r , rather than a constant of integration, since this is a partial integration. We take the partial derivative of Eq. 4 with respect to r to obtain

$$\frac{\partial P}{\partial r} = g'(r) = \rho \frac{K^2}{r^3} \quad (5)$$

where we have equated our result to Eq. 2 for consistency. We integrate Eq. 5 to obtain the function $g(r)$:

$$g(r) = -\frac{1}{2} \rho \frac{K^2}{r^2} + C \quad (6)$$

where C is an arbitrary constant of integration. Finally, we substitute Eq. 6 into Eq. 4 to obtain our final expression for $P(r, \theta)$. The result is

$$P(r, \theta) = -\frac{1}{2} \rho \frac{K^2}{r^2} + C \quad (7)$$

Thus the pressure field for a line vortex decreases like $1/r^2$ as we approach the origin. (The origin itself is a singular point.) This flow field is a simplistic model of a tornado or hurricane, and the low pressure at the center is the “eye of the storm” (Fig. 9–51). We note that this flow field is irrotational, and thus Bernoulli’s equation can be used instead to calculate the pressure. If we call the pressure P_∞ far away from the origin ($r \rightarrow \infty$), where the local velocity approaches zero, Bernoulli’s equation shows that at any distance r from the origin,

$$\text{Bernoulli equation: } P + \frac{1}{2} \rho V^2 = P_\infty \rightarrow P = P_\infty - \frac{1}{2} \rho \frac{K^2}{r^2} \quad (8)$$

Equation 8 agrees with our solution (Eq. 7) from the Navier–Stokes equation if we set constant C equal to P_∞ . A region of rotational flow near the origin would avoid the singularity there and would yield a more physically realistic model of a tornado.

Discussion For practice, try to obtain Eq. 7 by starting with Eq. 2 rather than Eq. 1; you should get the same answer.

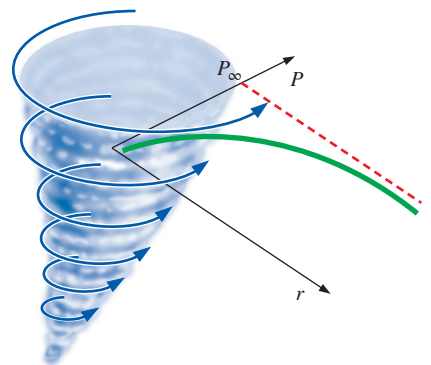


FIGURE 9–51

The two-dimensional line vortex is a simple approximation of a tornado; the lowest pressure is at the center of the vortex.

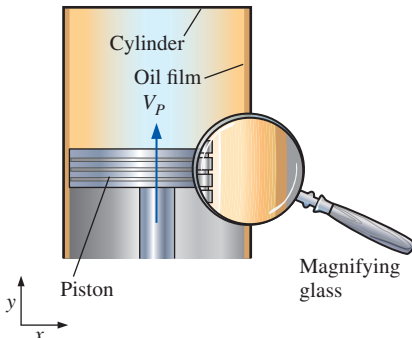
Exact Solutions of the Continuity and Navier–Stokes Equations

The remaining example problems in this section are exact solutions of the differential equation set consisting of the incompressible continuity and Navier–Stokes equations. As you will see, these problems are by necessity simple, so that they are solvable. Most of them assume infinite boundaries and fully developed conditions so that the advective terms on the left side of the Navier–Stokes equation disappear. In addition, they are laminar, two-dimensional, and either steady or dependent on time in a predefined manner. There are six basic steps in the procedure used to solve these problems, as listed in Fig. 9–52. Step 2 is especially critical, since the boundary conditions determine the uniqueness of the solution. Step 4 is not possible analytically except for simple problems. In step 5, enough boundary conditions must be available to solve for all the constants of integration produced in step 4. Step 6 involves verifying that all the differential equations and boundary conditions

- Step 1: Set up the problem and geometry (sketches are helpful), identifying all relevant dimensions and parameters.
- Step 2: List all appropriate assumptions, approximations, simplifications, and boundary conditions.
- Step 3: Simplify the differential equations of motion (continuity and Navier–Stokes) as much as possible.
- Step 4: Integrate the equations, leading to one or more constants of integration.
- Step 5: Apply boundary conditions to solve for the constants of integration.
- Step 6: Verify your results.

FIGURE 9–52

Procedure for solving the incompressible continuity and Navier–Stokes equations.

**FIGURE 9-53**

A piston moving at speed V_p in a cylinder. A thin film of oil is sheared between the piston and the cylinder; a magnified view of the oil film is shown. The *no-slip boundary condition* requires that the velocity of fluid adjacent to a wall equal that of the wall.

are satisfied. We advise you to follow these steps, even in cases where some of the steps seem trivial, in order to learn the procedure.

While the examples shown here are simple, they adequately illustrate the procedure used to solve these differential equations. In Chap. 15 we discuss how computers have enabled us to solve the Navier–Stokes equations *numerically* for much more complicated flows using computational fluid dynamics (CFD). You will see that the same procedure is used there—specification of geometry, application of boundary conditions, integration of the differential equations, etc., although the steps are not always followed in the same order.

Boundary Conditions

Since boundary conditions are so critical to a proper solution, we discuss the types of boundary conditions that are commonly encountered in fluid flow analyses. The most-used boundary condition is the **no-slip condition**, which states that for a fluid in contact with a solid wall, *the velocity of the fluid must equal that of the wall*,

No-slip boundary condition:

$$\vec{V}_{\text{fluid}} = \vec{V}_{\text{wall}} \quad (9-65)$$

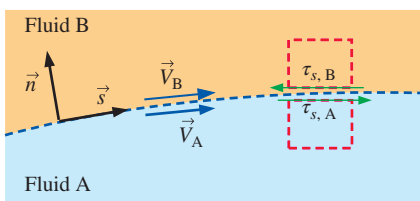
In other words, as its name implies, there is no “slip” between the fluid and the wall. Fluid particles adjacent to the wall adhere to the surface of the wall and move at the same velocity as the wall. A special case of Eq. 9-65 is for a stationary wall with $\vec{V}_{\text{wall}} = 0$; *the fluid adjacent to a stationary wall has zero velocity*. For cases in which temperature effects are also considered, the temperature of the fluid must equal that of the wall, i.e., $T_{\text{fluid}} = T_{\text{wall}}$. You must be careful to assign the no-slip condition according to your chosen *frame of reference*. Consider, for example, the thin film of oil between a piston and its cylinder wall (Fig. 9-53). From a stationary frame of reference, the fluid adjacent to the cylinder is at rest, and the fluid adjacent to the moving piston has velocity $\vec{V}_{\text{fluid}} = \vec{V}_{\text{wall}} = V_p \hat{j}$. From a frame of reference *moving with the piston*, however, the fluid adjacent to the piston has zero velocity, but the fluid adjacent to the cylinder has velocity $\vec{V}_{\text{fluid}} = \vec{V}_{\text{wall}} = -V_p \hat{j}$. An exception to the no-slip condition occurs in rarefied gas flows, such as during reentry of a spaceship or in the study of motion of extremely small (submicron) particles. In such flows the air can actually slip along the wall, but these flows are beyond the scope of the present text.

When two fluids (fluid A and fluid B) meet at an interface, the **interface boundary conditions** are

Interface boundary conditions:

$$\vec{V}_A = \vec{V}_B \quad \text{and} \quad \tau_{s,A} = \tau_{s,B} \quad (9-66)$$

where, in addition to the condition that the velocities of the two fluids must be equal, the shear stress τ_s acting on a fluid particle adjacent to the interface in the direction parallel to the interface must also match between the two fluids (Fig. 9-54). Note that in the figure, $\tau_{s,A}$ is drawn on the *top* of the fluid particle in fluid A, while $\tau_{s,B}$ is drawn on the *bottom* of the fluid particle in fluid B, and we have considered the *direction* of shear stress carefully. Because of the sign convention on shear stress, the direction of the arrows in Fig. 9-54 is opposite (a consequence of Newton's third law). We note that although velocity is continuous across the interface, its slope is *not*. Also, if temperature effects are considered, $T_A = T_B$ at the interface, but there may be a discontinuity in the slope of temperature at the interface as well.

**FIGURE 9-54**

At an interface between two fluids, the velocity of the two fluids must be equal. In addition, the shear stress parallel to the interface must be the same in both fluids.

What about pressure at an interface? If surface tension effects are negligible or if the interface is nearly flat, $P_A = P_B$. If the interface is sharply curved, however, as in the meniscus of liquid rising in a capillary tube, the pressure on one side of the interface can be substantially different than that on the other side. You should recall from Chap. 2 that the pressure jump across an interface is inversely proportional to the radius of curvature of the interface, as a result of surface tension effects.

A degenerate form of the interface boundary condition occurs at the *free surface* of a liquid, meaning that fluid A is a liquid and fluid B is a gas (usually air). We illustrate a simple case in Fig. 9–55 where fluid A is liquid water and fluid B is air. The interface is flat and surface tension effects are negligible, but the water is moving horizontally (like water flowing in a calm river). In this case, the air and water velocities must match at the surface and the shear stress acting on a water particle on the surface of the water must equal that acting on an air particle just above the surface. According to Eq. 9–66,

Boundary conditions at water-air interface:

$$u_{\text{water}} = u_{\text{air}} \quad \text{and} \quad \tau_{s, \text{water}} = \mu_{\text{water}} \frac{\partial u}{\partial y} \Big|_{\text{water}} = \tau_{s, \text{air}} = \mu_{\text{air}} \frac{\partial u}{\partial y} \Big|_{\text{air}} \quad (9-67)$$

A quick glance at the fluid property tables reveals that μ_{water} is over 50 times greater than μ_{air} . In order for the shear stresses to be equal, Eq. 9–67 requires that slope $(\partial u / \partial y)_{\text{air}}$ be more than 50 times greater than $(\partial u / \partial y)_{\text{water}}$. Thus, it is reasonable to approximate the shear stress acting at the surface of the water as negligibly small compared to shear stresses elsewhere in the water. Another way to say this is that the moving water drags air along with it with little resistance from the air; in contrast, the air doesn't slow down the water by any significant amount. In summary, for the case of a liquid in contact with a gas, and with negligible surface tension effects, the **free-surface boundary conditions** are

Free-surface boundary conditions: $P_{\text{liquid}} = P_{\text{gas}}$ and $\tau_{s, \text{liquid}} \approx 0$ (9-68)

Other boundary conditions arise depending on the problem setup. For example, we often need to define **inlet boundary conditions** at a boundary of a flow domain where fluid enters the domain. Likewise, we define **outlet boundary conditions** at an outflow. **Symmetry boundary conditions** are useful along an axis or plane of symmetry. For example, the appropriate symmetry boundary conditions along a horizontal plane of symmetry are illustrated in Fig. 9–56. For unsteady flow problems we also need to define **initial conditions** (at the starting time, usually $t = 0$).

In Examples 9–15 through 9–19, we apply boundary conditions from Eqs. 9–65 through 9–68 where appropriate. These and other boundary conditions are discussed in much greater detail in Chap. 15 where we apply them to CFD solutions.

EXAMPLE 9–15 Fully Developed Couette Flow

Consider steady, incompressible, laminar flow of a Newtonian fluid in the narrow gap between two infinite parallel plates (Fig. 9–57). The top plate is moving at speed V , and the bottom plate is stationary. The distance between these two plates is h , and gravity acts in the negative z -direction (into the page in Fig. 9–57). There is no applied pressure other than hydrostatic pressure due to gravity. This

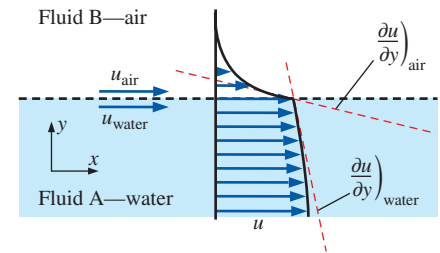


FIGURE 9–55

Along a horizontal *free surface* of water and air, the water and air velocities must be equal and the shear stresses must match. However, since $\mu_{\text{air}} \ll \mu_{\text{water}}$, a good approximation is that the shear stress at the water surface is negligibly small.

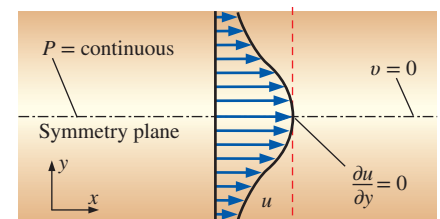


FIGURE 9–56

Boundary conditions along a plane of symmetry are defined so as to ensure that the flow field on one side of the symmetry plane is a *mirror image* of that on the other side, as shown here for a horizontal symmetry plane.

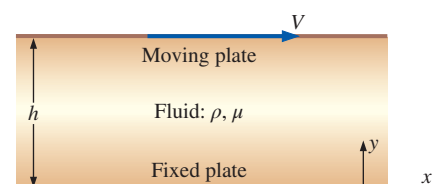


FIGURE 9–57

Geometry of Example 9–15: viscous flow between two infinite plates; upper plate moving and lower plate stationary.

flow is called **Couette flow**. Calculate the velocity and pressure fields, and estimate the shear force per unit area acting on the bottom plate.

SOLUTION For a given geometry and set of boundary conditions, we are to calculate the velocity and pressure fields, and then estimate the shear force per unit area acting on the bottom plate.

Assumptions 1 The plates are infinite in x and z . 2 The flow is steady, i.e., $\partial/\partial t$ of anything is zero. 3 This is a parallel flow (we assume that the y -component of velocity, v , is zero). 4 The fluid is incompressible and Newtonian with constant properties, and the flow is laminar. 5 Pressure $P = \text{constant}$ with respect to x . In other words, there is no applied pressure gradient pushing the flow in the x -direction; the flow establishes itself due to viscous stresses caused by the moving upper plate. 6 The velocity field is purely two-dimensional, meaning here that $w = 0$ and $\partial/\partial z$ of any velocity component is zero. 7 Gravity acts in the negative z -direction (into the page in Fig. 9–57). We express this mathematically as $\vec{g} = -g\vec{k}$, or $g_x = g_y = 0$ and $g_z = -g$.

Analysis To obtain the velocity and pressure fields, we follow the step-by-step procedure outlined in Fig. 9–52.

Step 1 Set up the problem and the geometry. See Fig. 9–57.

Step 2 List assumptions and boundary conditions. We have numbered and listed seven assumptions (above). The boundary conditions come from imposing the no-slip condition: (1) At the bottom plate ($y = 0$), $u = v = w = 0$. (2) At the top plate ($y = h$), $u = V$, $v = 0$, and $w = 0$.

Step 3 Simplify the differential equations. We start with the incompressible continuity equation in Cartesian coordinates, Eq. 9–61a,

$$\frac{\partial u}{\partial x} + \underbrace{\frac{\partial v}{\partial y}}_{\text{assumption 3}} + \underbrace{\frac{\partial w}{\partial z}}_{\text{assumption 6}} = 0 \rightarrow \frac{\partial u}{\partial x} = 0 \quad (1)$$

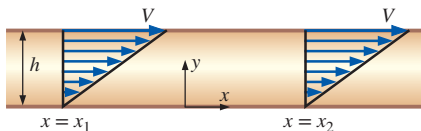


FIGURE 9–58

A *fully developed* region of a flow field is a region where the velocity profile does not change with downstream distance. Fully developed flows are encountered in long, straight channels and pipes. Fully developed Couette flow is shown here—the velocity profile at x_2 is identical to that at x_1 .

Equation 1 tells us that u is not a function of x . In other words, it doesn't matter where we place our origin—the flow is the same at any x -location. The phrase **fully developed** is often used to describe this situation (Fig. 9–58). This can also be obtained directly from assumption 1, which tells us that there is nothing special about any x -location since the plates are infinite in length. Furthermore, since u is not a function of time (assumption 2) or z (assumption 6), we conclude that u is at most a function of y ,

$$\text{Result of continuity:} \quad u = u(y) \text{ only} \quad (2)$$

We now simplify the x -momentum equation (Eq. 9–61b) as far as possible. It is good practice to list the reason for crossing out a term, as we do here:

$$\begin{aligned} \rho \left(\underbrace{\frac{\partial u}{\partial t}}_{\text{assumption 2}} + \underbrace{u \frac{\partial u}{\partial x}}_{\text{continuity}} + \underbrace{v \frac{\partial u}{\partial y}}_{\text{assumption 3}} + \underbrace{w \frac{\partial u}{\partial z}}_{\text{assumption 6}} \right) &= - \underbrace{\frac{\partial P}{\partial x}}_{\text{assumption 5}} + \underbrace{\rho g_x}_{\text{assumption 7}} \\ &+ \mu \left(\underbrace{\frac{\partial^2 u}{\partial x^2}}_{\text{continuity}} + \underbrace{\frac{\partial^2 u}{\partial y^2}}_{\text{assumption 6}} + \underbrace{\frac{\partial^2 u}{\partial z^2}}_{\text{assumption 6}} \right) \rightarrow \frac{d^2 u}{dy^2} = 0 \quad 3) \end{aligned}$$

Notice that the material acceleration (left-hand side of Eq. 3) is zero, implying that fluid particles are not accelerating in this flow field, neither by local (unsteady) acceleration, nor by advective acceleration. Since the advective acceleration terms make the Navier–Stokes equation nonlinear, this greatly simplifies the problem. In fact, all other terms in Eq. 3 have disappeared except for a lone viscous term, which must then itself equal zero. Also notice that we have changed from a partial derivative ($\partial/\partial y$) to a total derivative (d/dy) in Eq. 3 as a direct result of Eq. 2. We do not show the details here, but you can show in similar fashion that every term except the pressure term in the y -momentum equation (Eq. 9–61c) goes to zero, forcing that lone term to also be zero,

$$\frac{\partial P}{\partial y} = 0 \quad (4)$$

In other words, P is not a function of y . Since P is also not a function of time (assumption 2) or x (assumption 5), P is at most a function of z ,

Result of y-momentum: $P = P(z)$ only (5)

Finally, by assumption 6 the z -component of the Navier–Stokes equation (Eq. 9–61d) simplifies to

$$\frac{\partial P}{\partial z} = -\rho g \quad \rightarrow \quad \frac{dP}{dz} = -\rho g \quad (6)$$

where we used Eq. 5 to convert from a partial derivative to a total derivative.

Step 4 Solve the differential equations. Continuity and y -momentum have already been “solved,” resulting in Eqs. 2 and 5, respectively. Equation 3 (x -momentum) is integrated twice to get

$$u = C_1 y + C_2 \quad (7)$$

where C_1 and C_2 are constants of integration. Equation 6 (z -momentum) is integrated once, resulting in

$$P = -\rho g z + C_3 \quad (8)$$

Step 5 Apply boundary conditions. We begin with Eq. 8. Since we have not specified boundary conditions for pressure, C_3 remains an arbitrary constant. (Recall that for incompressible flow, the absolute pressure can be specified only if P is known somewhere in the flow.) For example, if we let $P = P_0$ at $z = 0$, then $C_3 = P_0$ and Eq. 8 becomes

Final solution for pressure field: $P = P_0 - \rho g z \quad (9)$

Alert readers will notice that Eq. 9 represents a simple **hydrostatic pressure distribution** (pressure decreasing linearly as z increases). We conclude that, at least for this problem, *hydrostatic pressure acts independently of the flow*. More generally, we make the following statement (see also Fig. 9–59):

For incompressible flow fields without free surfaces, hydrostatic pressure does not contribute to the dynamics of the flow field.

In fact, in Chap. 10 we show how hydrostatic pressure can actually be removed from the equations of motion through use of a modified pressure.

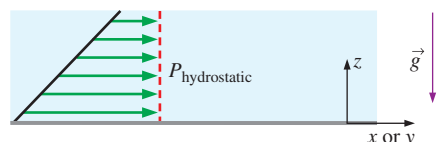
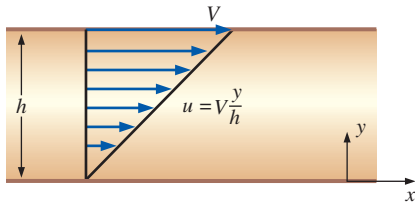
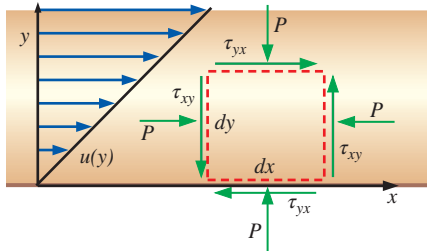


FIGURE 9–59

For incompressible flow fields *without free surfaces*, hydrostatic pressure does not contribute to the dynamics of the flow field.

**FIGURE 9-60**

The linear velocity profile of Example 9-15: Couette flow between parallel plates.

**FIGURE 9-61**

Stresses acting on a (greatly magnified) differential two-dimensional rectangular fluid element whose bottom face is in contact with the bottom plate of Example 9-15. Note that we are ignoring gravity in this case; otherwise pressure would increase in the direction of the gravitational acceleration.

We next apply boundary conditions (1) and (2) from step 2 to obtain constants C_1 and C_2 .

$$\text{Boundary condition (1): } u = C_1 \times 0 + C_2 = 0 \rightarrow C_2 = 0$$

and

$$\text{Boundary condition (2): } u = C_1 \times h + 0 = V \rightarrow C_1 = V/h$$

Finally, Eq. 7 becomes

$$\text{Final result for velocity field: } \mathbf{u} = \frac{\mathbf{V} y}{h} \quad (10)$$

The velocity field reveals a simple linear velocity profile from $u = 0$ at the bottom plate to $u = V$ at the top plate, as sketched in Fig. 9-60.

Step 6 Verify the results. Using Eqs. 9 and 10, you can verify that all the differential equations and boundary conditions are satisfied.

To calculate the shear force per unit area acting on the bottom plate, we consider a rectangular fluid element whose bottom face is in contact with the bottom plate (Fig. 9-61). Mathematically positive viscous stresses are shown. In this case, these stresses are in the proper direction since fluid above the differential element pulls it to the right while the wall below the element pulls it to the left. From Eq. 9-56, we write out the components of the viscous stress tensor,

$$\tau_{ij} = \begin{pmatrix} 2\mu \frac{\partial u}{\partial x} & \mu \left(\frac{\partial u}{\partial y} + \frac{\partial v}{\partial x} \right) & \mu \left(\frac{\partial u}{\partial z} + \frac{\partial w}{\partial x} \right) \\ \mu \left(\frac{\partial v}{\partial x} + \frac{\partial u}{\partial y} \right) & 2\mu \frac{\partial v}{\partial y} & \mu \left(\frac{\partial v}{\partial z} + \frac{\partial w}{\partial y} \right) \\ \mu \left(\frac{\partial w}{\partial x} + \frac{\partial u}{\partial z} \right) & \mu \left(\frac{\partial w}{\partial y} + \frac{\partial v}{\partial z} \right) & 2\mu \frac{\partial w}{\partial z} \end{pmatrix} = \begin{pmatrix} 0 & \frac{V}{h} & 0 \\ \frac{V}{h} & 0 & 0 \\ 0 & 0 & 0 \end{pmatrix} \quad (11)$$

Since the dimensions of stress are force per unit area by definition, the force per unit area acting on the bottom face of the fluid element is equal to $\tau_{yx} = \mu V/h$ and acts in the negative x -direction, as sketched. The shear force per unit area on the wall is equal and opposite to this (Newton's third law); hence,

$$\text{Shear force per unit area acting on the wall: } \frac{\vec{F}}{A} = \mu \frac{V}{h} \vec{i} \quad (12)$$

The direction of this force agrees with our intuition; namely, the fluid tries to pull the bottom wall to the right, due to viscous effects (friction).

Discussion The z -component of the linear momentum equation is *uncoupled* from the rest of the equations; this explains why we get a hydrostatic pressure distribution in the z -direction, even though the fluid is not static, but moving. Equation 11 reveals that the viscous stress tensor is constant *everywhere* in the flow field, not just at the bottom wall (notice that none of the components of τ_{ij} is a function of location).

You may be questioning the usefulness of the final results of Example 9-15. After all, when do we encounter two infinite parallel plates, one of which is moving? Actually there *are* several practical flows for which the Couette flow solution is a very good approximation. One such flow occurs inside a **rotational viscometer** (Fig. 9-62), an instrument used

to measure viscosity. It is constructed of two concentric circular cylinders of length L —a solid, rotating inner cylinder of radius R_i and a hollow, stationary outer cylinder of radius R_o . (L is into the page in Fig. 9–62; the z -axis is out of the page.) The gap between the two cylinders is very small and contains the fluid whose viscosity is to be measured. The magnified region of Fig. 9–62 is a nearly identical setup as that of Fig. 9–57 since the gap is small, i.e., $(R_o - R_i) \ll R_o$. In a viscosity measurement, the angular velocity of the inner cylinder, ω , is measured, as is the applied torque, T_{applied} , required to rotate the cylinder. From Example 9–15, we know that the viscous shear stress acting on a fluid element adjacent to the inner cylinder is approximately equal to

$$\tau = \tau_{yx} \cong \mu \frac{V}{R_o - R_i} = \mu \frac{\omega R_i}{R_o - R_i} \quad (9-69)$$

where the speed V of the moving upper plate in Fig. 9–57 is replaced by the counterclockwise speed ωR_i of the rotating wall of the inner cylinder. In the magnified region at the bottom of Fig. 9–62, τ acts to the right on the fluid element adjacent to the inner cylinder wall; hence, the force per unit area acting on the inner cylinder at this location acts to the left with magnitude given by Eq. 9–69. The total clockwise torque acting on the inner cylinder wall due to fluid viscosity is thus equal to this shear stress times the wall area times the moment arm,

$$T_{\text{viscous}} = \tau A R_i \cong \mu \frac{\omega R_i}{R_o - R_i} (2\pi R_i L) R_i \quad (9-70)$$

Under steady conditions, the clockwise torque T_{viscous} is balanced by the applied counterclockwise torque T_{applied} . Equating these and solving Eq. 9–70 for the fluid viscosity yields

$$\text{Viscosity of the fluid: } \mu = T_{\text{applied}} \frac{(R_o - R_i)}{2\pi\omega R_i^3 L}$$

A similar analysis can be performed on an unloaded journal bearing in which a viscous oil flows in the small gap between the inner rotating shaft and the stationary outer housing. (When the bearing is loaded, the inner and outer cylinders cease to be concentric and a more involved analysis is required.)

EXAMPLE 9–16 Couette Flow with an Applied Pressure Gradient

Consider the same geometry as in Example 9–15, but instead of pressure being constant with respect to x , let there be an applied pressure gradient in the x -direction (Fig. 9–63). Specifically, let the pressure gradient in the x -direction, $\partial P/\partial x$, be some constant value given by

$$\text{Applied pressure gradient: } \frac{\partial P}{\partial x} = \frac{P_2 - P_1}{x_2 - x_1} = \text{constant} \quad (1)$$

where x_1 and x_2 are two arbitrary locations along the x -axis, and P_1 and P_2 are the pressures at those two locations. Everything else is the same as for Example 9–15. (a) Calculate the velocity and pressure field. (b) Plot a family of velocity profiles in dimensionless form.

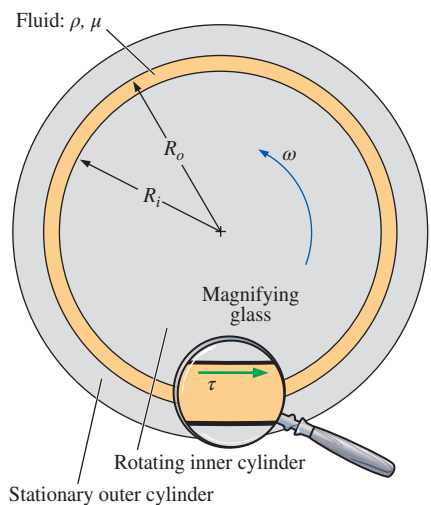


FIGURE 9–62

A rotational viscometer; the inner cylinder rotates at angular velocity ω , and a torque T_{applied} is applied, from which the viscosity of the fluid is calculated.

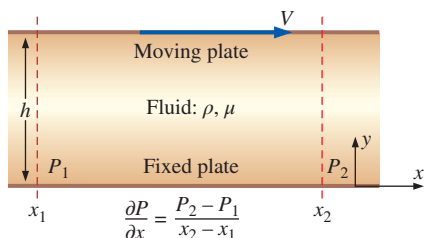


FIGURE 9–63

Geometry of Example 9–16: viscous flow between two infinite plates with a constant applied pressure gradient $\partial P/\partial x$; the upper plate is moving and the lower plate is stationary.

SOLUTION We are to calculate the velocity and pressure field for the flow sketched in Fig. 9–63 and plot a family of velocity profiles in dimensionless form.

Assumptions The assumptions are identical to those of Example 9–15, except assumption 5 is replaced by the following: A constant pressure gradient is applied in the x -direction such that pressure changes linearly with respect to x according to Eq. 1.

Analysis (a) We follow the same procedure as in Example 9–15. Much of the algebra is identical, so to save space we discuss only the differences.

Step 1 See Fig. 9–63.

Step 2 Same as Example 9–15 except for assumption 5.

Step 3 The continuity equation is simplified in the same way as in Example 9–15,

$$\text{Result of continuity:} \quad u = u(y) \text{ only} \quad (2)$$

The x -momentum equation is simplified in the same manner as in Example 9–15 except that the pressure gradient term remains. The result is

$$\text{Result of } x\text{-momentum:} \quad \frac{d^2u}{dy^2} = \frac{1}{\mu} \frac{\partial P}{\partial x} \quad (3)$$

Likewise, the y -momentum and z -momentum equations simplify to

$$\text{Result of } y\text{-momentum:} \quad \frac{\partial P}{\partial y} = 0 \quad (4)$$

and

$$\text{Result of } z\text{-momentum:} \quad \frac{\partial P}{\partial z} = -\rho g \quad (5)$$

We cannot convert from a partial derivative to a total derivative in Eq. 5, because P is a function of both x and z in this problem, unlike in Example 9–15 where P was a function of z only.

Step 4 We integrate Eq. 3 (x -momentum) twice, noting that $\partial P/\partial x$ is a constant,

$$\text{Integration of } x\text{-momentum:} \quad u = \frac{1}{2\mu} \frac{\partial P}{\partial x} y^2 + C_1 y + C_2 \quad (6)$$

where C_1 and C_2 are constants of integration. Equation 5 (z -momentum) is integrated once, resulting in

$$\text{Integration of } z\text{-momentum:} \quad P = -\rho g z + f(x) \quad (7)$$

Note that since P is now a function of both x and z , we add a function of x instead of a constant of integration in Eq. 7. This is a *partial* integration with respect to z , and we must be careful when performing partial integrations (Fig. 9–64).

Step 5 From Eq. 7, we see that the pressure varies hydrostatically in the z -direction, and we have specified a linear change in pressure in the x -direction. Thus the function $f(x)$ must equal a constant plus $\partial P/\partial x$ times x . If we set $P = P_0$ along the line $x = 0, z = 0$ (the y -axis), Eq. 7 becomes

$$\text{Final result for pressure field:} \quad P = P_0 + \frac{\partial P}{\partial x} x - \rho g z \quad (8)$$

CAUTION!

WHEN PERFORMING A
PARTIAL INTEGRATION,
ADD A FUNCTION OF THE
OTHER VARIABLE(S)

FIGURE 9–64

A caution about partial integration.

We next apply the velocity boundary conditions (1) and (2) from step 2 of Example 9–15 to obtain constants C_1 and C_2 .

Boundary condition (1):

$$u = \frac{1}{2\mu} \frac{\partial P}{\partial x} \times 0 + C_1 \times 0 + C_2 = 0 \quad \rightarrow \quad C_2 = 0$$

and

Boundary condition (2):

$$u = \frac{1}{2\mu} \frac{\partial P}{\partial x} h^2 + C_1 \times h + 0 = V \quad \rightarrow \quad C_1 = \frac{V}{h} - \frac{1}{2\mu} \frac{\partial P}{\partial x} h$$

Finally, Eq. 6 becomes

$$u = \frac{Vy}{h} + \frac{1}{2\mu} \frac{\partial P}{\partial x} (y^2 - hy) \quad (9)$$

Equation 9 indicates that the velocity field consists of the superposition of two parts: a linear velocity profile from $u = 0$ at the bottom plate to $u = V$ at the top plate, and a parabolic distribution that depends on the magnitude of the applied pressure gradient. If the pressure gradient is zero, the parabolic portion of Eq. 9 disappears and the profile is linear, just as in Example 9–15; this is sketched as the dashed red line in Fig. 9–65. If the pressure gradient is negative (pressure decreasing in the x -direction, causing flow to be pushed from left to right), $\partial P/\partial x < 0$ and the velocity profile looks like the one sketched in Fig. 9–65. A special case is when $V = 0$ (top plate stationary); the linear portion of Eq. 9 vanishes, and the velocity profile is parabolic and symmetric about the center of the channel ($y = h/2$); this is sketched as the dotted line in Fig. 9–65.

Step 6 You can use Eqs. 8 and 9 to verify that all the differential equations and boundary conditions are satisfied.

(b) We use dimensional analysis to generate the dimensionless groups (Π groups). We set up the problem in terms of velocity component u as a function of y , h , V , μ , and $\partial P/\partial x$. There are six variables (including the dependent variable u), and since there are three primary dimensions represented in the problem (mass, length, and time), we expect $6 - 3 = 3$ dimensionless groups. When we pick h , V , and μ as our repeating variables, we get the following result using the method of repeating variables (details are left for you to do on your own—this is a good review of Chap. 7 material):

$$\text{Result of dimensional analysis: } \frac{u}{V} = f\left(\frac{y}{h}, \frac{h^2}{\mu V} \frac{\partial P}{\partial x}\right) \quad (10)$$

Using these three dimensionless groups, we rewrite Eq. 9 as

$$\text{Dimensionless form of velocity field: } u^* = y^* + \frac{1}{2} P^* y^* (y^* - 1) \quad (11)$$

where the dimensionless parameters are

$$u^* = \frac{u}{V} \quad y^* = \frac{y}{h} \quad P^* = \frac{h^2}{\mu V} \frac{\partial P}{\partial x}$$

In Fig. 9–66, u^* is plotted as a function of y^* for several values of P^* , using Eq. 11.

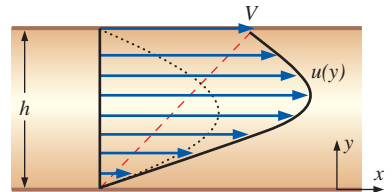
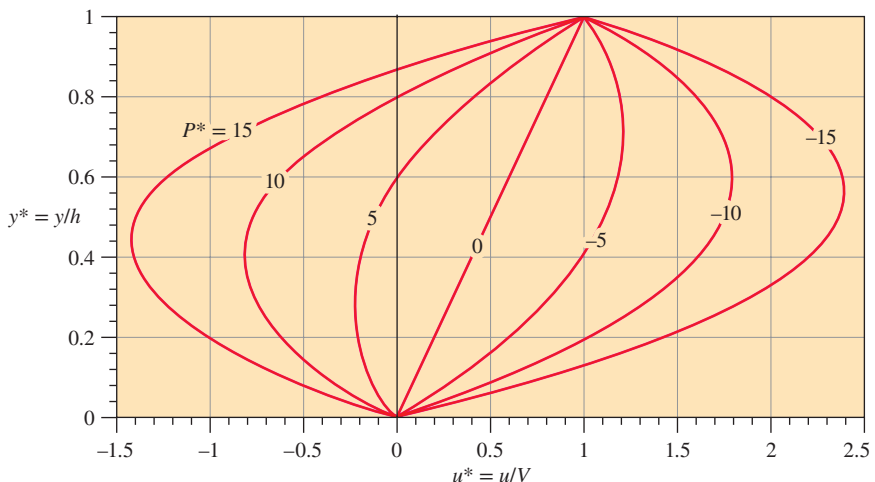
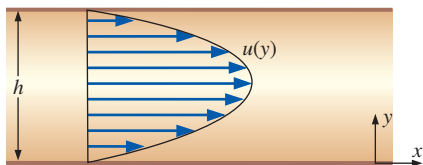


FIGURE 9–65

The velocity profile of Example 9–16: Couette flow between parallel plates with an applied negative pressure gradient; the dashed red line indicates the profile for a zero pressure gradient, and the dotted line indicates the profile for a negative pressure gradient with the upper plate stationary ($V = 0$).

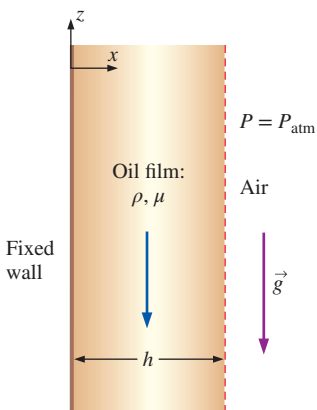
**FIGURE 9-66**

Nondimensional velocity profiles for Couette flow with an applied pressure gradient; profiles are shown for several values of nondimensional pressure gradient.

**FIGURE 9-67**

The velocity profile for fully developed two-dimensional channel flow (planar Poiseuille flow).

Discussion When the result is nondimensionalized, we see that Eq. 11 represents a *family* of velocity profiles. We also see that when the pressure gradient is *positive* (flow being pushed from right to left) and of sufficient magnitude, we can have *reverse flow* in the bottom portion of the channel. For all cases, the boundary conditions reduce to $u^* = 0$ at $y^* = 0$ and $u^* = 1$ at $y^* = 1$. If there is a pressure gradient but both walls are stationary, the flow is called two-dimensional channel flow, or **planar Poiseuille flow** (Fig. 9-67). We note, however, that most authors reserve the name *Poiseuille flow* for fully developed *pipe* flow—the axisymmetric analog of two-dimensional channel flow (see Example 9-18).

**FIGURE 9-68**

Geometry of Example 9-17: a viscous film of oil falling by gravity along a vertical wall.

EXAMPLE 9-17 Oil Film Flowing Down a Vertical Wall by Gravity

Consider steady, incompressible, parallel, laminar flow of a film of oil falling slowly down an infinite vertical wall (Fig. 9-68). The oil film thickness is h , and gravity acts in the negative z -direction (downward in Fig. 9-68). There is no applied (forced) pressure driving the flow—the oil falls by gravity alone. Calculate the velocity and pressure fields in the oil film and sketch the normalized velocity profile. You may neglect changes in the hydrostatic pressure of the surrounding air.

SOLUTION For a given geometry and set of boundary conditions, we are to calculate the velocity and pressure fields and plot the velocity profile.

Assumptions 1 The wall is infinite in the yz -plane (y is into the page for a right-handed coordinate system). 2 The flow is steady (all partial derivatives with respect to time are zero). 3 The flow is parallel (the x -component of velocity, u , is zero everywhere). 4 The fluid is incompressible and Newtonian with constant properties, and the flow is laminar. 5 Pressure $P = P_{\text{atm}} = \text{constant}$ at the free surface. In other words, there is no applied pressure gradient pushing the flow; the flow establishes itself due to a balance between gravitational forces and viscous forces. In addition, since there is no gravity force in the horizontal direction, $P = P_{\text{atm}}$ everywhere. 6 The velocity field is purely two-dimensional, which implies that velocity

component $v = 0$ and all partial derivatives with respect to y are zero. Gravity acts in the negative z -direction. We express this mathematically as $\vec{g} = -g\vec{k}$, or $g_x = g_y = 0$ and $g_z = -g$.

Analysis We obtain the velocity and pressure fields by following the step-by-step procedure for differential fluid flow solutions (Fig. 9–52).

Step 1 Set up the problem and the geometry. See Fig. 9–68.

Step 2 List assumptions and boundary conditions. We have listed seven assumptions. The boundary conditions are: (1) There is no slip at the wall; at $x = 0$, $u = v = w = 0$. (2) At the free surface ($x = h$), there is negligible shear (Eq. 9–68), which for a vertical free surface in this coordinate system means $\partial w/\partial x = 0$ at $x = h$.

Step 3 Write out and simplify the differential equations. We start with the incompressible continuity equation in Cartesian coordinates,

$$\underbrace{\frac{\partial u}{\partial x}}_{\text{assumption 3}} + \underbrace{\frac{\partial v}{\partial y}}_{\text{assumption 6}} + \frac{\partial w}{\partial z} = 0 \rightarrow \frac{\partial w}{\partial z} = 0 \quad (1)$$

Equation 1 tells us that w is not a function of z ; i.e., it doesn't matter where we place our origin—the flow is the same at *any* z -location. In other words, the flow is *fully developed*. Since w is not a function of time (assumption 2), z (Eq. 1), or y (assumption 6), we conclude that w is at most a function of x ,

Result of continuity: $w = w(x)$ only (2)

We now simplify each component of the Navier–Stokes equation as far as possible. Since $u = v = 0$ everywhere, and gravity does not act in the x - or y -directions, the x - and y -momentum equations are satisfied exactly (in fact all terms are zero in both equations). The z -momentum equation reduces to

$$\begin{aligned} \rho \left(\underbrace{\frac{\partial w}{\partial t}}_{\text{assumption 2}} + \underbrace{u \frac{\partial w}{\partial x}}_{\text{assumption 3}} + \underbrace{v \frac{\partial w}{\partial y}}_{\text{assumption 6}} + \underbrace{w \frac{\partial w}{\partial z}}_{\text{continuity}} \right) &= - \underbrace{\frac{\partial p}{\partial z}}_{\text{assumption 5}} + \underbrace{\rho g_z}_{-\rho g} \\ + \mu \left(\underbrace{\frac{\partial^2 w}{\partial x^2}}_{\text{assumption 6}} + \underbrace{\frac{\partial^2 w}{\partial y^2}}_{\text{continuity}} + \underbrace{\frac{\partial^2 w}{\partial z^2}}_{\text{continuity}} \right) &\rightarrow \frac{d^2 w}{dx^2} = \frac{\rho g}{\mu} \end{aligned} \quad (3)$$

The material acceleration (left side of Eq. 3) is zero, implying that fluid particles are not accelerating in this flow field, neither by local nor advective acceleration. Since the advective acceleration terms make the Navier–Stokes equation nonlinear, this greatly simplifies the problem. We have changed from a partial derivative ($\partial/\partial x$) to a total derivative (d/dx) in Eq. 3 as a direct result of Eq. 2, reducing the partial differential equation (PDE) to an ordinary differential equation (ODE). ODEs are of course much easier than PDEs to solve (Fig. 9–69).

Step 4 Solve the differential equations. The continuity and x - and y -momentum equations have already been “solved.” Equation 3 (z -momentum) is integrated twice to get

$$w = \frac{\rho g}{2\mu} x^2 + C_1 x + C_2 \quad (4)$$

NOTICE

If $u = u(x)$ only,
change from
PDE to ODE:

$$\frac{\partial u}{\partial x} \rightarrow \frac{du}{dx}$$

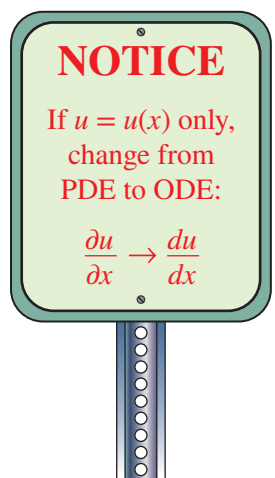
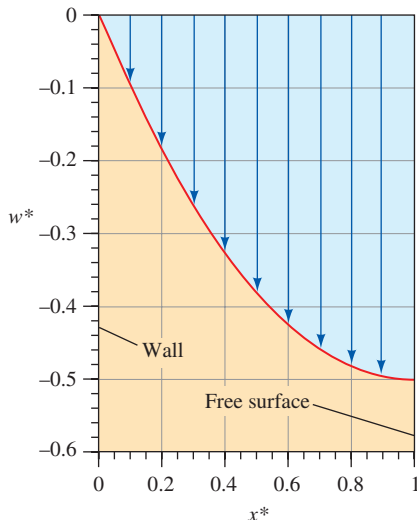


FIGURE 9–69

In Examples 9–15 through 9–18, the equations of motion are reduced from *partial differential equations* to *ordinary differential equations*, making them much easier to solve.

**FIGURE 9-70**

The normalized velocity profile of Example 9-17: an oil film falling down a vertical wall.

Step 5 Apply boundary conditions. We apply boundary conditions (1) and (2) from step 2 to obtain constants C_1 and C_2 ,

$$\text{Boundary condition (1): } w = 0 + 0 + C_2 = 0 \quad C_2 = 0$$

and

$$\text{Boundary condition (2): } \left. \frac{dw}{dx} \right|_{x=h} = \frac{\rho g}{\mu} h + C_1 = 0 \rightarrow C_1 = -\frac{\rho gh}{\mu}$$

Finally, Eq. 4 becomes

$$\text{Velocity field: } w = \frac{\rho g}{2\mu} x^2 - \frac{\rho g}{\mu} h x = \frac{\rho g x}{2\mu} (x - 2h) \quad (5)$$

Since $x < h$ in the film, w is negative everywhere, as expected (flow is downward). The pressure field is trivial; namely, $P = P_{\text{atm}}$ everywhere.

Step 6 Verify the results. You can verify that all the differential equations and boundary conditions are satisfied.

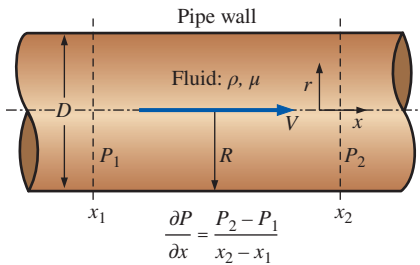
We normalize Eq. 5 by inspection: we let $x^* = x/h$ and $w^* = w\mu/(\rho gh^2)$. Equation 5 becomes

$$\text{Normalized velocity profile: } w^* = \frac{x^*}{2} (x^* - 2) \quad (6)$$

We plot the normalized velocity field in Fig. 9-70.

Discussion The velocity profile has a large slope near the wall due to the no-slip condition there ($w = 0$ at $x = 0$), but zero slope at the free surface, where the boundary condition is zero shear stress ($\partial w/\partial x = 0$ at $x = h$). We could have introduced a factor of -2 in the definition of w^* so that w^* would equal 1 instead of $-\frac{1}{2}$ at the free surface.

The solution procedure used in Examples 9-15 through 9-17 in Cartesian coordinates can also be used in any other coordinate system. In Example 9-18 we present the classic problem of fully developed flow in a round pipe, for which we use cylindrical coordinates.

**FIGURE 9-71**

Geometry of Example 9-18: steady laminar flow in a long round pipe with an applied pressure gradient $\partial P/\partial x$ pushing fluid through the pipe. The pressure gradient is usually produced by a pump and/or gravity.

EXAMPLE 9-18 Fully Developed Flow in a Round Pipe—Poiseuille Flow

Consider steady, incompressible, laminar flow of a Newtonian fluid in an infinitely long round pipe of diameter D or radius $R = D/2$ (Fig. 9-71). We ignore the effects of gravity. A constant pressure gradient $\partial P/\partial x$ is applied in the x -direction,

$$\text{Applied pressure gradient: } \frac{\partial P}{\partial x} = \frac{P_2 - P_1}{x_2 - x_1} = \text{constant} \quad (1)$$

where x_1 and x_2 are two arbitrary locations along the x -axis, and P_1 and P_2 are the pressures at those two locations. Note that we adopt a modified cylindrical coordinate system here with x instead of z for the axial component, namely, (r, θ, x) and (u_r, u_θ, u) . Derive an expression for the velocity field inside the pipe and estimate the viscous shear force per unit surface area acting on the pipe wall.

SOLUTION For flow inside a round pipe we are to calculate the velocity field, and then estimate the viscous shear stress acting on the pipe wall.

Assumptions 1 The pipe is infinitely long in the x -direction. 2 The flow is steady (all partial time derivatives are zero). 3 This is a parallel flow (the r -component of velocity, u_r , is zero). 4 The fluid is incompressible and Newtonian with constant properties, and the flow is laminar (Fig. 9–72). 5 A constant pressure gradient is applied in the x -direction such that pressure changes linearly with respect to x according to Eq. 1. 6 The velocity field is axisymmetric with no swirl, implying that $u_\theta = 0$ and all partial derivatives with respect to θ are zero. 7 We ignore the effects of gravity.

Analysis To obtain the velocity field, we follow the step-by-step procedure outlined in Fig. 9–52.

Step 1 Lay out the problem and the geometry. See Fig. 9–71.

Step 2 List assumptions and boundary conditions. We have listed seven assumptions. The first boundary condition comes from imposing the no-slip condition at the pipe wall: (1) at $r = R$, $\vec{V} = 0$. The second boundary condition comes from the fact that the centerline of the pipe is an axis of symmetry: (2) at $r = 0$, $\partial u / \partial r = 0$.

Step 3 Write out and simplify the differential equations. We start with the incompressible continuity equation in cylindrical coordinates, a modified version of Eq. 9–62a,

$$\underbrace{\frac{1}{r} \frac{\partial(ru_r)}{\partial r}}_{\text{assumption 3}} + \underbrace{\frac{1}{r} \frac{\partial(u_\theta)}{\partial \theta}}_{\text{assumption 6}} + \frac{\partial u}{\partial x} = 0 \quad \rightarrow \quad \frac{\partial u}{\partial x} = 0 \quad (2)$$

Equation 2 tells us that u is not a function of x . In other words, it doesn't matter where we place our origin—the flow is the same at any x -location. This can also be inferred directly from assumption 1, which tells us that there is nothing special about any x -location since the pipe is infinite in length—the flow is fully developed. Furthermore, since u is not a function of time (assumption 2) or θ (assumption 6), we conclude that u is at most a function of r ,

$$\text{Result of continuity:} \quad u = u(r) \text{ only} \quad (3)$$

We now simplify the axial momentum equation (a modified version of Eq. 9–62d) as far as possible:

$$\begin{aligned} \rho \left(\underbrace{\frac{\partial u}{\partial t}}_{\text{assumption 2}} + \underbrace{u_r \frac{\partial u}{\partial r}}_{\text{assumption 3}} + \underbrace{\frac{u_\theta}{r} \frac{\partial u}{\partial \theta}}_{\text{assumption 6}} + \underbrace{u \frac{\partial u}{\partial x}}_{\text{continuity}} \right) \\ = -\frac{\partial P}{\partial x} + \underbrace{\rho g_x}_{\text{assumption 7}} + \mu \left(\frac{1}{r} \frac{\partial}{\partial r} \left(r \frac{\partial u}{\partial r} \right) + \underbrace{\frac{1}{r^2} \frac{\partial^2 u}{\partial \theta^2}}_{\text{assumption 6}} + \underbrace{\frac{\partial^2 u}{\partial x^2}}_{\text{continuity}} \right) \end{aligned}$$

or

$$\frac{1}{r} \frac{d}{dr} \left(r \frac{du}{dr} \right) = \frac{1}{\mu} \frac{\partial P}{\partial x} \quad (4)$$

As in Examples 9–15 through 9–17, the material acceleration (entire left side of the x -momentum equation) is zero, implying that fluid particles are not

CAUTION: EXACT SOLUTIONS POSSIBLE FOR LAMINAR FLOW ONLY

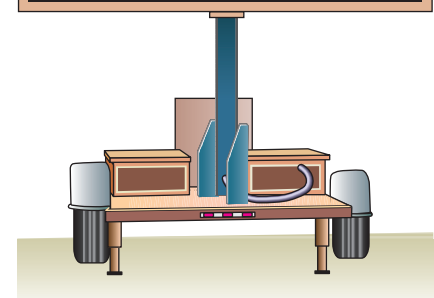


FIGURE 9–72

Exact analytical solutions of the Navier–Stokes equations, as in the examples provided here, are not possible if the flow is turbulent.

The Navier–Stokes Equation

$$\rho \left(\frac{\partial \vec{V}}{\partial t} + (\vec{V} \cdot \vec{\nabla}) \vec{V} \right) = -\vec{\nabla} P + \vec{\rho} g + \mu \nabla^2 \vec{V}$$

Nonlinear term

FIGURE 9–73

For incompressible flow solutions in which the advective terms in the Navier–Stokes equation are zero, the equation becomes *linear* since the advective term is the only nonlinear term in the equation.

accelerating at all in this flow field, and linearizing the Navier–Stokes equation (Fig. 9–73). We have replaced the partial derivative operators for the u -derivatives with total derivative operators because of Eq. 3.

In similar fashion, every term in the r -momentum equation (Eq. 9–62b) except the pressure gradient term is zero, forcing that lone term to also be zero,

$$r\text{-momentum: } \frac{\partial P}{\partial r} = 0 \quad (5)$$

In other words, P is not a function of r . Since P is also not a function of time (assumption 2) or θ (assumption 6), P can be at most a function of x ,

$$\text{Result of } r\text{-momentum: } P = P(x) \text{ only} \quad (6)$$

Therefore, we replace the partial derivative operator for the pressure gradient in Eq. 4 by the total derivative operator since P varies only with x . Finally, all terms of the θ -component of the Navier–Stokes equation (Eq. 9–62c) go to zero.

Step 4 Solve the differential equations. Continuity and r -momentum have already been “solved,” resulting in Eqs. 3 and 6, respectively. The θ -momentum equation has vanished, and thus we are left with Eq. 4 (x -momentum). After multiplying both sides by r , we integrate once to obtain

$$r \frac{du}{dr} = \frac{r^2}{2\mu} \frac{dP}{dx} + C_1 \quad (7)$$

where C_1 is a constant of integration. Note that the pressure gradient dP/dx is a constant here. Dividing both sides of Eq. 7 by r , we integrate a second time to get

$$u = \frac{r^2}{4\mu} \frac{dP}{dx} + C_1 \ln r + C_2 \quad (8)$$

where C_2 is a second constant of integration.

Step 5 Apply boundary conditions. First, we apply boundary condition (2) to Eq. 7,

$$\text{Boundary condition (2): } 0 = 0 + C_1 \rightarrow C_1 = 0$$

An alternative way to interpret this boundary condition is that u must remain finite at the centerline of the pipe. This is possible only if constant C_1 is equal to 0, since $\ln(0)$ is undefined in Eq. 8. Now we apply boundary condition (1),

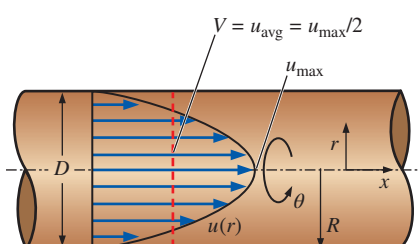
$$\text{Boundary condition (1): } u = \frac{R^2}{4\mu} \frac{dP}{dx} + 0 + C_2 = 0 \rightarrow C_2 = -\frac{R^2}{4\mu} \frac{dP}{dx}$$

Finally, Eq. 8 becomes

$$\text{Axial velocity: } u = \frac{1}{4\mu} \frac{dP}{dx} (r^2 - R^2) \quad (9)$$

The axial velocity profile is thus in the shape of a paraboloid, as sketched in Fig. 9–74.

Step 6 Verify the results. You can verify that all the differential equations and boundary conditions are satisfied.

**FIGURE 9–74**

Axial velocity profile of Example 9–18: steady laminar flow in a long round pipe with an applied constant-pressure gradient dP/dx pushing fluid through the pipe.

We calculate some other properties of fully developed laminar pipe flow as well. For example, the maximum axial velocity obviously occurs at the centerline of the pipe (Fig. 9–74). Setting $r = 0$ in Eq. 9 yields

$$\text{Maximum axial velocity: } u_{\max} = -\frac{R^2}{4\mu} \frac{dP}{dx} \quad (10)$$

The volume flow rate through the pipe is found by integrating Eq. 9 through a cross section of the pipe,

$$\dot{V} = \int_{\theta=0}^{2\pi} \int_{r=0}^R ur dr d\theta = \frac{2\pi}{4\mu} \frac{dP}{dx} \int_{r=0}^R (r^2 - R^2)r dr = -\frac{\pi R^4}{8\mu} \frac{dP}{dx} \quad (11)$$

Since volume flow rate is also equal to the average axial velocity times cross-sectional area, we easily determine the average axial velocity V :

$$\text{Average axial velocity: } V = \frac{\dot{V}}{A} = \frac{(-\pi R^4/8\mu) (dP/dx)}{\pi R^2} = -\frac{R^2}{8\mu} \frac{dP}{dx} \quad (12)$$

Comparing Eqs. 10 and 12 we see that for fully developed laminar pipe flow, the average axial velocity is equal to exactly half of the maximum axial velocity.

To calculate the viscous shear force per unit surface area acting on the pipe wall, we consider a differential fluid element adjacent to the bottom portion of the pipe wall (Fig. 9–75). Pressure stresses and mathematically positive viscous stresses are shown. From Eq. 9–63 (modified for our coordinate system), we write the viscous stress tensor as

$$\tau_{ij} = \begin{pmatrix} \tau_{rr} & \tau_{r\theta} & \tau_{rx} \\ \tau_{\theta r} & \tau_{\theta\theta} & \tau_{\theta x} \\ \tau_{xr} & \tau_{x\theta} & \tau_{xx} \end{pmatrix} = \begin{pmatrix} 0 & 0 & \mu \frac{\partial u}{\partial r} \\ 0 & 0 & 0 \\ \mu \frac{\partial u}{\partial r} & 0 & 0 \end{pmatrix} \quad (13)$$

We use Eq. 9 for u , and set $r = R$ at the pipe wall; component τ_{rx} of Eq. 13 reduces to

$$\text{Viscous shear stress at the pipe wall: } \tau_{rx} = \mu \frac{du}{dr} = \frac{R}{2} \frac{dP}{dx} \quad (14)$$

For flow from left to right, dP/dx is negative, so the viscous shear stress on the bottom of the fluid element at the wall is in the direction opposite to that indicated in Fig. 9–75. (This agrees with our intuition since the pipe wall exerts a retarding force on the fluid.) The shear force per unit area on the wall is equal and opposite to this; hence,

$$\text{Viscous shear force per unit area acting on the wall: } \frac{\vec{F}}{A} = -\frac{R}{2} \frac{dP}{dx} \vec{i} \quad (15)$$

The direction of this force again agrees with our intuition; namely, the fluid tries to pull the bottom wall to the right, due to friction, when dP/dx is negative.

Discussion Since $du/dr = 0$ at the centerline of the pipe, $\tau_{rx} = 0$ there. You are encouraged to try to obtain Eq. 15 by using a control volume approach instead, taking your control volume as the fluid in the pipe between any two x -locations,

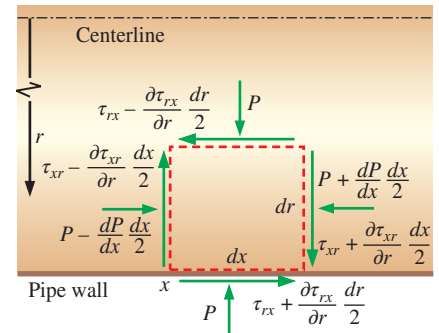
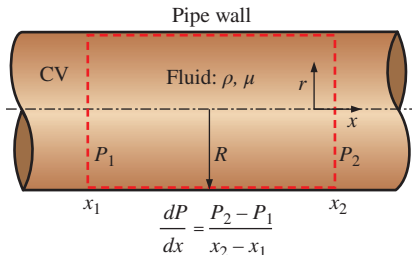


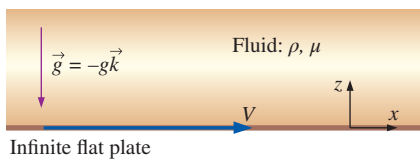
FIGURE 9–75

Pressure and viscous shear stresses acting on a differential fluid element whose bottom face is in contact with the pipe wall. Note that we are ignoring gravity in this case; otherwise pressure would increase in the direction of the gravitational acceleration.

**FIGURE 9-76**

Control volume used to obtain Eq. 15 of Example 9-18 by an alternative method.

x_1 and x_2 (Fig. 9-76). You should get the same answer. (*Hint:* Since the flow is fully developed, the axial velocity profile at location 1 is identical to that at location 2.) Note that when the volume flow rate through the pipe exceeds a critical value, instabilities in the flow occur, and the solution presented here is no longer valid. Specifically, flow in the pipe becomes turbulent rather than laminar; turbulent pipe flow is discussed in more detail in Chap. 8. This problem is also solved in Chap. 8 using an alternative approach.

**FIGURE 9-77**

Geometry and setup for Example 9-19; the y -coordinate is into the page.

EXAMPLE 9-19 Sudden Motion of an Infinite Flat Plate

Consider a viscous Newtonian fluid on top of an infinite flat plate lying in the xy -plane at $z = 0$ (Fig. 9-77). The fluid is at rest until time $t = 0$, when the plate suddenly starts moving at speed V in the x -direction. Gravity acts in the $-z$ -direction. Determine the pressure and velocity fields.

SOLUTION The velocity and pressure fields are to be calculated for the case of fluid on top of an infinite flat plate that suddenly starts moving.

Assumptions 1 The wall is infinite in the x - and y -directions; thus, nothing is special about any particular x - or y -location. 2 The flow is *parallel* everywhere ($w = 0$). 3 Pressure $P = \text{constant}$ with respect to x . In other words, there is no applied pressure gradient pushing the flow in the x -direction; flow occurs due to viscous stresses caused by the moving plate. 4 The fluid is incompressible and Newtonian with constant properties, and the flow is laminar. 5 The velocity field is two-dimensional in the xz -plane; therefore, $v = 0$, and all partial derivatives with respect to y are zero. 6 Gravity acts in the $-z$ -direction.

Analysis To obtain the velocity and pressure fields, we follow the step-by-step procedure outlined in Fig. 9-52.

Step 1 Lay out the problem and the geometry. (See Fig. 9-77.)

Step 2 List assumptions and boundary conditions. We have listed six assumptions. The boundary conditions are: (1) At $t = 0$, $u = 0$ everywhere (no flow until the plate starts moving); (2) at $z = 0$, $u = V$ for all values of x and y (no-slip condition at the plate); (3) as $z \rightarrow \infty$, $u = 0$ (far from the plate, the effect of the moving plate is not felt); and (4) at $z = 0$, $P = P_{\text{wall}}$ (the pressure at the wall is constant at any x - or y -location along the plate).

Step 3 Write out and simplify the differential equations. We start with the incompressible continuity equation in Cartesian coordinates (Eq. 9-61a),

$$\frac{\partial u}{\partial x} + \underbrace{\frac{\partial v}{\partial y}}_{\text{assumption 5}} + \underbrace{\frac{\partial w}{\partial z}}_{\text{assumption 2}} = 0 \quad \rightarrow \quad \frac{\partial u}{\partial x} = 0 \quad (1)$$

Equation 1 tells us that u is not a function of x . Furthermore, since u is not a function of y (assumption 5), we conclude that u is at most a function of z and t ,

Result of continuity: $u = u(z, t)$ only (2)

The y -momentum equation reduces to

$$\frac{\partial P}{\partial y} = 0 \quad (3)$$

by assumptions 5 and 6 (all terms with v , the y -component of velocity, vanish, and gravity does not act in the y -direction). Equation 3 simply tells us that pressure is not a function of y ; hence,

Result of y -momentum: $P = P(z, t)$ only (4)

Similarly the z -momentum equation reduces to

$$\frac{\partial P}{\partial z} = -\rho g \quad (5)$$

We now simplify the x -momentum equation (Eq. 9–61b) as far as possible.

$$\begin{aligned} \rho \left(\frac{\partial u}{\partial t} + u \underbrace{\frac{\partial u}{\partial x}}_{\text{continuity}} + v \underbrace{\frac{\partial u}{\partial y}}_{\text{assumption 5}} + w \underbrace{\frac{\partial u}{\partial z}}_{\text{assumption 2}} \right) &= -\frac{\partial P}{\partial x} + \underbrace{\rho g_x}_{\text{assumption 6}} \\ &+ \mu \left(\underbrace{\frac{\partial^2 u}{\partial x^2}}_{\text{continuity}} + \underbrace{\frac{\partial^2 u}{\partial y^2}}_{\text{assumption 5}} + \frac{\partial^2 u}{\partial z^2} \right) \rightarrow \rho \frac{\partial u}{\partial t} = \mu \frac{\partial^2 u}{\partial z^2} \end{aligned} \quad (6)$$

It is convenient to combine the viscosity and density into the kinematic viscosity, defined as $\nu = \mu/\rho$. Equation 6 reduces to the well-known **one-dimensional diffusion equation** (Fig. 9–78),

Result of x -momentum: $\frac{\partial u}{\partial t} = \nu \frac{\partial^2 u}{\partial z^2}$ (7)

Step 4 Solve the differential equations. Continuity and y -momentum have already been “solved,” resulting in Eqs. 2 and 4, respectively. Equation 5 (z -momentum) is integrated once, resulting in

$$P = -\rho g z + f(t) \quad (8)$$

where we have added a function of time instead of a constant of integration since P is a function of two variables, z and t (see Eq. 4). Equation 7 (x -momentum) is a linear partial differential equation whose solution is obtained by combining the two independent variables z and t into one independent variable. The result is called a **similarity solution**, the details of which are beyond the scope of this text. Note that the one-dimensional diffusion equation occurs in many other fields of engineering, such as diffusion of species (mass diffusion) and diffusion of heat (conduction); details about the solution can be found in books on these subjects. The solution of Eq. 7 is intimately tied to the boundary condition that the plate is impulsively started, and the result is

Integration of x -momentum: $u = C_1 \left[1 - \operatorname{erf} \left(\frac{z}{2\sqrt{\nu t}} \right) \right]$ (9)

where **erf** in Eq. 9 is the **error function**, defined as

Error function: $\operatorname{erf}(\xi) = \frac{2}{\sqrt{\pi}} \int_0^{\xi} e^{-\eta^2} d\eta$ (10)

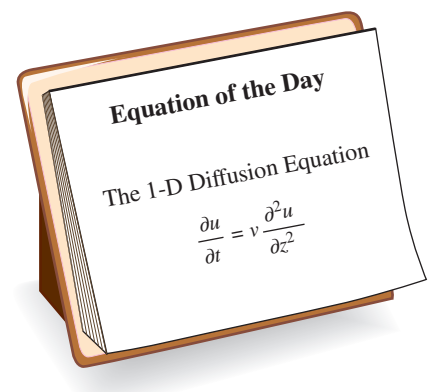
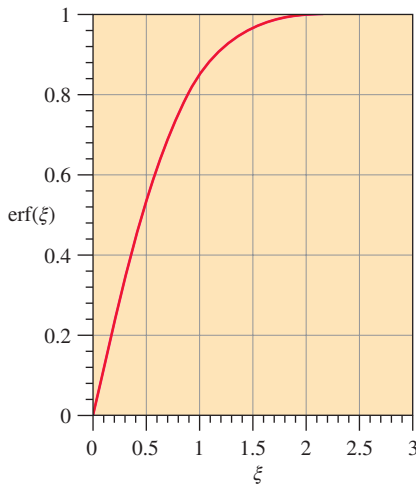
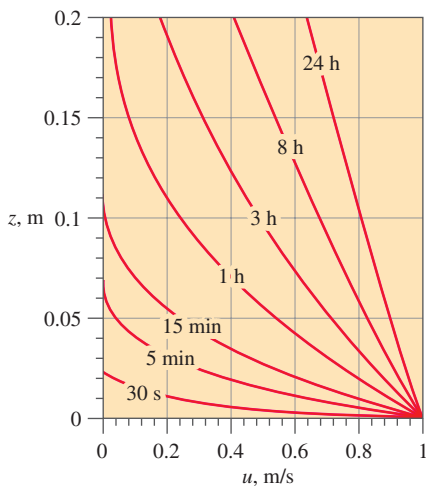


FIGURE 9–78

The one-dimensional diffusion equation is *linear*, but it is a *partial differential equation* (PDE). It occurs in many fields of science and engineering.

**FIGURE 9-79**

The error function ranges from 0 at $\xi = 0$ to 1 as $\xi \rightarrow \infty$.

**FIGURE 9-80**

Velocity profiles of Example 9-19: flow of water above an impulsively started infinite plate; $v = 1.004 \times 10^{-6} \text{ m}^2/\text{s}$ and $V = 1.0 \text{ m/s}$.

The error function is commonly used in probability theory and is plotted in Fig. 9-79. Tables of the error function can be found in many reference books, and some calculators and spreadsheets can calculate the error function directly.

Step 5 Apply boundary conditions. We begin with Eq. 8 for pressure. Boundary condition (4) requires that $P = P_{\text{wall}}$ at $z = 0$ for all times, and Eq. 8 becomes

$$\text{Boundary condition (4): } P = 0 + f(t) = P_{\text{wall}} \rightarrow f(t) = P_{\text{wall}}$$

In other words, the arbitrary function of time, $f(t)$, turns out not to be a function of time at all, but merely a constant. Thus,

$$\text{Final result for pressure field: } P = P_{\text{wall}} - \rho g z \quad (11)$$

which is simply hydrostatic pressure. We conclude that *hydrostatic pressure acts independently of the flow*. Boundary conditions (1) and (3) from step 2 have already been applied in order to obtain the solution of the x -momentum equation in step 4. Since $\text{erf}(0) = 0$, the second boundary condition yields

$$\text{Boundary condition (2): } u = C_1(1 - 0) = V \rightarrow C_1 = V$$

and Eq. 9 becomes

$$\text{Final result for velocity field: } u = V \left[1 - \text{erf} \left(\frac{z}{2\sqrt{vt}} \right) \right] \quad (12)$$

Several velocity profiles are plotted in Fig. 9-80 for the specific case of water at room temperature ($v = 1.004 \times 10^{-6} \text{ m}^2/\text{s}$) with $V = 1.0 \text{ m/s}$. At $t = 0$, there is no flow. As time goes on, the motion of the plate is felt farther and farther into the fluid, as expected. Notice how long it takes for viscous diffusion to penetrate into the fluid—after 15 min of flow, the effect of the moving plate is not felt beyond about 10 cm above the plate!

We define normalized variables u^* and z^* as

$$\text{Normalized variables: } u^* = \frac{u}{V} \quad \text{and} \quad z^* = \frac{z}{2\sqrt{vt}}$$

Then we rewrite Eq. 12 in terms of nondimensional parameters:

$$\text{Normalized velocity field: } u^* = 1 - \text{erf}(z^*) \quad (13)$$

The combination of unity minus the error function occurs often in engineering and is given the special name **complementary error function** and symbol **erfc**. Thus Eq. 13 can also be written as

$$\text{Alternative form of the velocity field: } u^* = \text{erfc}(z^*) \quad (14)$$

The beauty of the normalization is that this one equation for u^* as a function of z^* is valid for any fluid (with any kinematic viscosity v) above a plate moving at any speed V and at any location z in the fluid at any time t ! The normalized velocity profile of Eq. 13 is sketched in Fig. 9-81. All the profiles of Fig. 9-80 collapse into the single profile of Fig. 9-81; such a profile is called a **similarity profile**.

Step 6 Verify the results. You can verify that all the differential equations and boundary conditions are satisfied.

Discussion The time required for momentum to diffuse into the fluid seems much longer than we would expect based on our intuition. This is because the solution presented here is valid only for laminar flow. It turns out that if the plate's speed is large enough, or if there are significant vibrations in the plate or disturbances in the fluid, the flow will become turbulent. In a turbulent flow, large eddies mix rapidly moving fluid near the wall with slowly moving fluid away from the wall. This mixing process occurs rather quickly, so that turbulent diffusion is usually orders of magnitude faster than laminar diffusion.

Examples 9–15 through 9–19 are for incompressible laminar flow. The same set of differential equations (incompressible continuity and Navier–Stokes) is valid for incompressible *turbulent* flow. However, turbulent flow solutions are much more complicated because the flow contains disordered, unsteady, three-dimensional eddies that mix the fluid. Furthermore, these eddies may range in size over several orders of magnitude. In a turbulent flow field, none of the terms in the equations can be ignored (with the exception of the gravity term in some cases), and thus solutions can be obtained only through numerical computations. Computational fluid dynamics (CFD) is discussed in Chap. 15.

Differential Analysis of Biofluid Mechanics Flows*

In Example 9–18 we derived fully developed flow in a round pipe, or what is commonly referred to as Poiseuille flow. The solution to the Navier–Stokes equation for this particular example is quite straightforward but is based on a number of assumptions and approximations. These approximations hold true for standard pipe flow with most water systems, for example. However, when applied to blood flow in the human body, the approximations must be closely monitored and evaluated for their applicability. Traditionally as a first-order attempt, cardiovascular fluid dynamists have used the Poiseuille flow derivation to understand blood flow in arteries. This can provide the engineer with a first-order approximation for the velocity and flow rate, but if the engineer were interested in a more sophisticated and, frankly realistic, understanding of blood flow, it is important to examine the main approximations used to arrive at Poiseuille flow.

Before delving in, let's retain the basic approximations about the fluid, or blood in this case. The fluid will remain incompressible, the flow will continue to be laminar, and gravity remains negligible. The approximation of fully developed flow will also remain, though in reality this is not applicable in the cardiovascular system. Based on only these approximations, this leaves the other main approximations of steady, parallel, axisymmetric Newtonian flow, and the pipe approximated as a rigid circular tube.

Recall that the heart pumps blood continuously at an average rate of 75 beats per minute for a healthy adult human at rest. As an example of the flow waveform generated by the ventricular contraction simulated in a mock circulatory system (Fig. 9–82), the flow rate changes temporally for this 800 ms cycle. Therefore, fundamentally to model blood flow through

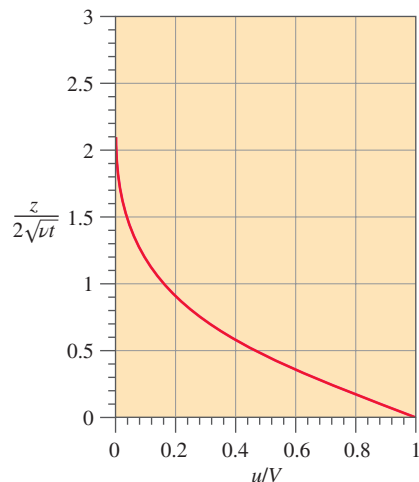


FIGURE 9–81

Normalized velocity profile of Example 9–19: laminar flow of a viscous fluid above an impulsively started infinite plate.

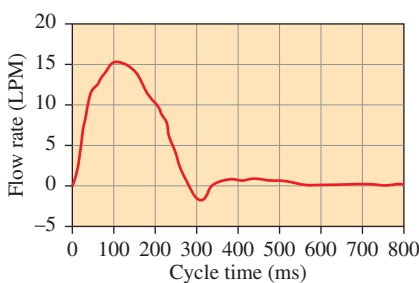


FIGURE 9–82

The flow waveform created during ejection from a ventricular assist device in a mock circulatory loop. This is similar to the waveform created during left ventricular ejection.

* This section was contributed by Professor Keefe Manning of Penn State University.

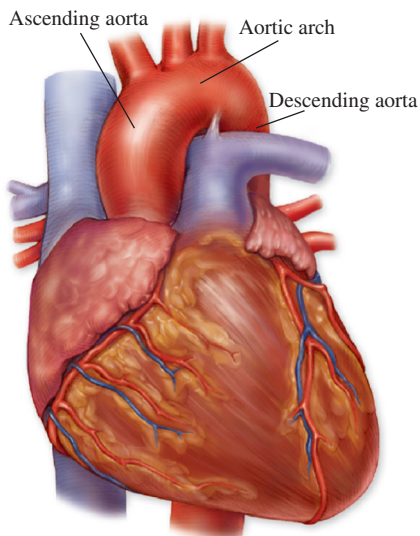


FIGURE 9–83

An anatomical figure illustrating the ascending aorta, aortic arch, and descending aorta coming from the left ventricle (on the backside of the heart in this view). The illustration demonstrates how the aorta moves toward the spinal cord.

McGraw-Hill Companies, Inc.

the arteries, the steady flow approximation is inappropriate, making modeling blood flow as Poiseuille flow unsuitable for just this one approximation alone. There is a rapid acceleration and deceleration of flow within a short time period (~300 ms). However, the wave propagation that is initiated at the heart diminishes with distance from it, and as the arteries become progressively smaller to the capillary level, the magnitude of pulsatility decreases. When focused on the venous side as blood returns to the heart, the steady flow approximation can be applied with more confidence, but it should be noted that there remains flow disruption, in particular, from the lower limbs as venous valves (similar to heart valves) help bring blood back to the heart.

The rigid, circular tube approximation is equally as inappropriate when applied to cardiovascular blood flow. As mentioned in Chap. 8, the blood vessels continually taper from the main vessel (the aorta) to smaller vessels (arteries, arterioles, and capillaries). There are no abrupt changes in diameter as might be seen in a commercial piping network. Therefore, one geometric consideration is the fact that a segment of blood vessel from one end to the other end will have a continual change in diameter. With respect to a circular tube cross section, the vessels are not perfectly circular but rather more elliptical in their cross section, so there is a major axis and minor axis. The most important approximation here that applies to Poiseuille flow is the fact that pipes are typically considered rigid. However, healthy vessels are *not* rigid; these structures are compliant and flexible. For example, the aorta emanating from the left ventricle can double in diameter to accommodate the sharp increase in blood volume during left ventricular ejection over a brief time period. One of the major exceptions to using this approximation is when studying pathologic states like atherosclerosis or studying blood flow in the elderly. The basic result of both is that the vessels will harden. In doing so, the rigidity approximation can be applied. There is also a secondary effect as the vessels harden, namely, the pulsatility of blood dampens more quickly, which can influence the steady flow approximation in the arterioles in these particular patient populations.

With respect to parallel flow and axisymmetric flow, these both can be invalidated as inappropriate approximations applied to blood flow, by focusing on one location of the cardiovascular system. Considering the aorta in Fig. 9–83 (ascending from the left ventricle, the aortic arch, and descending from the arch), there are significant changes in geometry that influence the flow field. What is commonly not displayed in two-dimensional pictures of the cardiovascular system (like Fig. 8–83) is the fact that the aorta does not remain in one plane as typically depicted. Actually, the aorta (as one looks at another person) will start from the left ventricle and move towards the spinal column (towards the back of the person) moving the flow into other planes due to pure anatomy. What this geometry does is create Dean flow in this region. As a result, the flow that is created moving around this bend and backwards, is a double helical swirling pattern (think about the DNA helix but the helices are streamlines). With all this swirling, the approximations of parallel and axisymmetric flow are inappropriate. This is the most extreme case of flow in the human body (except for cases of pathology or with medical device intervention). The parallel and axisymmetric flow approximations can be used with more confidence in the rest of the circulatory system.

It should be mentioned that flow within the capillaries is *not* Poiseuille flow since the red blood cells have to squeeze into these vessels and what results is a two-phase flow where a red blood cell is followed by plasma, which is in turn followed by a red blood cell; this continues, creating a unique flow field to facilitate oxygen and nutrient exchange. Finally, blood is not Newtonian, as illustrated in Example 9–20.

EXAMPLE 9–20 Fully Developed Flow in a Round Pipe with a Simple Blood Viscosity Model

Consider Example 9–18 and all the approximations to arrive at Poiseuille flow and the axial velocity profile shown in Fig. 9–74. In this example, we will change the basic assumption of a Newtonian fluid and instead use a non-Newtonian fluid viscosity model. Blood behaves as a viscoelastic fluid but for our purposes, we assume a shear thinning or pseudoplastic model and apply a generalized power law viscosity model. The power law model effectively comes from the viscous stress tensor and is $\tau_{rz} = -\mu \left(\frac{du}{dr} \right)^n$ where we introduce a negative sign for direction, and where $0 < n < 1$.

SOLUTION We take Example 9–18 up to Equation 4 in that example:

$$\frac{1}{r} \frac{d}{dr} \left(r \frac{du}{dr} \right) = \frac{1}{\mu} \frac{dP}{dx}. \text{ Through rearrangement and one integration with respect}$$

$$\text{to } r, \text{ we arrive at } \frac{r}{2} \frac{dP}{dx} = \mu \frac{dP}{dx}, \text{ which is also } \frac{r}{2} \frac{dP}{dx} = \mu \frac{dP}{dx} = \tau_{rz}.$$

Then we can equate the power law model to this as well, and arrive at a new relationship, $\frac{r}{2} \frac{dP}{dx} = -\mu \left(\frac{du}{dr} \right)^n$. When we move the negative sign to the other side, multiple by $1/n$ on both sides, and solve for $\frac{du}{dr}$, we arrive at

$$\frac{du}{dr} = \left(-\frac{r}{2\mu} \frac{dP}{dx} \right)^{\frac{1}{n}}.$$

We integrate and then apply the second boundary condition from Example 9–18 (centerline of the pipe is an axis of symmetry). Our velocity then becomes

$$u = \frac{R^{\left(\frac{n+1}{n}\right)} - r^{\left(\frac{n+1}{n}\right)}}{\left(\frac{n+1}{n}\right)} \left(\frac{1}{2\mu} \frac{dP}{dx} \right)^{\frac{1}{n}}$$

We now have a generalized velocity profile for a power law fluid or a type of non-Newtonian fluid, which might be a rudimentary model for blood. As mentioned, we approximate blood as a pseudoplastic fluid; as such, we arbitrarily set $n = 0.5$. The actual velocity then becomes

$$u = \frac{R^3 - r^3}{3} \left(\frac{1}{2\mu} \frac{dP}{dx} \right)^2$$

Note that if we were to use $n = 1$ instead, we would get the following, $u = (R^2 - r^2) \left(\frac{1}{4\mu} \frac{dP}{dx} \right)$, which is the axial velocity for a Newtonian fluid.

We plot both the Newtonian and pseudoplastic velocity profiles in Fig. 9–84. Note how the viscosity alters the flow profile making it more blunt. To calculate

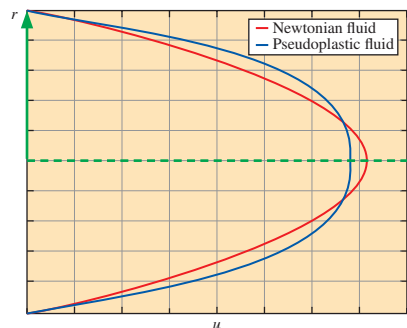


FIGURE 9–84

Assuming all values are the same in the velocity equations and the pipe is the same diameter, the pseudoplastic fluid causes the velocity profile to be more blunt compared to the parabolic profile generated for a Newtonian fluid.

the volume flow rate, we integrate over the cross section of the pipe using the equation $\dot{V} = \int_0^R 2\pi r u \, dr$ and using the generalized form for u . Once we integrate and do some algebraic manipulation, our flow rate becomes

$$\dot{V} = \frac{n\pi R^3}{3n+1} \left(\frac{R}{2\mu} \frac{dP}{dx} \right)^{\frac{1}{n}}$$

For our example pseudoplastic fluid ($n = 0.5$), the flow rate simplifies to

$$\dot{V} = \frac{\pi R^5}{5} \left(\frac{1}{2\mu} \frac{dP}{dx} \right)^2$$

Discussion When $n = 1$, the general equation for volume flow rate reduces to that for Poiseuille flow, as it must.

SUMMARY

In this chapter we derive the differential forms of conservation of mass (the *continuity equation*) and the linear momentum equation (the *Navier–Stokes equation*). For incompressible flow of a Newtonian fluid with constant properties, the continuity equation is

$$\vec{\nabla} \cdot \vec{V} = 0$$

and the Navier–Stokes equation is

$$\rho \frac{D\vec{V}}{Dt} = -\vec{\nabla}P + \rho\vec{g} + \mu\nabla^2\vec{V}$$

For incompressible two-dimensional flow, we also define the stream function ψ . In Cartesian coordinates,

$$u = \frac{\partial\psi}{\partial y} \quad v = -\frac{\partial\psi}{\partial x}$$

We show that the difference in the value of ψ from one streamline to another is equal to the volume flow rate per

unit width between the two streamlines and that curves of constant ψ are streamlines of the flow.

We provide several examples showing how the differential equations of fluid motion are used to generate an expression for the pressure field for a given velocity field and to generate expressions for both velocity and pressure fields for a flow with specified geometry and boundary conditions. The solution procedure learned here can be extended to much more complicated flows whose solutions require the aid of a computer.

The Navier–Stokes equation is the cornerstone of fluid mechanics. Although we know the necessary differential equations that describe fluid flow (continuity and Navier–Stokes), it is another matter to *solve* them. For some simple (usually infinite) geometries, the equations reduce to equations that we can solve analytically. For more complicated geometries, the equations are nonlinear, coupled, second-order, partial differential equations that cannot be solved with pencil and paper. We must then resort to either *approximate* solutions (Chap. 10) or *numerical* solutions (Chap. 15).

REFERENCES AND SUGGESTED READING

1. R. W. Fox and A. T. McDonald. *Introduction to Fluid Mechanics*, 8th ed. New York: Wiley, 2011.
2. P. M. Gerhart, R. J. Gross, and J. I. Hochstein. *Fundamentals of Fluid Mechanics*, 2nd ed. Reading, MA: Addison-Wesley, 1992.
3. R. J. Heinsohn and J. M. Cimbala. *Indoor Air Quality Engineering*. New York: Marcel-Dekker, 2003.
4. P. K. Kundu, I. M. Cohen., and D. R. Dowling. *Fluid Mechanics*, ed. 5. San Diego, CA: Academic Press, 2011.
5. R. L. Panton. *Incompressible Flow*, 2nd ed. New York: Wiley, 2005.
6. M. R. Spiegel. *Vector Analysis, Schaum's Outline Series, Theory and Problems*. New York: McGraw-Hill Trade, 1968.
7. M. Van Dyke. *An Album of Fluid Motion*. Stanford, CA: The Parabolic Press, 1982.



APPLICATION SPOTLIGHT ■ The No-Slip Boundary Condition

Guest Author: Minami Yoda, Georgia Institute of Technology

The boundary conditions for a fluid in contact with a solid states that there is no “slip” between the fluid and the solid. The boundary condition for a fluid in contact with a different fluid also states that there is no slip between the two fluids. Yet why would different substances—fluid and solid molecules, or molecules of different fluids—have the same behavior? The no-slip boundary condition is widely accepted because it has been verified by observation, and because measurements of quantities derived from the velocity field, such as the shear stress, are in agreement with a velocity profile that assumes that the tangential velocity component is zero at a stationary wall.

Interestingly, Navier (of the Navier–Stokes equations) did not propose a no-slip boundary condition. He instead proposed the *partial-slip* boundary condition (Fig. 9–85) for a fluid in contact with a solid boundary: the fluid velocity component parallel to the wall at the wall, u_f , is proportional to the fluid shear stress at the wall, τ_s :

$$u_f = b\tau_s = b\mu_f \frac{\partial u}{\partial y} \Big|_f \quad (1)$$

where the constant of proportionality b , which has dimensions of length, is called the *slip length*. The no-slip condition is the special case of Eq. 1 where $b = 0$. Although some recent studies in very small (< 0.1 mm diameter) channels suggest that the no-slip condition may not hold within a few nanometers of the wall (recall that $1 \text{ nm} = 10^{-9} \text{ m} = 10 \text{ Ångstroms}$), the no-slip condition appears to be the correct boundary condition for a fluid in contact with a wall for a fluid that is a continuum.

Nevertheless, engineers also exploit the no-slip boundary condition to reduce friction (or viscous) drag. As discussed in this chapter, the no-slip boundary condition at a free surface, or a water-air interface, makes the viscous stress τ_s , and thus the friction drag, very small in the liquid (Eq. 9–68). One way to create a free surface over a solid surface, like the hull of a ship, is to inject air to create a film of air that (at least partially) covers the hull surface (Fig. 9–86). In theory, the drag on the ship, and hence its fuel consumption, can be greatly reduced by creating a free-surface boundary condition over the ship hull. Maintaining a stable air film remains a major engineering challenge, however.

References

- Lauga, E., Brenner, M., and Stone, H., “Microfluidics: The No-Slip Boundary Condition,” *Springer Handbook of Experimental Fluid Mechanics* (eds. C. Tropea, A. Yarin, J. F. Foss), Ch. 19, pp. 1219–1240, 2007.
<http://www.nature.com/news/2008/080820/full/454924a.html>

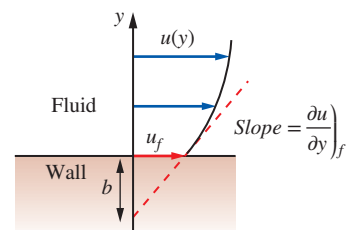


FIGURE 9–85
Navier’s partial-slip boundary condition.

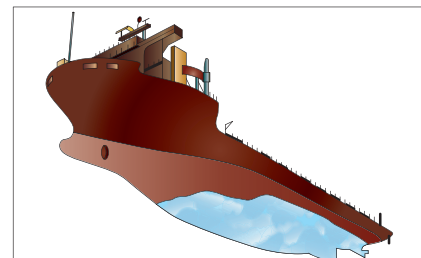


FIGURE 9–86
Proposed injection of air bubbles to form an air film over the bottom hull of a cargo ship [based on a picture courtesy of Y. Murai and Y. Oishi, Hokkaido University and the Monohakobi Technology Institute (MTI), Nippon Yusen Kaisha (NYK) and NYK-Hinode Lines].